ANION MOVEMENT IN A STRUCTURED SOIL

A thesis presented in partial fulfilment
of the requirements for the Degree of
Doctor of Philosophy
in Soil Science at
Massey University

PIMPAN KANCHANASUT

1980

ABSTRACT

Anion movement in soil was studied both in the laboratory and in the field, using structured "undisturbed" soil and sieved aggregates. The movement of chloride, bromide and phosphorus was investigated. Chloride and bromide being non-reactive in soil, were used to indicate whether the flow was more uniform or preferential, while phosphorus was used to indicate the behaviour of strongly adsorbed anions.

Experiments involving the movement of chloride and phosphorus through columns of 0.5-1 mm soil aggregates provided data on phosphate adsorption during miscible displacement. Chloride breakthrough curves were described well by conventional convective-dispersive theory. For phosphorus, linear adsorption isotherms were determined independently, using solution concentrations and equilibrium times similar to those pertaining in the aggregate columns. Conventional theory using these data predicted reasonably well the early part of the breakthrough curves, but did not predict the observed "tailing" of phosphorus breakthrough curves.

The movement of anions through artificial soil channels and planar cracks was studied. The breakthrough curves showed the movement of both chloride and phosphorus was highly preferential through 0.5 mm diameter channels and 0.17 mm wide planar cracks. The results agreed quite well with model predictions.

The movement of anions through 2.4 litre "undisturbed" soil cores was also studied. Under saturated conditions, both chloride and phosphorus moved preferentially. Dye studies indicated the major pathways were worm channels, root channels, and soil cracks. Under unsaturated conditions when the pressure potential was maintained at -0.02 bar (at which channels larger than 0.15 mm diameter and cracks wider than 0.07 mm would be drained), the breakthrough curves for bromide were much less preferential than under saturated conditions. The experimental set-up for this experiment was designed so that the blockage of natural

flow paths was minimized and the effects of porous plates at either end of the cores were avoided.

Two field experiments were conducted at a mole-tile drained site on Tokomaru silt loam (a Fragiaqualf). One experiment investigated the movement of chloride and phosphorus solution ponded on the soil surface. The breakthrough curves for both chloride and phosphorus percolating from the surface to the mole-drains indicated the movement was very preferential, both anions reaching the mole-drains located at 400 mm depth within a minute of their application to the soil surface. Dye staining indicated the movement occurred mostly through worm channels and plant root channels associated with planar cracks.

The other field experiment investigated the leaching of bromide under both ponded water and natural rainfall conditions. When the same amount of water was considered, leaching by rainfall was more effective than by ponding. However, under both water treatments, relatively large amounts of applied bromide remained unleached near the soil surface, while some bromide moved deep into the soil profile. Interception and stem flow appeared to be important factors causing non-uniform leaching under pasture by natural rainfall. Very considerable variation in bromide concentration between replicate soil samples was found, with a log-normal rather than normal distribution. Quite different leaching patterns were found in soil under pasture and in a soil which had been cultivated and cropped.

ACKNOWLEDGEMENT

I wish to express my sincere thanks to Dr D.R. Scotter, for his guidance, criticism, discussion, and encouragement throughout this study. Also for his friendship, interest, and help offered to me at all times.

Thanks are also extended to Mr R.W. Tillman, and Dr J.K. Syers, Soil Science Department, Massey University, for their help and valuable discussion.

The achievement of this study would not be possible without a Columbo Plan Scholarship offered by the New Zealand Government, and study leave given by Khon Kean University, Thailand, which I very much appreciate.

To Robin Tillman and John Sykes, thanks for their assistance with soil sampling, and to Tipvanna and Pisanu, for their assistance with the preparation of this manuscript.

To my family and Suvit, thanks for their continual support and encouragement at all times.

Finally to Miss Vivienne Mair, for excellent typing and preparation of this manuscript.

TABLE OF CONTENTS

Page

Page

Page

APPENDIX E

APPENDIX F

LIST OF FIGURES

Page

Page

Page

Page

Page

LIST OF TABLES

Page

LIST OF SYMBOLS

		DIMENSIONS
a	radius of a sphere	L
B	Brenner number (B = vd/E)	none
C	solution concentration	$M L^{-3}$
C_e	effluent concentration	$M L^{-3}$
C_i	influent concentration	$M L^{-3}$
C_{im}	concentration of solute in immobile region	$M L^{-3}$
C_m	concentration of solute in mobile region	$M L^{-3}$
C_o	initial solute concentration in the layer near the soil surface to depth z_o	$M L^{-3}$
D	molecular diffusion of solute in water	$L^2 T^{-1}$
D_s	molecular diffusion of solute in soil	$L^2 T^{-1}$
d	soil column length	L
E	dispersion coefficient	$L^2 T^{-1}$
E_{Cl}	dispersion coefficient of chloride	$L^2 T^{-1}$
ET	evapostranspiration	L
g	acceleration due to gravity	$L T^{-2}$
I	infiltration rate	$L T^{-1}$
i	depth of water input or interger	L or none
K	hydraulic conductivity	$L T^{-1}$
k	Freundlich solution distribution coefficient	L^3M^{-1}
k_I	Freundlich solution distribution coefficient for adsorption site I	L^3M^{-1}
k_1	adsorption rate coefficient	T^{-1}
k_2	desorption rate coefficient	T^{-1}
k_3	adsorption rate coefficient for site II	T^{-1}
k_4	desorption rate coefficient for site II	T^{-1}
N	a constant in the Freundlich equation	none
n	number of samples	none
Q	flow rate	L^3T^{-1}
q	Darcy flux density	$L T^{-1}$
R	retardation factor ($R = \frac{\rho_b}{\theta} k$)	
r	correlation coefficient, or radial distance in equation (B.1)	none or L
S	solute adsorbed per unit mass of soil solids	$M M^{-1}$

S_I	amount of solute adsorbed per unit mass of soil for site I	$M\ M^{-1}$
S_{II}	amount of solute adsorbed per unit mass of soil for site II	$M\ M^{-1}$
s	standard deviation of x	
s_L	standard deviation of ln x	
t	time	T
V	cumulative volume of effluent	L^3
V_o	liquid-filled pore volume	L^3
V_e	volume of effluent when $C_e/C_i = 0.5$	L^3
v	average pore water velocity ($v = q/\theta$)	$L\ T^{-1}$
x	variable (usually C or lnC)	
$\bar{x}$	mean of x	
$\bar{x}_L$	mean of ln x	
Z	z-vt	L
z	distance in direction of v	L
z_o	initial depth of solute near the soil surface	L
α	diffusional transfer coefficient	T^{-1}
η	viscosity of fluid	$M\ L^{-1}\ T^{-1}$
ψ	pressure potential	L or $M\ L^{-1}\ T^{-2}$
θ	volumetric water content in soil	$L^3\ L^{-3}$
ρ_b	bulk density	$M\ L^{-3}$
ρ_f	fluid density	$M\ L^{-3}$

CHAPTER 1

GENERAL INTRODUCTION

1.1 IMPORTANCE OF SOLUTE MOVEMENT IN SOILS

An important problem in agriculture, horticulture and forestry is the loss of fertilizers, herbicides, pesticides, and soil nutrients in leaching water draining below the root zone. Leached fertilizers and chemicals may ultimately contaminate ground water, streams and lakes, causing eutrophication of water sources. Leaching usually occurs when soil is relatively wet during autumn, winter and spring (Alison, 1968; McLean, 1977; Cameron et al., 1978). However leaching has also been observed to occur at other times after a large rainstorm or irrigation, particularly immediately after fertilizer application (Aylmore and Karim, 1968; Johnston et al., 1965; Balasubramanian et al., 1973; Kissel et al., 1974).

Significant loss of nitrogen fertilizer by leaching under natural field conditions has been reported by several investigators, including Wetselaar (1962), Johnston et al. (1965), Wild (1972), Calvert (1975), Cameron et al. (1978), Gast et al. (1974). In New Zealand, where rainfall intensity and distribution is relatively high, particularly during winter, Sharpley and Syers (1979b) observed a nitrogen loss in mole-tile drainage equalling approximately 2% of the amount applied within 4 weeks of application to Tokomaru silt loam soil under pasture. This percentage of nitrogen fertilizer lost was greater than that measured in similar studies overseas by Bolton et al. (1970) and Meek et al. (1969). Also in Tokomaru silt loam, but under cultivation, Gandar and Gregg (1979) found nitrate losses equal to 60% of the fertilizer applied in the drainage water over a year.

Although phosphorus is a very strongly adsorbed anion in soils, a significant amount of leaching has been found in sandy soils (Spencer, 1957; Humphrey and Prichett, 1971; Calvert, 1975), and organic soils (Black, 1968; Duxbury and Peverly, 1978). Leached phosphorus in natural subsurface drainage and artificial drains was observed to be a significant constituent of stream flow by Minshall (1969), Jackson et al. (1973), Burwell et al. (1975), and Sharpley and Syers (1979 a and b). Sharpley and Syers (1979 a) reported that in the watershed area near Massey University, approximately 67% and 28% of phosphorus in the stream flow are contributed from natural subsurface drainage and mole-tile drainage, respectively.

Leaching of phosphorus may occur rapidly. Kanchanasut et al. (1978) have reported that a significant increase in phosphorus concentration in mole-tile drainage was observed over-night, after 10 mm rainfall following fertilizer application.

Herbicides and pesticides are usually considered immobile in soil, due to strong adsorption and fast degradation, however significant amounts have been observed in groundwater as reported by LaFleur, et al. (1972), LaFleur et al. (1974), Hall and Hartwit (1978).

It is very important to understand and be able to predict the movement of these solutes in soils, particularly under field conditions and under different water management patterns. This thesis attempts to make a contribution in this regard.

1.2 MOVEMENT OF SOLUTES IN SOILS

1.2.1 Differential Equations Used to Describe Solute Movement

The two main processes which are involved in solute movement in soils are: (1) molecular diffusion in response to a concentration gradient, and (2) convection due to mass flow of the soil solution. When molecular diffusion and convection occur simultaneously, they interact to cause enhanced dispersion. Under steady state conditions, the longitudinal transport of solute in a uniform soil has usually been described by the following partial differential equation (Biggar and Nielsen, 1962)

$$\frac{\partial C}{\partial t} = E \frac{\partial^2 C}{\partial z^2} - v \frac{\partial C}{\partial z} \qquad (1.1)$$

where C = solution concentration ($M\ L^{-3}$)

E = dispersion coefficient ($L^2 T^{-1}$)

v = average pore velocity ($L\ T^{-1}$), obtained from q/θ where q is the Darcy flux density ($L\ T^{-1}$) and θ the volumetric water content ($L^3\ L^{-3}$)

z = distance in direction of v (L)

and t = time (T).

This equation, which forms the basis of conventional miscible displacement theory in soils, will be referred to as the convective-dispersive equation in the thesis.

When the flow velocity is sufficiently high that the direct effects of molecular diffusion can be neglected, transport of solute may be described by a simpler equation, derived for dispersion about a moving reference plane, as (Nielsen and Biggar, 1962; Gardner, 1965)

$$\frac{\partial C}{\partial t} = E \frac{\partial^2 C}{\partial Z^2} \qquad (1.2)$$

where $Z = z-vt$.

1.2.2 Solutions of Transport Equations

1.2.2.1 Miscible displacement research Miscible displacement is the process that occurs when one fluid mixes with and displaces another fluid. Day (1956), Biggar and Nielsen (1962, 1963, 1967), Nielsen and Biggar (1961, 1962), and Gardner (1965) were among the first to use miscible displacement theory to study solute transport in soils. Much miscible displacement research has concentrated on observing and analysing breakthrough curves, which are graphs of the ratio C_e/C_i versus the number of pore volumes of effluent collected (V/V_o), where C_i and C_e are the concentration of displacing and displaced solution respectively, V is the cumulative volume of effluent and V_o the volume of pores occupied by fluid. The position and shape of the breakthrough curves give information about the pore configuration in the porous media. Nielsen and Biggar (1961, 1962) and Biggar and Nielsen (1963) described generalized breakthrough curves for flow through various pore geometries in relation to flow velocity and water content.

The convective-dispersive equation (1.1) has been used extensively to predict non-reactive solute movement in soil. The deriviation of the analytical solution under the initial and boundary conditions

$$\begin{aligned} C(z,t) &= 0 \quad \text{for } z > 0 \text{ and } t = 0 \\ C(z,t) &= C_i \quad \text{for } z = 0 \text{ and } t > 0 \\ \lim_{z \to \infty} C(z,t) &= 0 \quad \text{for } t > 0 \end{aligned} \tag{1.3}$$

is given by Nielsen and Biggar (1962) and Kirkham and Powers (1972). The solution is

$$C/C_i = \tfrac{1}{2}\left(\operatorname{erfc}\left\{\frac{z-vt}{(4Et)^{\frac{1}{2}}}\right\} + \exp\left(\frac{vz}{E}\right) \operatorname{erfc}\left\{\frac{z+vt}{(4Et)^{\frac{1}{2}}}\right\}\right) \tag{1.4}$$

This solution is often used to describe the breakthrough curves from a column of finite length (d) with the exit concentration (C_e) approximated as C at z = d, and V/V_o found as vt/d. When plotted, equation (1.4) yields an approximately S-shaped curve, symmetrical about one pore volume.

The value of E may be obtained either directly from the slope of the experimental breakthrough curves (Kirkham and Powers, 1972) or by the log-normal distribution method suggested by Rose and Passioura (1971a).

1.2.2.2 Leaching Distribution of solute in the soil profile after leaching a thin surface layer of non-reactive solute may be described by equation (1.2), assuming a constant flow velocity and dispersion coefficient. The analytical solution for steady state conditions was given by Day (1956), as

$$C = C_o z_o (4\pi Et)^{-\frac{1}{2}} \exp\left(-(z-vt)^2/4Et\right) \tag{1.5}$$

where z_o is the initial depth of solute near the soil surface, and C_o the initial concentration there. Equation (1.5) gives bell-shaped distribution curves, which get deeper and flatter with increasing time. Gardner (1965) found this solution adequately described some field data for nitrate leaching under natural rainfall conditions. However, leaching under field conditions usually occurs under unsteady flow conditions. Bresler and Hanks (1969) and Warrick et al. (1971) have attempted to describe chloride movement in the field soil profile with unsteady flow. To avoid complicated computations, Bresler and Hanks (1969) assumed the contribution to flow from diffusion negligible

in comparison with convective flow, while Warrick et al. (1971) assumed constant E.

1.2.3 Transport Models for Reactive Solutes

Solutes moving through soil often undergo adsorption-desorption reactions with solid surfaces. Solutes usually considered non-reactive with soil are nitrate, chloride, bromide, and tritium. However, adsorption or exclusion of these solutes in soil systems has been observed to some extent, depending on soil chemical properties (Biggar and Nielsen, 1962; Thomas and Swoboda, 1970; Krupp et al., 1972).

Phosphorus, most pesticides and herbicides, and potassium are examples of reactive solutes which are frequently used in agriculture. To account for adsorption-desorption reactions during movement, it is necessary to add an additional term to the convective-dispersive equation (1.1), giving (Cho et al., 1970; Davidson and McDougal, 1973; van Genuchten et al., 1974; Selim et al., 1974; Mansell et al., 1977)

$$\frac{\partial C}{\partial t} = E \frac{\partial^2 C}{\partial z^2} - v \frac{\partial C}{\partial z} - \frac{\rho_b}{\theta} \frac{\partial S}{\partial t} \qquad (1.6)$$

where S is the amount of solute adsorbed per unit mass of soil solids ($M\ M^{-1}$) and ρ_b is the soil bulk density ($M\ L^{-3}$). The expression $\partial S/\partial t$, which represents the rate of adsorption by soil, has been described in a number of ways, some of which are given below.

a. Equilibrium adsorption isotherms The Freundlich equation is the most commonly used to describe adsorption of phosphorus in equation (1.6) (Cho et al., 1970; Selim et al., 1974; Mansell et al.,1976). It may be written as:

$$S = kC^N \qquad (1.7)$$

where k is the solution distribution coefficient ($L^3\ M^{-1}$) and N is a constant, which is usually less than unity, determined by regression analysis from isotherm data. When N = 1, the relationship becomes linear. Differentiation of equation (1.7) with respect to times gives

$$\frac{\partial S}{\partial t} = \frac{dS}{dC} \quad \frac{\partial C}{\partial t} = kNC^{N-1} \frac{\partial C}{\partial t} \qquad (1.8)$$

Substitution of equation (1.8) in equation (1.6) and rearranging gives

$$(1 + R) \frac{\partial C}{\partial t} = E \frac{\partial^2 C}{\partial z^2} - v \frac{\partial C}{\partial z} \qquad (1.9)$$

where $R = \frac{\rho_b}{\theta} kNC^{N-1}$. When $N = 1$, $R = \frac{\rho_b}{\theta} k$. The analytical solution for equation (1.9) when $N = 1$ is equation (1.4) with E replaced by $E/(1 + R)$ and v by $v/(1 + R)$. A positive value for R moves the breakthrough curve to the right of one pore volume. For other N values, numerical solutions must be found.

Using an equilibrium adsorption model in the convective-dispersive equation usually results in an over-estimate of the amount of adsorption occurring during miscible displacement (Kay and Elrick, 1968; Davidson and Chang, 1972; Mansell et al. 1977). Davidson and Chang (1972) have shown that equilibrium adsorption would not occur over a wide range of pore-water velocities. Equilibrium adsorption models can only give the upper bound for adsorption during the movement of reactive solutes.

b. Kinetic adsorption models Phosphorus adsorption by soil is in reality a kinetic process. The rate of adsorption is initially rapid, followed by a slower sorption reaction which may continue for a long period of time (Barrow, 1974; Ryden et al., 1977). Lapidus and Amundson (1952) introduced an equation for first order, reversible, kinetic sorption reactions which may be written

$$\frac{\partial S}{\partial t} = \frac{\theta}{\rho_b} k_1 C - k_2 S = k_2 \left(\frac{k_1 \theta}{k_2 \rho_b} C - S\right) \qquad (1.10)$$

where k_1 and k_2 are adsorption and desorption rate coefficients (T^{-1}), respectively. The numerical solution of equation (1.10) with equation (1.6) has generally described experimental data well at low pore-water velocities (Davidson and McDougal, 1973; van Genuchten et al., 1974). However, Mansell et al. (1977) found that this model did not adequately describe phosphate movement through cores of a sandy soil, the desorption rate constant (k_2) appearing to change when pore-water velocity changed.

c. Combination model Selim et al. (1976) and Cameron and Klute (1977) have development a two-site adsorption-desorption model for use in describing transport of reactive solutes. The two sites are those which appear to adsorb or react with solutes effectively instantaneously, and those which appear to adsorb more slowly, resulting in a kinetic reaction. This division is probably fairly arbitrary, and the physico-chemical significance of the two sites is not clear (Syers et al. 1973; Ryden et al., 1977; Bowden et al. 1980).

The two-site linear adsorption model can be expressed as:

$$\frac{\partial S_I}{\partial t} = k_I \frac{\partial C}{\partial t} \qquad (1.11)$$

$$\frac{\partial S_{II}}{\partial t} = \frac{\theta}{\rho_b} k_3 C - k_4 S_{II} \qquad (1.12)$$

where S_I and S_{II} are the amounts of solute adsorbed on site I and site II respectively, k_I is the solution distribution coefficient for site I, and k_3 and k_4 the adsorption and desorption rate coefficients respectively for site II. The differential equation resulting when these expressions are substituted into equation (1.6) is

$$(1 + R_I) \frac{\partial C}{\partial t} = E \frac{\partial^2 C}{\partial z^2} - v \frac{\partial C}{\partial z} - (k_3 C - \frac{\rho_b}{\theta} k_4 S_{II}) \qquad (1.13)$$

where $R_I = \frac{\rho_b}{\theta} k_I$. This adsorption model is more comprehensive than the ones described earlier. However, it is difficult to determine independently the appropriate adsorption-desortion parameters, hence they are usually estimated by curve-fitting to the experimental breakthrough data. Solving equation (1.13) numerically, de Camargo et al. (1979) found that pore-water velocity had a large influence on the adsorption and desorption rate coefficients (k_3 and k_4) needed to describe phosphorus movement through columns containing sieved soil. For pesticide movement, Rao et al. (1979) also found that two sets of k values were required to predict the breakthrough curves at two different input concentrations.

In general, if non-linear and/or kinetic adsorption reactions are assumed, solution of the resulting modified convective-dispersive equation must be found numerically using a computer, as analytical solutions are not available.

1.3 FAILURES OF CONVENTIONAL THEORY

Nearly 100 years ago, Lawes et al. (1882) wrote that "A large part of water added to soil profiles moves immediately through channels and interacts slightly with water in the soil itself". In New Zealand, Taylor (1956) stated that, "It has often been assumed that the moisture spreads evenly through the soils, whereas what happens is far more complex. Soil water percolated down cracks and through spaces between the structural surfaces and is adsorbed laterally into the soil aggregates".

The concept of rapid movement of infiltrating water described by Lawes et al. (1882) has been ignored until recently. For decades, soil physicists and soil scientists have treated soil as a uniform porous medium and applied the theory described in the preceding sections to predict water and solute movement. For example, disturbed, homogenised and repacked soil has been used extensively in miscible displacement experiments studying the movement of solutes (Davidson et al., 1968; Linstrom and Boesma, 1971; Davidson and Chang, 1972; Rao et al.,1979). However, some miscible displacement experiments using natural soil cores have been carried out. The resulting breakthrough curves from saturated soil cores usually show an earlier, and initially steeper, breakthrough than for packed uniform soil columns (Elrick and French, 1966; Kissel et al., 1973; Cassel et al., 1974; McMahon and Thomas, 1974). The differences have been attributed to different pore connecting patterns. In undisturbed cores the movement predominantly occurs through larger continuous channels, while in the more homogeneous repacked columns the movement is more uniform, and can be described by the convective-dispersive equation. Anderson and Bouma (1977a) and Bouma and Wösten (1979) have shown that the shape of the breakthrough curves is very sensitive to any differences in flow paths, either among the replicate cores of the same soil structure, or among different soil structural types.

Very often also it has been found that the distribution of surface applied solute after leaching in the soil profile is not bell-shaped, as would be predicted by convective-dispersive theory (Zimmerman et al., 1967; Boswell and Anderson, 1970; Wild, 1972; Shuford et al.,1977; Cameron et al.,1977; Wild and Babiker, 1976). The pronounced asymmetry of the leaching pattern

commonly observed has been attributed to non-uniform movement of soil water and solutes. This has been confirmed using dye staining techniques by Ritchie et al. (1972), Anderson and Bouma (1973), Bouman et al. (1977b); Bouma and Dekker (1978), Omoti and Wild (1979).

This kind of breakthrough curve or leaching pattern is referred to as "preferential flow" in this study. The evidence for its occurrence, and its importance in soil and ground water discharge and solute movement have recently been reviewed by Thomas and Phillips (1979).

As well as in undisturbed soil, deviations from convective-dispersive theory have also been observed in packed soil columns containing large aggregates (Biggar and Nielsen, 1962; Green et al., 1972; van Genuchten et al., 1974; van Genuchten and Wierenga, 1977). The microscopic flow velocities in media with complex pore geometries vary from point to point in both magnitude and direction. The velocity in a pore is at a maximum at the centre of the pore, whereas the fluid adjacent to the pore wall does not move. Also the velocity through larger pores exceeds the flow through smaller pores. Biggar and Nielsen (1962) have shown that when aggregate size is increased, the range of microscopic flow velocities increases, and most of the flow will occur through macropores between aggregates. Also, as the distances between macropores increase, molecular diffusion is much less effective in dissipating concentration gradients between the soil solution in the macropores and within the aggregates. Thus the mixing in the columns becomes less complete and affects the slope of the breakthrough curves. Solute moving through macropores is responsible for an early breakthrough, while slow solute movement through micropores within the aggregates is responsible for a long tail section in the breakthrough curves.

Non-uniform flow becomes more evident when reactive solutes are used. Davidson and McDougal (1973) suggested that in media with complex pore geometry, the observed tailing of the breakthrough curves could be due to both slow diffusion of solutes into the micropores, and to kinetic adsorption processes. Transport models including the effects of pore geometry will be discussed in the following section.

1.4 MODIFIED SOLUTE TRANSPORT MODELS

Recent advances in predicting solute transport in soils include efforts to incorporate the effects of pore geometry on flow velocity distribution in the transport models. Some of the models are:

a. Convective-Dispersive Model with Lateral Diffusion

In columns of saturated soil aggregates, soil pores can be partitioned into macropores, which are pores between aggregates and micropores which are pores inside aggregates. Convective viscous flow is assumed to occur only in the macropores or mobile regions, while diffusion occurs inside the aggregates or immobile regions. The convective-dispersive equation was modified to include lateral diffusion by Coats and Smith (1964) and van Genuchten and Wierenga (1976). The equation for non-reactive solute transport may be written:

$$\theta_m \frac{\partial C_m}{\partial t} + \theta_{im} \frac{\partial C_{im}}{\partial t} = \theta_m E \frac{\partial^2 C_m}{\partial z^2} - v_m \theta_m \frac{\partial C_m}{\partial z} \qquad (1.14)$$

and the exchange between mobile and immobile regions given by

$$\theta_{im} \frac{\partial C_{im}}{\partial t} = \alpha(C_m - C_{im}) \qquad (1.15)$$

In these equations θ_m and θ_{im} are the fractions of soil volume filled with mobile and stagnant liquid respectively, C_m and C_{im} are the concentrations of solute in the mobile and immobile regions respectively, v_m is the average pore water velocity in the mobile liquid, and α is a diffusional transfer coefficient (T^{-1}). Passioura (1971) derived and solved analytically an equation similar to equation (1.14).

Van Genuchten and Wierenga (1976a) included the effect of adsorption-desorption in equation (1.14) and (1.15). Analytical solutions of equation (1.14) and (1.15) with linear adsorption (N = 1) are given by van Genuchten and Wierenga (1976a), while for $N \neq 1$ a numerical solution is given by van Genuchten and Wierenga (1976b).

The diffusional transfer coefficient (α) has a large influence on the shape of the breakthrough curves. For non-reactive solutes, Rao et al. (1980) observed the diffusion into spherical aggregates and found the α values were dependent upon aggregate size, volumetric water content in the aggregate (θ_{im}), molecular diffusion in the aggregate, the fraction of water content in the mobile region (θ_m), and diffusion time. For reactive solutes, α was found to depend on flow velocity (van Genuchten and Wierenga, 1977), and input concentration (Rao et al., 1979). Thus treating α as a constant, as is usual, is not very satisfactory.

b. Viscous Flow with Lateral Diffusion

A model was developed by Scotter (1978) based on the assumption of viscous solution flow down vertical cylindrical channels or planar cracks, with simultaneous molecular diffusion of solute into the surrounding soil. The theory and related computations are given in Appendix C. He assumed the movement occurred through channels of the same size and uniformly distributed across the cross section of soil. The resulting breakthrough curves for strongly adsorbed solute did not differ significantly from for the non-reactive solute breakthrough curves, when channel diameter and planar crack width were greater than 0.2 and 0.1 mm respectively.

1.5 GENERAL OBJECTIVES

The work described in the following chapters aimed at investigating the characteristics of chloride, bromide and phosphorus movement in soil with different pore geometries under both laboratory and field conditions. It also aimed at assessing the usefulness of some of the theory outlined above to describe the observed solute movement, which occurred mostly under preferential flow conditions.

CHAPTER 2

ACCOUNTING FOR ADSORPTION DURING PHOSPHORUS MOVEMENT IN SOIL

2.1 INTRODUCTION

Phosphorus movement in soil is usually quite limited, as it is retarded by soil-phosphorus interaction. The interaction phenomenon is generally described by an adsorption-desorption isotherm, which is usually non-linear and time dependent (Fox and Kamprath, 1970; White and Taylor, 1977; Ryden et al., 1977). These isotherms are usually determined by the "batch method", which involves shaking suspensions of soil in various phosphorus solutions and measuring the amounts of phosphorus coming into or out of solution. The adsorption occurs rapidly in the first few hours, and then continues to occur slowly over a long period of time. Adsorption and desorption processes of phosphorus are not singular, and some of the adsorption reactions are irreversible, due to precipitation and chemisorption with high adsorption energy (Ryden et al., 1973; Barrow and Shaw, 1975; White and Taylor, 1977). Common adsorption-desorption models for phosphorus have been described in Chapter 1.

Phosphorus transport through soils has often been studied using miscible displacement techniques (e.g. Cho et al., 1970; Selim et al., 1974; de Camargo et al., 1979). The resulting breakthrough curves are not as would be expected from conventional convective-dispersive theory, as the curves are usually asymmetrical with significant "tailing". Many attempts have been made to quantify the influences of adsorption-desorption processes on breakthrough curves (e.g. Davidson and Chang, 1972; Davidson and McDougal, 1973; Kay and Elrick, 1967; van Genuchten et al., 1974; Mansell et al., 1977).

As phosphorus adsorption is time dependent, using equilibrium adsorption isotherms to account for adsorption during miscible displacement in soil often results in the predicted curves diverging from the experimental data (Selim et al., 1974; Mansell et al., 1977). The equilibrium adsorption isotherm can only give the upper bound of the amount of adsorption of reactive solute in soil (Davidson and McDougal, 1973; van Genuchten et al., 1974), and when used with the convective-dispersive equation is unable to predict correctly the shape of the breakthrough curves in packed soil columns (Davidson and Chang, 1972; Mansell et al.,1977).

For reactive solutes, the interaction between pore water velocity and adsorption has been studied by Linstrom and Boesma (1971), Selim et al. (1974), Mansell et al. (1977), and de Camargo et al. (1979). They found more adsorption occurred when pore-water velocity was decreased. This suggests that the use of adsorption isotherms obtained using equilibration times similar to the contact times for phosphorus in the soil column might be useful in predicting the breakthrough curves. This idea is investigated in this chapter.

Adsorption isotherm determinations usually aim to measure equilibrium adsorption, therefore the soil-phosphorus solution suspension is shaken until the adsorption rate is negligibly small. Little attention has been paid to the equilibration methods and times adopted in adsorption isotherm determinations, carried out for use in models of adsorption during miscible displacement. For example, Mansell et al. (1977) used adsorption isotherms determined after shaking 1:5 soil to phosphorus solution suspension for 7 days to predict phosphorus movement in short sand columns in which the displacement occurred in less than an hour. Similarly, de Camargo et al. (1979) used isotherms obtained from shaking a 1:20 soil to solution suspension intermittently for 24 hours to predict phosphorus movement in columns of < 2 and < 1 mm soil aggregate in which the displacement occurred within about 12 hours.

As stated earlier, the distribution and adsorption of phosphorus and other reactive solutes are affected by soil pore geometry or soil structure. The movement of solutes into stagnant pores, or micropores within soil aggregates and soil structural units, is considered to occur by molecular diffusion alone, while in the macropores between soil aggregates convection and hydrodynamic dispersion, induced by viscous flow, are the major transport mechanisms (Passioura, 1971; Skopp and Warrick, 1974; van Genuchten and Wierenga, 1976). The adsorption on soil aggregate surfaces, or onto the walls of macropores, would reach equilibrium faster than on soil surfaces within the aggregates. Therefore, even non-equilibrium adsorption isotherms determined using conventional methods, may be of limited use for describing adsorption during miscible displacement.

2.2 OBJECTIVES

The experiments described in this chapter aimed to compare the adsorption isotherms obtained from the conventional batch method and from leaching columns. Then to determine the feasibility of using isotherms obtained at appropriate equilibrium times and concentrations for predicting phosphorus movement through columns of soil aggregates.

2.3 MATERIALS AND METHODS

2.3.1 Conventional Batch Method Adsorption Isotherms

Phosphorus adsorption isotherms were obtained using a 1:40 soil to solution ratio. One gram of < 2 mm seived, air-dried soil (Tokomaru silt loam, A horizon) was shaken gently in an end-over-end shaker with 39 ml of 100 µg/ml chloride as potassium chloride solution (KCl). One ml of the appropriate concentration of phosphorus solution as potassium dihydrogen phosphate (KH_2PO_4) was added to the soil suspension at various times between 6 and 29 hours after commencing to shake the samples. This method, proposed by Ryden et al. (1977), kept the shaking time constant while allowing the time for equilibration to vary from 1 to 24 hours. Pre-shaking was needed because some aggregates were not broken down before 6 hours shaking. After 30 hours shaking, the soil suspension was centrifuged, filtered and a phosphorus determination was made on the clear supernatant using the method of Murphy and Riley (1962).

In addition, phosphorus adsorption by various soil aggregate size fractions (< 0.2, 0.2-0.5, 0.5-1.0, and < 2 mm) was determined at 10 hour equilibration time in 28.5 µg/ml phosphorus and 100 µg/ml chloride solution. As the aggregates were broken down during shaking, this allowed any differences in adsorption of different aggregate sizes, conceivably due to different clay or organic matter contents, to be assessed.

In all cases potassium chloride solution was added to obtain the same total ionic strength as in the leaching method described below (Section 2.3.2), and in the soil aggregate columns (Section 2.3.3). Three replicate determinations were made at each concentration level.

2.3.2 Continuous-Leaching Method Isotherms

A miscible displacement technique was also used to determine the phosphorus adsorption isotherm. A small plastic tube 18 mm in inside diameter and 40 mm long was packed with 5 g of < 2 mm seived, air-dried soil, and was set-up vertically. The soil in the column was initially saturated with distilled water. Phosphorus solution was then percolated upwards through the soil column at 0.5 ml/min. The three concentrations used were 1, 5, and 10 µg/ml phosphorus as potassium dihydrogen phosphate. The effluent was collected at regular time intervals by an automatic fraction collector. One hundred µg/ml of chloride as potassium chloride was mixed with the phosphorus solution to act as a marker. The experiment was continued until the concentration of the effluent was the same as the influent concentration, within the limits of measurement.

The relative concentration of the effluent solution (C_e/C_i) was plotted against the volume of the effluent, and the area between the chloride and phosphorus breakthrough curves was obtained by integration using Simpson's rule. This area was considered to represent the amount of phosphorus adsorption.

2.3.3 Phosphorus and Chloride Movement in Columns of Soil Aggregates

Seived, air dried soil aggregates, 0.5-1 mm in effective diameter, were uniformly packed into 30 mm inside diameter, 90 mm long perspex tubing. These soil columns were set-up vertically, with the input solution entering the lower end, and the effluent solution collected from the top of the column through the out-flow tube located on the side of the column (Fig. 2.1).

"Dead space" at the base of the soil column was minimized by using a single layer of nylon mesh (60 µm) instead of a porous plate at the lower end of the soil column. At the top, the effluent solution was collected through the small outflow-tube, minimizing "dead space" there also. The volume of effluent in the outflow-tube was negligible in comparison with soil pore volume (less than 0.04%).

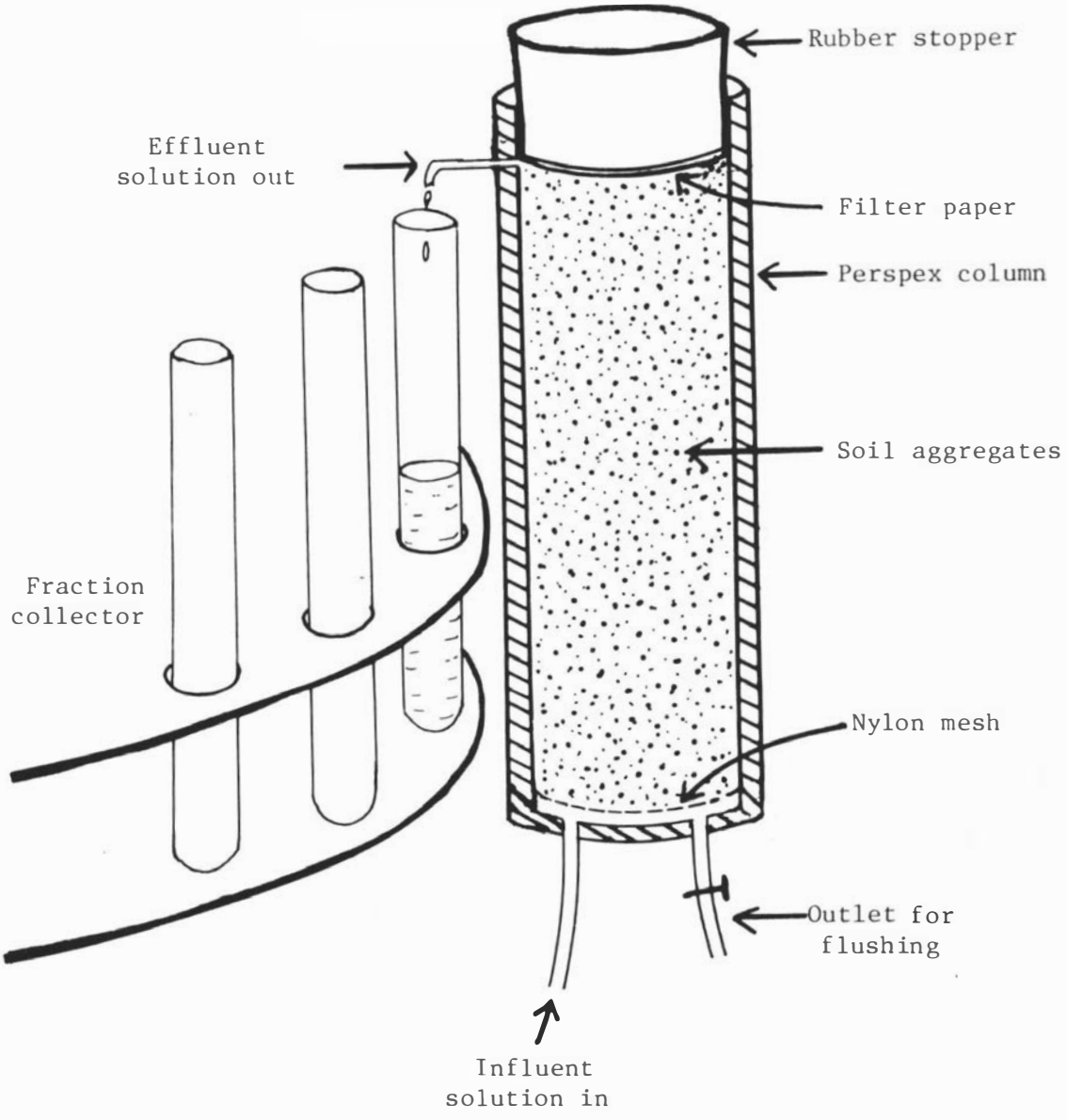

Fig. 2.1 Schematic diagram of experimental set-up for studying phosphorus and chloride movement in soil-aggregate columns.

The soil column was saturated slowly from below with a solution containing 293 µg/ml potassium nitrate (KNO_3) and was leached with the same solution for at least 14 hours to ensure the soil in the column was completely saturated. Potassium nitrate was used to equalise the density of the displaced solution and the displacing solutions, so that there was no gravity segregation effect during the displacement (Rose and Passioura, 1971b; Starr and Parlange, 1976). The displacing solution, containing 20 µg/ml phosphorus as potassium dihydrogen phosphate and 100 µg/ml chloride as potassium chloride, was applied to the column after the previous solution in the chamber underneath the nylon mesh had been flushed out. The flux density (q) of the displacing solution was maintained by a peristaltic pump at 9×10^{-6} or 4.7×10^{-5} m s^{-1}. The higher flux density was approximately half of the saturated hydraulic conductivity of the aggregates. Duplicate experiments were conducted at each flux density. Effluent aliquots were taken at appropriate time-intervals and analysed for chloride and phosphorus concentration. A chloride selective-ion electrode was used to measure chloride in the solution.

2.4 RESULTS AND DISCUSSION

2.4.1 Conventional Batch-Method Adsorption Isotherms

Phosphorus adsorption data obtained using the conventional batch method at 3 and 10 hour equilibration times are shown in Fig. 2.2. The adsorption isotherms are non-linear and described fairly well by the Freundlich equation, equation (1.7). The Freundlich constants (k and N) for the five equilibration times used are given in Table 2.1. Also given are the correlation coefficients (r). Phosphorus adsorption was strongly time-dependent, as can be seen from Fig. 2.3. The curves in this figure were obtained using a power-curve fitting procedure. The data indicate a large part of the adsorption occurred during the first hour, perhaps almost instantaneously. The rate of adsorption decreased markedly as the equilibration time lengthened.

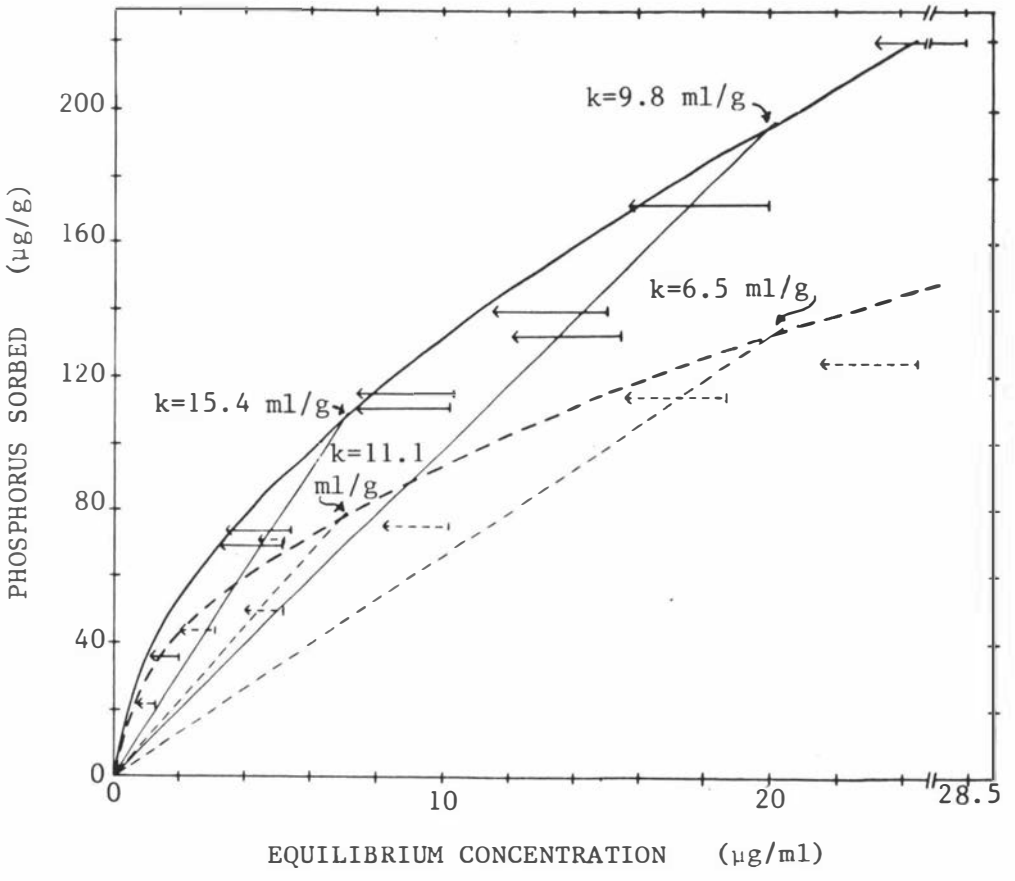

Fig. 2.2 Adsorption data and the fitted Freundlich isotherms, at two equilibration times; 3 hours (– – –) and 10 hours (——), obtained from the batch method. Arrows indicate the change in phosphorus concentration in the solution due to adsorption. The linear isotherms also shown were forced through the Freundlich isotherms at 7 and 20 µg/ml. They were used to obtain solution distribution coefficients (k) for predicting phosphorus movement in the soil columns.

The tail and head of the arrows indicate initial phosphorus concentration and the concentration after adsorption, respectively.

Table 2.1 Freundlich constants for batch method isotherms.

Equilibration Time (hr)	k (ml/g)	N	r
1	17.3	0.589	0.978
3	28.0	0.531	0.979
6	28.9	0.568	0.983
10	31.9	0.615	0.996
24	52.8	0.504	0.992

The amount of phosphorus adsorbed by different aggregate size fractions was checked, and the results are presented in Table 2.2. The fractions, 0.2-0.5 and 0.5-1 mm adsorbed significantly more phosphorus after 10 hour equilibration than the other two fractions (differences significant at the 95% confidence limit using a t-test). The soil aggregates were obtained by grinding and sieving the soil samples, and they must therefore have been bonded strongly enough to resist the force involved. The aggregate cementing materials usually observed in soil include clay minerals, colloidal oxides of iron and manganese and colloidal organic matter (Foth, 1978). These cementing materials are presented in this soil, as shown in Tables A.1, A.2 and A.3 in Appendix A, and are known to be strong phosphorus adsorbers (Hsu, 1964; John, 1972). The fraction < 0.2 mm, which consisted mostly of single grain particles, adsorbed the least phosphorus, while the fraction < 2 mm, which consisted mainly of fine material, also adsorbed less than two aggregate fractions.

Table 2.2 Phosphorus adsorption data for different soil aggregate size fractions after 10 hr equilibration.

Aggregate fraction (mm)	Solution phosphorus concentration after equilibration (µg/ml)	Adsorbed phosphorus (µg/g soil)
<0.2	23.4	206
0.2-0.5	22.2	252
0.5-1.0	22.4	245
<2.0	23.0	222

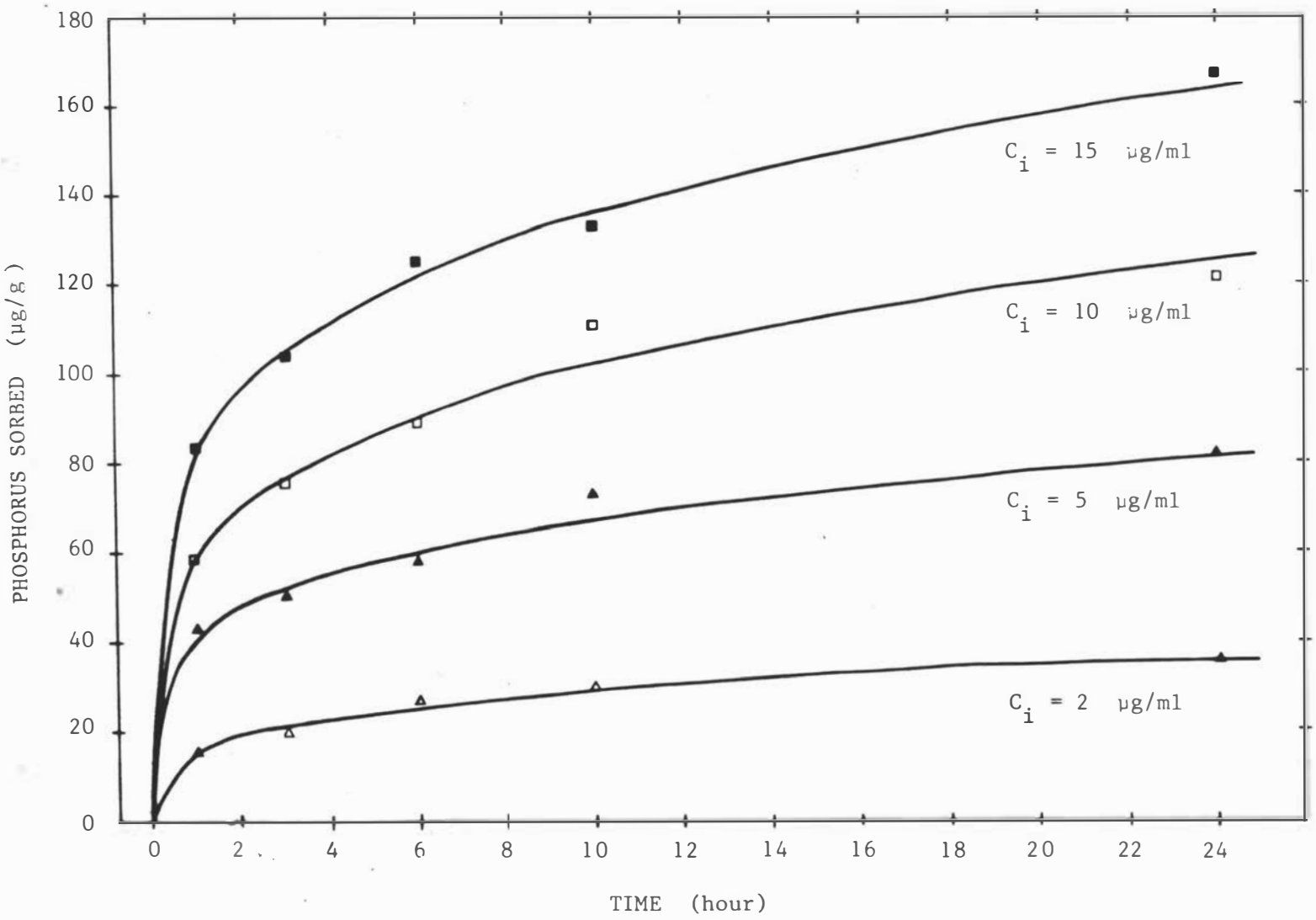

Fig. 2.3 Phosphorus adsorption rates for different initial solution concentrations (C_i). The curves shown were fitted to the experimental data using a power curve fitting procedure.

2.4.2 Continuous-Leaching Method Isotherms

Phosphorus and chloride breakthrough curves for continuous leaching experiments are shown in Fig. 2.4. Only one replicate is shown, however amounts of phosphorus adsorption were obtained from the average of the 4 replicates. The chloride curves indicate the displacement by the influent solution was completed in less than one hour. Adsorption of phosphorus occurred rapidly in the first few hours, then the adsorption rate became slow after the relative concentration of the effluent reached 0.8. The time required until adsorption approached equilibrium depended on the influent concentration. It took 7.5 ± 1.4 hours or approximately 12 pore volumes when the influent concentration contained 10 µg/ml phosphorus, while it took 25 ± 10.4 hours or approximately 36 pore volumes when the influent concentration was 1 µg/ml.

The actual maximum adsorption could not be obtained using this experimental technique, due to the very slow adsorption occurring at long times, when the relative concentration was near unity. The long tailing observed was probably influenced by both slow kinetic adsorption-desorption reactions and slow diffusion into soil aggregates.

As the diffusion of phosphorus is slow in comparison to the flow velocity, the effluent concentration measured might not be the same as the soil solution concentration within the aggregates. In contrast, using the batch method the solution concentration is uniform, due to the shaking and breakdown of the soil aggregates. Couchat et al. (1980) have pointed out that the leaching method for measuring adsorption gives erroneous results if the reaction of solute and soil is very slow.

The adsorption isotherms found after 6 and 10 hours of leaching are presented in Fig. 2.5. Also shown for comparison are the results obtained from the batch method at the same times. The amount of adsorption obtained from the leaching method was lower than from the batch method at both times, however the results from the two methods seem to diverge less at 6 hours than at 10 hours. The differences between the results obtained by the two methods may be attributed to:-

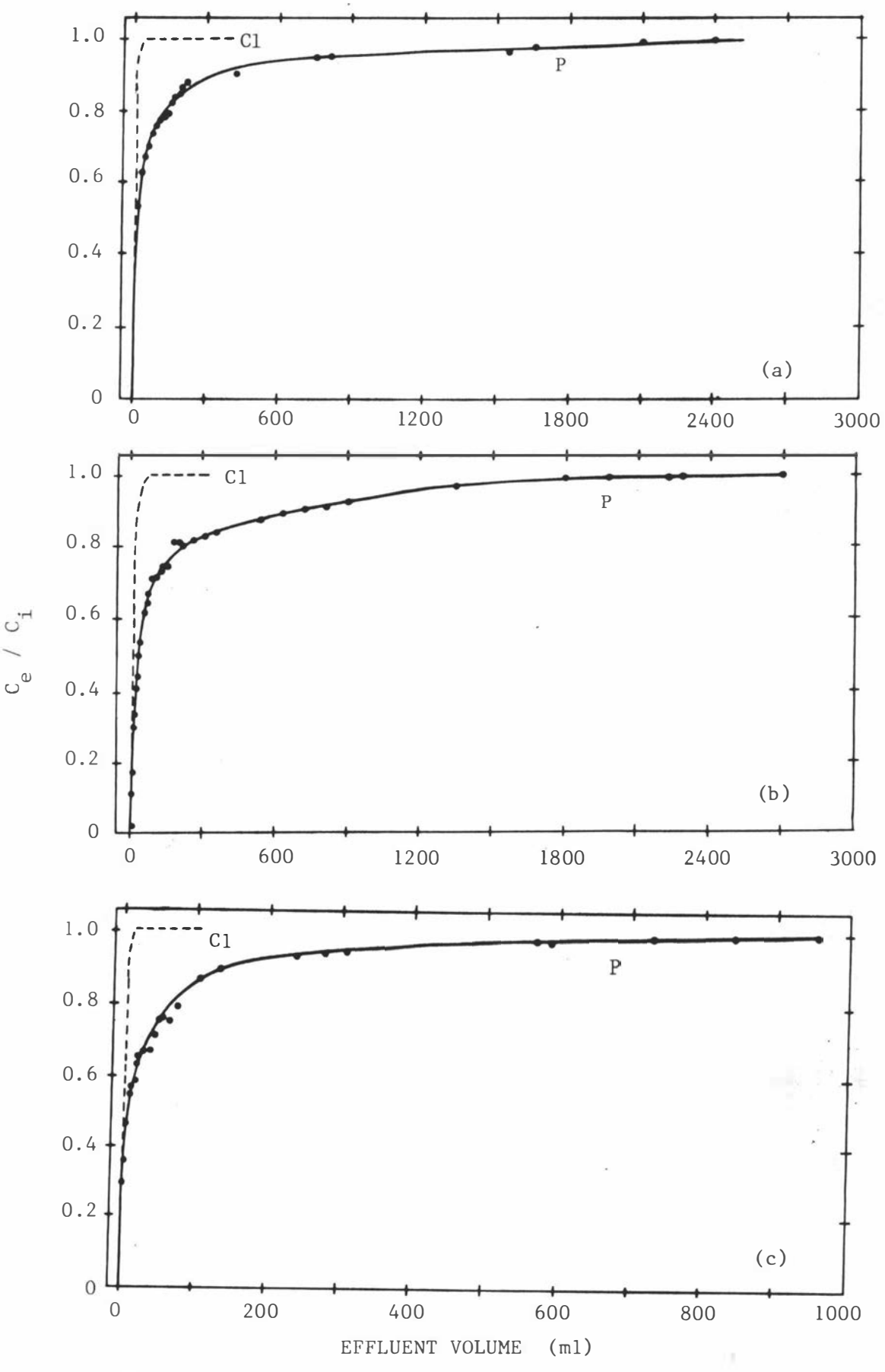

Fig. 2.4 Phosphorus and chloride breakthrough curves for continuous leaching experiments. The three levels of phosphorus concentration are: (a) 1, (b) 5, and (c) 10 µg/ml.

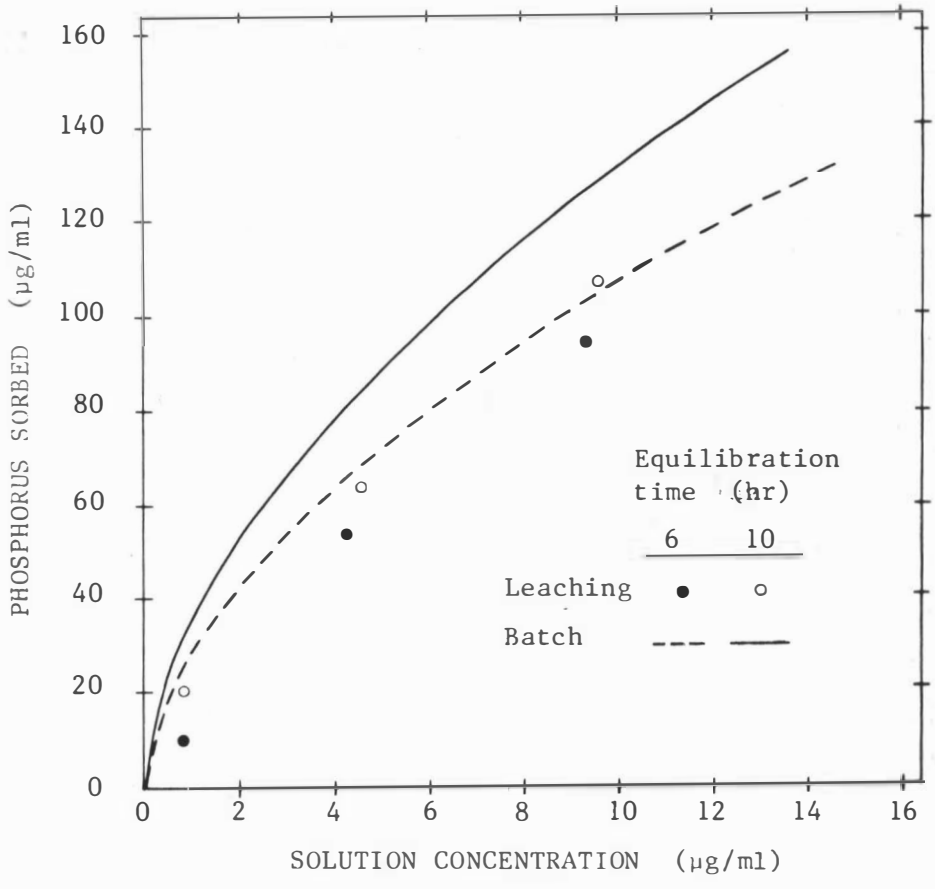

Fig. 2.5 Comparison of adsorption isotherms obtained from batch and and continuous leaching methods at 6 and 10 hour equilibration time. For the batch method the curves shown are the Freundlich isotherms.

a. Soil structure differences Soil samples in the leaching columns consisted of some aggregates, in which adsorption rate was limited by slow diffusion. Soil aggregates in the batch method had been broken down by shaking the soil suspension, so that adsorption would occur mostly directly onto the primary particles. The adsorption rate for the leaching method would depend on both the kinetic adsorption reactions and the diffusion rate into the soil aggregates, while for the batch method the adsorption rate would depend only on the kinetic reaction rate.

Diffusion of phosphorus into soil aggregates has been studied by Gunary (1964) and Evan and Syers (1971), using radiographic methods. The rate of diffusion observed was very slow, but varied from soil to soil. Table 2.3 shows calculated times for chloride and phosphorus diffusion into spherical soil-aggregates with constant concentration at the surface. Details relating to the calculations are given in Appendix B. It takes only 3 minutes for the average chloride concentration inside the largest aggregates (2 mm) to reach 80% of the concentration at infinite time, while it takes as long as 7 hours for phosphorus at 10 µg/ml surface solution concentration. The solution distribution coefficients (k) obtained from the linear Freundlich isotherms were used in these calculations.

Table 2.3 Calculated times for chloride and phosphorus to diffuse into spherical soil aggregates, assuming a linear adsorption isotherm for phosphorus (see Appendix B for details).

		Time for 80% replacement of soil solution (min) Aggregate diameter (mm)			
		0.5	0.75	1.0	2.0
Chloride		0.2	0.5	0.8	3.2
Phosphorus					
Concentration (µg/ml)	k (ml/g)				
1.0	36.0	69	137	274	1096
5.0	17.6	34	67	134	536
7.0	15.4	30	60	120	479
10.0	13.2	25	50	100	420

b. Phosphorus addition methods Phosphorus was applied gradually to the soil at a constant rate in the leaching method, while in the batch method, as adsorption occurred phosphorus was removed from solution and not replaced. Thus in the leaching method, the solution concentration increased while adsorption was taking place, but the concentration decreased in the batch method (see Fig. 2.3). As phosphorus adsorption and desorption are hysteretic, this would lead to more adsorption relative to the final solution concentration in the batch method. Also Barrow and Shaw (1975) found that adsorption of phosphorus was slightly less when small portions of phosphorus were repeatedly added to soil than when the total amount was added at once. This was attributed to blocking of some of the adsorption sites by the previous additions.

2.4.3 Phosphorus and Chloride Movement in Columns of Soil Aggregates

Breakthrough data for phosphorus and chloride through columns of 0.5-1 mm soil aggregates are shown in Figs 2.6 and 2.7 for 9.2×10^{-6} and 4.7×10^{-5} m s^{-1} flux density respectively. The physical data for each column are given in Table 2.4. Chloride breakthrough appeared earlier than expected at the lower flux density, with C_e/C_i reaching 0.5 after approximately 0.8 pore volumes. Early solute breakthrough has been variously attributed to anion exclusion from the negatively charged clay surfaces (Biggar and Nielsen, 1967; Krupp et al., 1972; Thomas and Swoboda, 1970), incomplete mixing in the stagnant pores (Biggar and Nielsen, 1962), and preferential flow between the soil aggregates (Biggar and Nielsen, 1962; van Genuchten and Wierenga, 1977; Green et al., 1972). If anion exclusion had occurred, the area under the breakthrough curves would be less than one pore volume. The area under the breakthrough curves was obtained by integration using Simpson's rule. In fact, the areas obtained for the lower flux density experiment (Core 1 and Core 2) were 0.98 and 0.92, suggesting anion exclusion was not a significant factor. Also if it was important, it would be expected to affect the results at both flux densities.

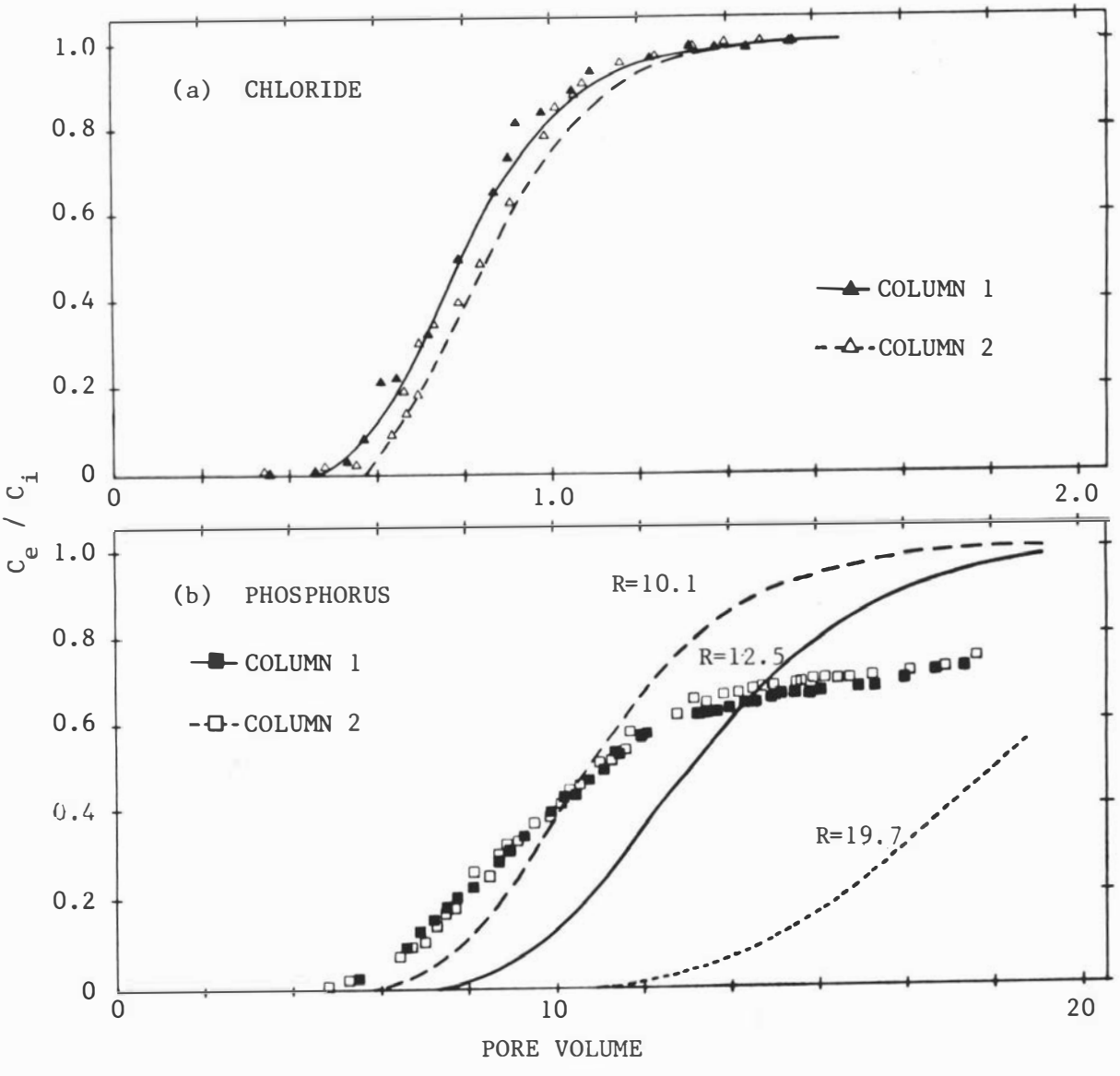

Fig. 2.6 Duplicate experimental and calculated breakthrough curves for (a) chloride and (b) phosphorus at 9 x 10^{-6} m s^{-1} flux density.

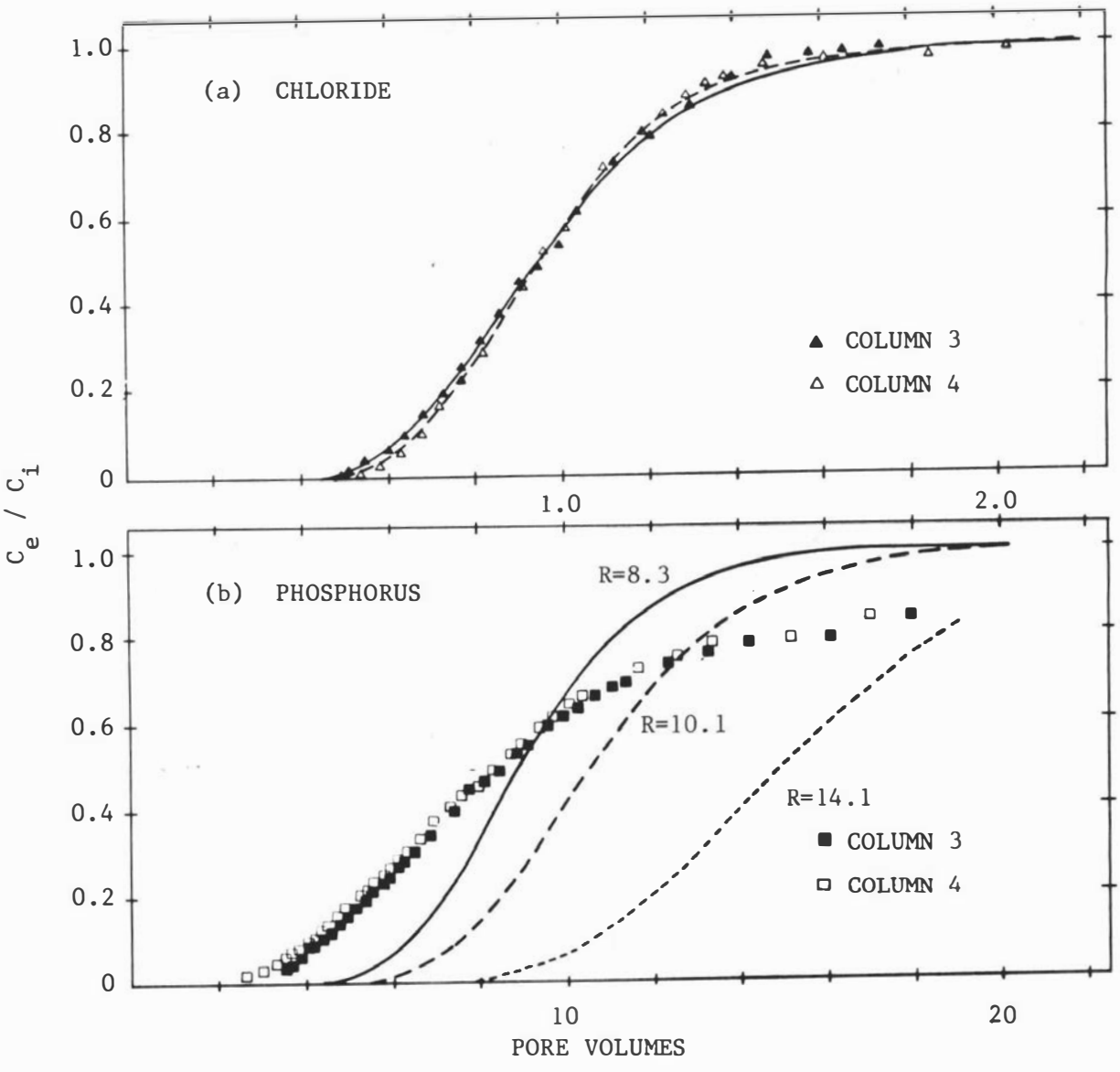

Fig. 2.7 Duplicate experimental and calculated breakthrough curves for (a) chloride and (b) phosphorus at 4.7×10^{-5} m s^{-1} flux density.

When the flux density was increased approximately 5 times, the resulting breakthrough curves of chloride shifted to the right and became somewhat flatter, with the effluent concentration reaching C_e/C_i = 0.5 at 0.95 pore volumes (Fig. 2.7a). The areas under the curves for the faster flux density experiment were 1.03 and 1.05 pore volumes (Core 3 and Core 4, respectively). The slight deviations from one pore volume in the area measured at both flux densities were probably due to experimental error.

Phosphorus appeared in the effluent much later than chloride. It appeared after 5 pore volumes, or 9 hours after application to the soil columns at the lower flux density, and after 2 pore volumes or 0.7 hours in the higher flux density columns. The concentration in the effluent also rose relatively more quickly from the higher flux density columns, C_e/C_i reaching 0.5 after 8.5 pore volumes, compared to 11 pore volumes for the lower flux density columns. The differences in position and shape of phosphorus breakthrough curves at the different flux densities indicate more adsorption occurred when residence time increased. This behaviour is in agreement with previous studies reported by Selim et al. (1974) and de Camargo et al. (1979) for phosphorus movement in soil columns.

The slope of the phosphorus breakthrough curves decreased markedly after C_e/C_i reached 0.75. The tailing of the breakthrough curves was probably influenced by an interaction between slow kinetic adsorption and diffusion in the complex soil pore geometry in the aggregate soil columns (Davidson and McDougal, 1971; Skopp and Warrick, 1974; van Genuchten and Wierenga, 1976).

2.4.4 Modelling of Phosphorus Movement in Soil Columns

No attempt was made to simulate in detail the experimental breakthrough data; only a simple, approximate model was used. The movement of phosphorus through the soil aggregate column was described using equation (1.9), for which an analytical solution is available (see Chapter 1). Use of this equation meant phosphorus adsorption was assumed to follow a linear Freundlich isotherm.

Table 2.4 Physical data for column experiments using 0.5-1 mm aggregates.

Experiment	v (10^{-5} m s^{-1})	ρ_b (kg m^{-3})	Column length (mm)	θ	E_{Cl} (10^{-8} m^2 s^{-1})	Time for one pore volume (hr)	V_e/V_o	B
Column 1	1.35	871	88	0.681	4.58	1.81	0.80	32.5
Column 2	1.34	855	90	0.685	3.72	1.86	0.86	37.8
Column 3	6.86	877	88	0.687	23.3	0.36	0.95	27.3
Column 4	6.61	860	90	0.713	29.5	0.38	0.95	21.2

B = Brenner number

v = the fluid average velocity given by the flux density (q) divided by the water filled porosity (θ)

E_{Cl} = dispersion coefficient for chloride

V_e = volume of the effluent when relative concentration is 0.5, (L^3)

V_o = pore volume (L^3)

ρ_b = bulk density ($M\ L^{-3}$)

As phosphorus adsorption is very dependent on time and the initial solution concentration, the linear solution distribution coefficients (k) used in the model were obtained from the batch method adsorption isotherms so that the equilibration times and solution concentrations were similar to the contact times and effluent concentrations in the soil columns. Two solution concentrations were used to calculated k values. One was the influent concentration (20 µg/ml), and the other (7 µg/ml) was approximately half the final concentration of phosphorus in the effluent. Equilibration times were estimated as half the time required for C_e/C_i to reach 0.5 in the soil columns. Thus k values for the slow flux density column (Column 1 and 2) were obtained from the adsorption isotherm at 10 hours, while for the fast flux density columns (Column 3 and 4) 3 hour isotherm data were used. For comparison, isotherm data after 6 hours equilibration time, with 20 µg/ml solution concentration, (R = 10.1) were also used in the model. The corresponding retardation factors (R) are given in Table 2.5.

Table 2.5 Retardation factor values (R) at 7 (R_7) and 20 (R_{20}) µg/ml solution concentration, obtained from batch method isotherms, for use in modelling movement through soil columns.

Experiment simulated	Equilibration time (hr)	R_7	R_{20}
Column 1	10	19.7	12.5
	6		10.1
Column 2	10	19.1	12.2
	6		9.9
Column 3	3	14.1	8.3
	6		10.1
Column 4	3	13.3	7.9
	6		9.5

The experimental chloride breakthrough data were used to determine dispersion coefficients (E_{Cl}), using equation (1.1) and the method of analysis proposed by Rose and Passioura (1971a). An adjustment was made to account for C_e/C_i reaching 0.5 before one pore volume. This was accomplished by replacing the pore volume (V_o) by an effective pore volume (V_e) in the calculations. The parameter V_e is the volume of the effluent corresponding to a relative concentration of 0.5. This method of adjustment was suggested by Rose and Passioura (1971a) and has been used by Cassel et al. (1975), Cagauan et al. (1962), and Selim et al. (1974). The resulting Brenner numbers (B = vd/E) and E values are given in Table 2.4. The predicted curves for chloride agree well with the experimental data, as shown in Figs. 2.6a and 2.7a.

The shape of the predicted phosphorus breakthrough curves does not agree so well with the experimental data, as might be expected (Figs. 2.6b and 2.7b). In all of the predicted curves, phosphorus appears in the effluent later than was found experimentally, and then the predicted concentration rises more steeply than the experimental data.

In Fig. 2.6b, the curve using k at 6 hour equilibration time and 20 µg/ml solution concentration isotherm (R = 10.1) gives the best approximation of the experimental breakthrough data, while the curve using k at 10 hour and 7 µg/ml concentration (R = 19.7) appears much later. However, k at 10 hour and 20 µg/ml concentration (R = 12.5) is also reasonably close to the experimental data. For the fast flux density columns, k at 3 hour and 20 µg/ml (R = 8.3) gives the best prediction (Fig. 2.7b). The results indicate the importance of equilibration time when adsorption isotherms are used for predicting the movement of reactive solutes in soil.

A problem arises if the simple model used here is to be used predictively. The phosphorus adsorption parameters were obtained independently of the miscible displacement experiment (differing from most other work in this regard), but the appropriate equilibration times for these parameters were inferred from the phosphorus breakthrough data. However, equilibration times can also be estimated, without any breakthrough information, using a simple iterative procedure.

Knowing the mass of soil in the column and the rate at which phosphorus will be added, and using initially say the 24 hour adsorption value at the solution concentration to be applied (in this case 243 µg P/g soil), the time needed for enough phosphorus to enter the column to satisfy the adsorption demand and replace the soil solution is calculated. Half of this time is then used as an estimate of the average time phosphorus will have to equilibrate in the column during miscible displacement. This equilibration time is used to find a new adsorption value from the batch method data, and the whole calculation is repeated. After 3 iterations, the equilibration time estimates for the column experiment were found as 13 and 1.5 hours for the low and high flux density columns respectively. These times result in R values (for 20 µg/ml solution concentration) of 13 and 7. These values are very similar to the values inferred from the breakthrough data of 12 and 8 (Table 2.5) and would result in similar predicted breakthrough curves to the ones in Figs. 2.6b and 2.7b.

2.5 GENERAL DISCUSSION

The results show the usefulness of using linear adsorption isotherms, obtained at appropriate equilibration times, for predicting when phosphorus will appear in the effluent from soil columns. The calculations involved can be done simply using a pocket calculator.

The same approach could be used to describe phosphorus movement under field conditions, when the flow through the soil is uniform enough for conventional convective-dispersive theory to apply and for a dispersion coefficient to be found. However, as will be shown in the following chapters, if preferential flow is dominant, convective-dispersive theory is of no use, and in fact adsorption has little effect on phosphorus movement. The various conditions determining whether flow tends to be uniform or preferential are discussed later in the thesis.

2.6 CONCLUSIONS

1. More phosphorus adsorption occurred using the conventional "batch" method than the leaching column method at comparable equilibration times, particularly at longer equilibration times.

2. Chloride breakthrough curves, used as an indicator of water movement in both leaching columns and soil aggregate columns, indicated the displacement in the soil columns occurred relatively uniform. The curves for the soil aggregate columns were described well by the convective-dispersive equation.

3. Phosphorus breakthrough curves were asymmetrical with "tailing". The shape of the breakthrough curves could not be described adequately using convective-dispersive theory with a simple linear-adsorption isotherm. However, this theory, using distribution coefficients (k) determined independently at appropriate solution concentrations and equilibration times, predicted fairly well the position of the breakthrough curves, and so the time delay between phosphorus and chloride breakthrough.

4. Phosphorus adsorption, and the resulting shape of the breakthrough curves, were influenced by the contact time of phosphorus in the soil columns. Increasing flux density decreased the amount of phosphorus adsorption.

5. Tailing of phosphorus breakthrough curves was probably due to slow diffusion of phosphorus into the aggregates, coupled with kinetic sorption reactions.

CHAPTER 3

ANION MOVEMENT THROUGH ARTIFICIAL SOIL CHANNELS AND PLANAR CRACKS

3.1 INTRODUCTION

Several workers have suggested that water and solute movement in natural soils often occurs preferentially through large soil pores such as worm channels (Williams and Allman, 1969; Ehlers, 1973; Bouma et al., 1977a), fissures or planar cracks (Ritchie et al., 1972; Blake et al., 1973), worm channels and cracks (Wild, 1972; Bouma and Dekker, 1978; Omoti and Wild, 1979), and root channels (Wild, 1972; Williams and Allman, 1969). Such preferential flow has been usually thought to occur in relatively large channels. Williams and Allman (1969) refer to channels 2-10 mm in diameter while Bouma and Dekker (1978) and Omoti and Wild (1979) suggest cracks greater than 2 mm wide are resposible. Such large pores would only be effective in conducting water when the soil is effectively saturated. Jongerious (1957) and Brewer (1964) indicated that worm channels are only effective in saturated soil. However, most cracks are closed by swelling once the soil is saturated.

Flow in the smaller pores becomes significant in the absence of large pores, or when the large pores are empty. Omoti and Wild (1979) observed planar cracks about 0.05-0.1 mm wide conducting water in a weakly structured loamy sand in which no cracks were apparent to the unaided eye. Bouma et al. (1977b), using dye tracer and morphometric techniques, observed cores of medium, subangular blocky, structured soils. The conducting pores observed included mostly channels and vughs[1] 0.1-1 mm in diameter, 0.1-1 mm wide cracks, and a few pores greater than 1 mm in diameter.

Anderson and Bouma (1977a), using chloride as a tracer, found preferential flow in saturated soil cores similar in structure to those studied by Bouma et al. (1977b). In a subsequent paper, Anderson and Bouma (1977b) used a thin crust at the soil surface to obtain a matric potential of -250 mm under the crust and unsaturated flow in the top part of the cores. Presumably free water flowed out the base of the cores, the chloride breakthrough curves from these cores showed much less evidence of preferential flow than the saturated cores.

---

[1] relatively large voids, usually irregular and not normally interconnected with other voids of comparable size (Brewer, 1964).

At a matric potential of -250 mm, cyclindrical pores greater than 0.12 mm in diameter and cracks greater than 0.06 mm wide would be air-filled. Thus their work indicated that such pores larger than this were responsible for most of the preferential flow. However, chloride still appeared in the effluent somewhat earlier than expected even under partially unsaturated conditions, probably due partly to saturated flow near the bottom of the cores and possibly also anion exclusion.

Comparable differences between saturated and unsaturated breakthrough curves were also obtained by Elrick and French (1966) and Kissel et al. (1973) in natural undisturbed soil cores, and by Bouma and Anderson (1977) in artificial soil columns containing vertical channels 5 mm in diameter. However, the porous plates or crusts, which were used in all the unsaturated flow experiments, would reduce the effects of any preferential solute movement through the soil. Thus the breakthrough curves obtained, for example by Anderson and Bouma (1977b), would be influenced to some extent by the hydrodynamic dispersion in the crust on the top of the cores.

While many works have attributed the early appearance of applied solutes in the effluent to preferential flow through larger soil pores, no experimental work indicating the minimum size of pore allowing preferential flow appears to have been done. A theoretical model developed by Scotter (1978), using a simplified pore geometry, suggests that vertical channels 0.3 mm in diameter and cracks 0.1 mm wide are the minimum size of conducting pores for both reactive and non-reactive solute movement to occur preferentially. Unfortunately, due to the regular shape of channel and crack assumed in the theory and the irregular pore shape in real soil, the results of the model predictions cannot be quantitatively compared with experiments using natural soil.

3.2 OBJECTIVE

The experiments described in this chapter aimed to observe the movement of sorbed and non-sorbed anions through soil columns containing artificial vertical channels and planar cracks of regular shape.

3.3 MATERIALS AND METHODS

The soil was taken from the Ah2 horizon (approximately 150 mm depth) of Tokomaru silt loam (Appendix A). Soil samples were air-dried and passed through a 2 mm sieve. Soil cylinders containing an artificial channel, approximately 47 mm in diameter and 50 mm long, were made by casting a soil slurry around a length of nylon line 0.3 mm in diameter. The soil slurry was made by mixing air-dried soil with 330 µg/ml calcium nitrate solution ($Ca(NO_3)_2$). After pouring, the casts were air-dried and then oven-dried at 105C. The presence of calcium ions and oven-drying, stabilised the soil structure. The cast was then slowly rewet to a small positive pressure potential and the nylon line was then removed. The side and most of the bottom of some casts was coated with paraffin wax. Other casts were coated all over except for a 5 mm uncoated annulus around the entry and exit of the channel. Soil casts containing a single planar slit were prepared in a similar manner using brass shim 0.15 mm thick and 12 mm wide, and the side and most of the bottom of these casts was also coated with wax.

Each soil cast was saturated slowly from below with a solution containing 164 µg/ml calcium nitrate, and 100 µg/ml sodium azide (NaN_3) to control microbial growth. It was then leached with the same solution until the flux was approximately constant. Next the Mariotte supply was removed, and as soon as free solution had disappeared from the soil surface, the displacing solution, containing 10 µg/ml phosphorus as potassium dihydrogen phosphate (KH_2PO_4), 350 µg/ml chloride as potassium chloride (NCl), 115 µg/ml calcium nitrate, and 100 µg/ml sodium azide, was applied and effluent aliquots taken at suitable time intervals. The calcium nitrate concentration in the displacing solution was chosen so that the displaced and displacing solution had the same density. The analysis method of Murphy and Riley (1962) was used for phosphorus, and titration with silver nitrate (Bower and Wilcox, 1965) or a specific ion electrode, for chloride.

3.4 COMPUTATIONS

Breakthrough curves for chloride and phosphorus were computed assuming viscous flow of solution down vertical cylindrical channels and planar cracks, with simultaneous molecular diffusion of solutes into the surrounding soil. Details of the theory are given by Scotter (1978) and are presented in Appendix C (Section C.1) with a typical CSMP programme (Section C.3).

The retardation factor (R) for phosphorus was arbitrarily selected by fitting the calculated curves from the model to the experimental data for phosphorus movement through packed aggregate columns containing the same soil materials (Kanchanasut et al., 1978). The channel size in the aggregate soil columns was estimated from the retentivity curves. The R values used were 69 for phosphorus and zero for chloride.

As some slight swelling and shrinkage was unavoidable during preparation of the casts, the actual effective diameters of the channels and widths of the slits were calculated from the flow rates, using equations (1) and (6) in Appendix C.1, respectively.

3.5 RESULTS AND DISCUSSION

Physical data for the soil casts are given in Table 3.1. The breakthrough data for chloride and phosphorus in the soil casts containing channels are shown in Fig. 3.1. Blocking the channels at the conclusion of the experiment typically reduced the flow to 1% of its previous value, indicating nearly all of the flow was through the channel rather than uniformly through the soil. The movement of a rhodamine B dye-water mixture subsequently applied to the casts also supported this conclusion, with only the channel wall or planar crack wall, and less than 1 mm thickness of the surrounding soil matrix being affected by dye, as shown in Fig. 3.2.

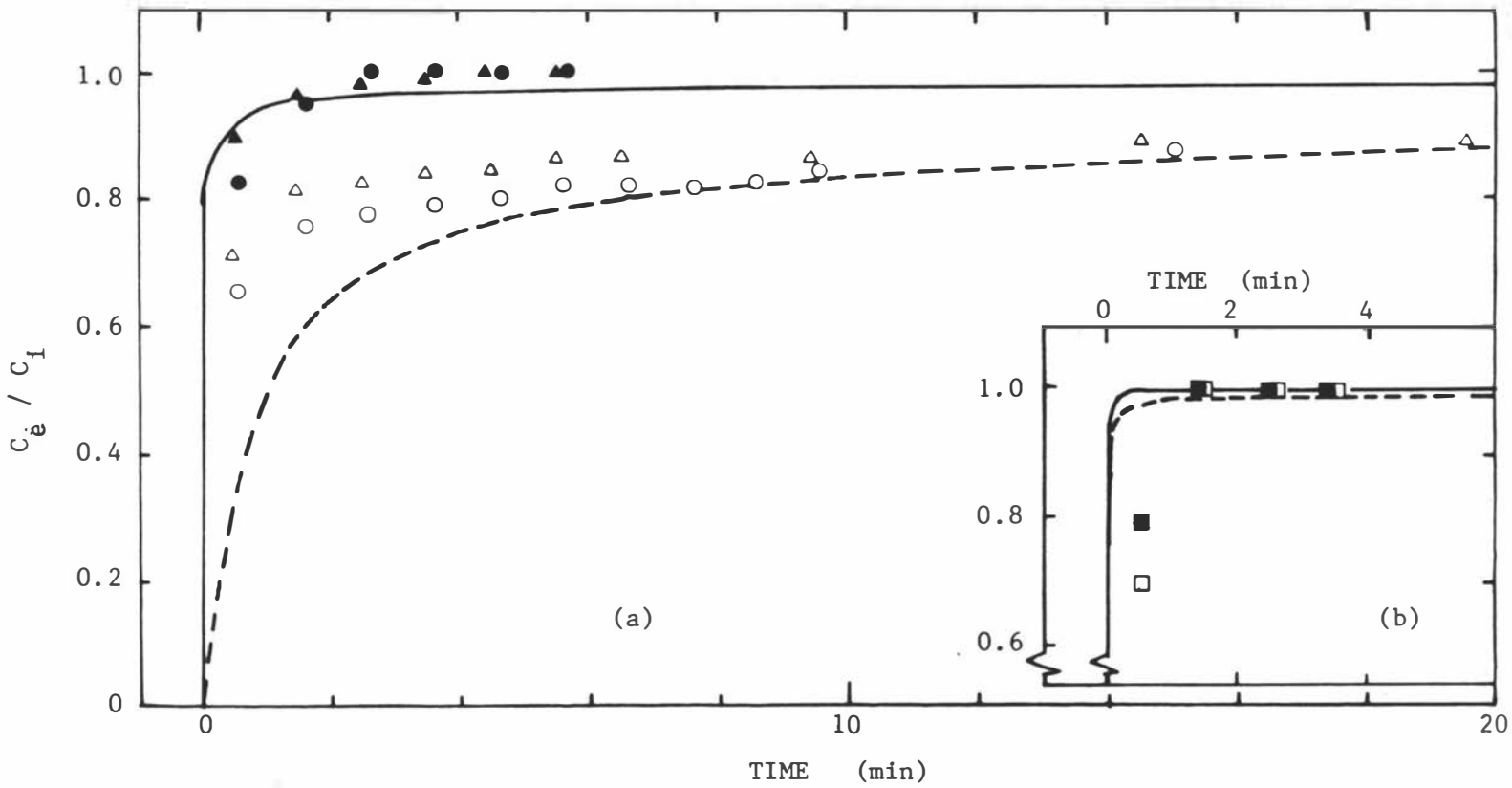

Fig. 3.1 Breakthrough data for soil casts containing a single channel. (a) Breakthrough data for soil casts with exposed soil surface; Cast I, chloride (●) and phosphorus (○); Cast II, chloride (▲) and phosphorus (△). (b) Breakthrough data for soil cast with almost completely wax-coated surface; Cast III, chloride (■) and phosphorus (□). Also shown are predicted breakthrough curves for Cast I and III, chloride (——) and phosphorus (— —) assuming R=69 for phosphorus.

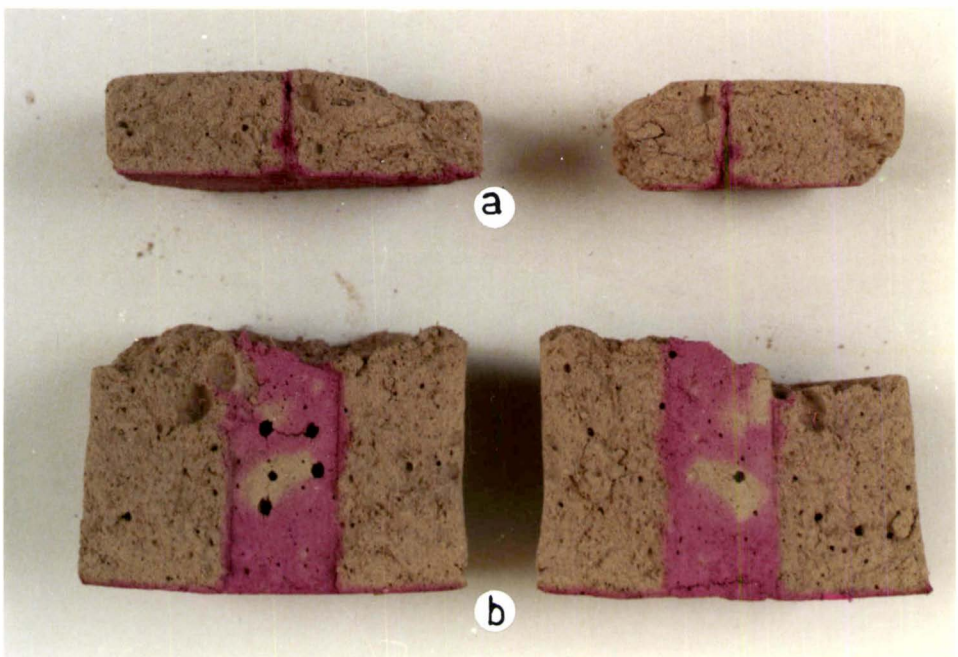

Fig. 3.2 Movement of Rhodamine B dye solution in the soil casts containing artificial (a) vertical channel, and (b) planar crack.

Table 3.1 Physical data for soil casts containing a channel or crack.

		ρ_b (kg m^{-3})	θ	K (10^{-5} m s^{-1})	Diameter or width (mm)	Time for one pore volume (min.)	k ($ml\ g^{-1}$)	Pressure potential to drain (mm)
Channel	I	1550	0.38	0.67	0.47	35	16.9	-63
	II	1530	0.38	1.18	0.53	22	17.1	-55
	III	1590	0.35	1.04	0.51	23	15.2	-58
Crack	IV	1350	0.46	3.00	0.17	10	20.7	-86
	V	1310	0.46	2.50	0.16	11	24.4	-92

ρ_b = bulk density

K = hydraulic conductivity

k = adsorption distribution coefficient of phosphorus

θ = volumetric water content.

Fig. 3.1b shows the breakthrough data for chloride and phosphorus in the soil cast completely wax-coated, except for just around the channel. The exit concentrations of both chloride and phosphorus rose steeply with relative concentration (C_e/C_i) reaching unity in less than 2 minutes. This was in good agreement with breakthrough curves computed using the simple theory in Appendix C.1.

In Fig. 3.1a are shown the data for two casts with slightly different channel sizes and without wax coating on the surface. The chloride concentration did not rise as rapidly as in Fig. 3.1b, although the relative concentration of both casts still reached 0.5 in less than a minute, after only a small fraction of a pore volume had percolated,

indicating preferential movement down the channel. However, as nearly all the flow was down a single channel, reference to the number of pore volumes has little significance. The phosphorus concentration also rose rapidly, indicating preferential movement, and in 10 min. reached a relative concentration of approximately 0.84. A correction discussed in Appendix C was included in the computer programme to account for diffusion across the surface from the ponded solution as well as radial diffusion out of the channel. The difference between Figs. 3.1a and b shows the effect of diffusion across the surface of the casts.

Breakthrough data for chloride and phosphorus in the duplicate casts containing planar cracks are shown in Fig. 3.3. The computed theoretical curves take approximate account of diffusion across the surface of the casts, in the manner already referred to. Again, pronounced preferential movement of chloride and phosphorus occurred and the theoretical and experimental data are in reasonable agreement.

The breakthrough data for the duplicate casts with slightly different sized channels or cracks indicate the sensitivity of flow to the size of conducting pore. Scotter (1978) has shown the predicted breakthrough curves for different channel and crack sizes in Figs. 2,3, and 4 in Appendix C. The shape of the curve is strongly dependent on pore size.

The value of R used gave phosphorus breakthrough curves in reasonable agreement with the experimental data. The values of the adsorption distribution coefficient (k) for each cast were calculated ($R = \frac{\rho_b}{\theta} k$, see Section 1.2.3), in order to compare them with the values obtained from the adsorption isotherm experiments described in Chapter 2. The k values obtained are given in Table 3.1. They are all somewhat higher than the measured isotherm values at 6 and 10 hour equilibration times, which were 10.7 and 13.2 ml g^{-1} at 10 µg/ml phosphorus concentration, respectively (Fig. 2.5). k values smaller than the measured isotherm values might be expected, due to the time dependence of phosphorus adsorption, and the phosphorus movement through the channels and cracks occurring within a few minutes after application. However, soils in the casts had been mixed with calcium ions during preparation of the

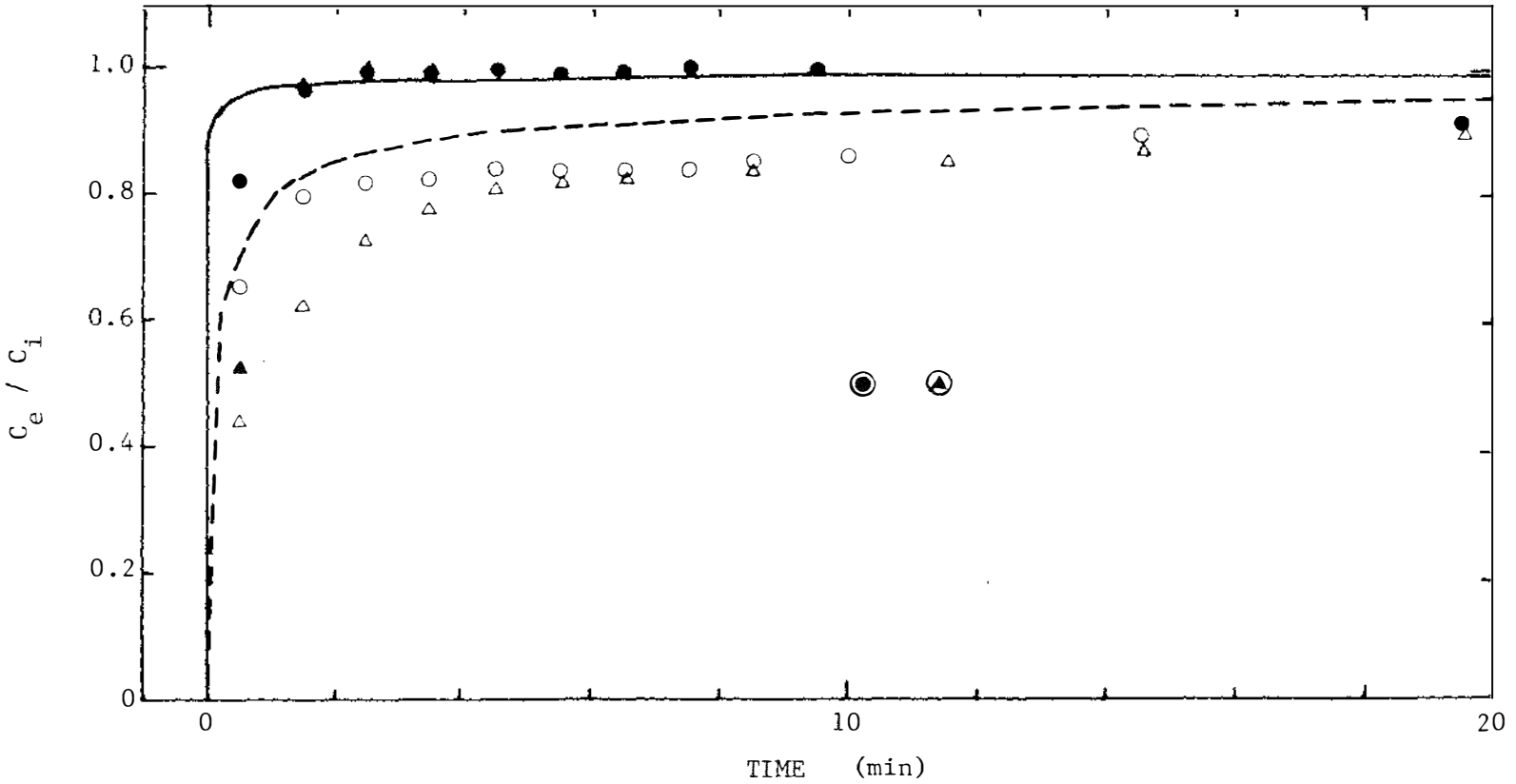

Fig. 3.3 Breakthrough data for soil casts containing a single crack; Cast IV, chloride (●) and phosphorus (○); and Cast V, chloride (▲) and phosphorus (△). Also shown are predicted breakthrough curves for Cast IV, chloride (——) and phosphorus (— —) assuming R=69 for phosphorus. The circled symbols indicate time for one pore volume.

casts, which would increase the adsorption capacity for phosphorus (John, 1972). The relatively small difference between the chloride and phosphorus breakthrough curves when preferential flow occurs (Figs.3.1 and 3.3) indicates however that the actual k values chosen are of little importance.

The results of this experiment support the theory proposed by Scotter (1978). It was found that solute adsorption has little effect on preferential flow through channels at least 0.47 mm in diameter and cracks at least 0.17 mm wide.

While the movement through channels or cracks closer to the critical size could not be studied, it is reasonable to assume that the theory will still be valid for such flows. Table 3.1, and Tables 1 and 2 in Appendix C.1, show the pressure potentials needed to drain channels and cracks of a range of sizes. The pressure potential needed to drain the critical sized pores is -200 mm, thus preferential flow would only be expected to occur in soil close to or at saturation, and not in soil at "field capacity" or drier.

Channels larger than 0.2 mm in diameter and cracks wider than 0.1 mm are probably quite common in natural soil, as many roots, planar cracks or fissures, and soil organisms are of these magnitudes or larger. If such soil pores are water-filled, and continuous or interconnecting with other large pores, preferential flow would be expected.

3.6 CONCLUSIONS

1. Chloride and phosphorus moved almost instantaneously through cast soil columns approximately 50 mm long containing a single channel about 0.5 mm in diameter, or crack about 0.17 mm by 12 mm. The effluent concentration of both anions reached 50% of the influent concentration less than a minute after their application to the surface. Dye patterns confirmed that almost all of the solution moved through these pores rather than uniformly through the soil.

2. Experimental breakthrough data for both chloride and phosphorus are in general agreement with model predictions, assuming all the viscous flow is down the channel or crack, while molecular diffusion transports solute into the soil around the channel or crack. The model implies that preferential flow will occur only if vertical, continuous, water-filled channels at least 0.2 mm in diameter and/or cracks 0.1 mm wide are present in soil.

CHAPTER 4

ANION MOVEMENT IN SOIL CORES

4.1 INTRODUCTION

Miscible displacement experiments carried out in the laboratory usually involve using soil columns of disturbed and repacked soils (e.g. Davidson and Chang, 1972; Thomas and Swoboda, 1970; van Genuchten et al., 1974). The pore geometry in such repacked soil columns is very different to soil under field conditions, and the extrapolation of the results obtained to field situations may lead to large errors. Differences in solute movement in packed soil columns and relatively undisturbed soil cores have been shown by Elrick and French (1966), Kissel et al. (1973), McMahon and Thomas (1974) and Cassel et al. (1974). The breakthrough curves for chloride obtained from the undisturbed soil cores showed chloride appearing earlier, and the relative concentration in the effluent rising more rapidly than in the repacked columns, for which the classical "S-shaped" breakthrough curves were found.

The rapid movement of solutes through undisturbed soil cores has been attributed to the viscous flow occurring predominantly through only a few relatively large continuous pores. This has been confirmed using dye-tracing techniques by Ritchie et al. (1972), Omoti and Wild (1979) and Anderson and Bouma (1973).

Information on soil pore geometry and connecting patterns within a soil can be inferred from the breakthrough curves. Anderson and Bouma (1977a) found different breakthrough curve shapes for soil cores with blocky structure and those with prismatic structure. The rapid movement of chloride through the block-structured soil indicated more continuity of the conducting pores than in the prismatic structured soil. However, distinct differences between similar structured soils and replicate cores were observed by Anderson and Bouma (1977a) and Bouma and Wösten (1979), and even between replicates with similar volumetric water contents and hydraulic conductivities by Elrick and French (1966). The differences were attributed to soil heterogeneity caused by cracks, root channels, worm channels and disturbances caused by agricultural practices.

To minimize the effects of soil heterogeneity, Ritchie et al. (1972) suggested the use of large cylindrical soil cores with the diameter larger than the length, in order to reduce the effects of discontinuities in conducting pores caused by the core walls. Although only small differences in hydraulic conductivity were observed in cores of different lengths, breakthrough curves for chloride shown by Kissel et al. (1973) were significantly different. More pronounced preferential flow occurred through the shorter core (64 mm long) than the longer core (600 mm long).

Observed breakthrough curves for unsaturated solute flow through undisturbed soil cores have been less variable than for saturated cores. When soil is unsaturated large conducting pores are drained, and the movement of water and solutes is through the smaller pores, with a narrower size range. The movement is thus slower and more uniform. At a soil pressure potential of about -300 mm (-30 mbar), Elrick and French (1966) found chloride movement occurred relatively uniformly and results for replicate cores were in close agreement, in contrast to the saturated flow data referred to above.

Using the same soil cores as in the previously described saturated flow experiments (Anderson and Bouma, 1977a), Anderson and Bouma (1977b) observed the movement of chloride became less preferential when unsaturated flow was induced by a surface gypsum crust 5 mm thick. The corresponding pressure potentials were about -250 and -350 mm for blocky and prismatic structured soil respectively. At these pressure potentials, channels at least 0.12 mm in diameter and cracks at least 0.06 mm wide would be drained. These sizes are slightly less than the critical sizes for preferential flow proposed by Scotter (1978). However, the resulting breakthrough curves still indicated significant preferential flow, probably due partly to the experimental method used, as discussed in Section 3.1. Using a much higher pressure potential of -50 mm (at which channels greater than 0.5 mm in diameter would be drained), Bouma and Wösten (1979) still observed a significant shift to the right of the chloride breakthrough curves for saturated undisturbed cores.

Conducting pores in the undisturbed Tokomaru silt loam soil have been investigated using dye tracing techniques. Corker (1977) and McAuliffe (1978) applied dye solution to saturated soil cores after hydraulic conductivity measurements and observed worm channels, plant roots, and cracks were the major pathways for water movement. The hydraulic conductivity of these soil was greatly influenced by worm activities. McAuliffe (1978) observed changes in flow paths and hydraulic conductivity with time due to worm activity.

4.2 OBJECTIVES

The work described in this chapter aimed to study the saturated and unsaturated movement of anions through relatively large undisturbed soil cores. The effect of anion sorption on preferential flow under saturated conditions was investigated. Unsaturated flow was investigated to test whether the critical sizes of cylindrical channels and cracks for preferential flow proposed by Scotter (1978) were valid in natural soil cores. Improved techniques for unsaturated miscible displacement were aimed for, providing a uniform matric potential throughout a fairly large core, and avoiding the effects of porous plates at either end of the core.

4.3 MATERIALS AND METHODS

4.3.1 Experimental Set-up

Miscible displacement of anions was investigated using "undisturbed" soil cores under both saturated and unsaturated flow conditions. The equipment used is illustrated in Fig. 4.1. It was operated so that there was a steady state flux within the soil and the gravitational potential was the major driving force. Such conditions imply an hydraulic gradient close to unity and a near constant pressure potential throughout the soil during steady flow.

Cylindrical cores were obtained during winter 1979 from the top 150 mm of Tokomaru silt loam (Horizon A) in the non-tile drained area growing pasture in Dairy Farm No.4, Massey University, Palmerston North. The area is adjacent to the other experimental sites described in Sections 5.3 and 6.3. Cylindrical aluminium corers, 143 mm in inside

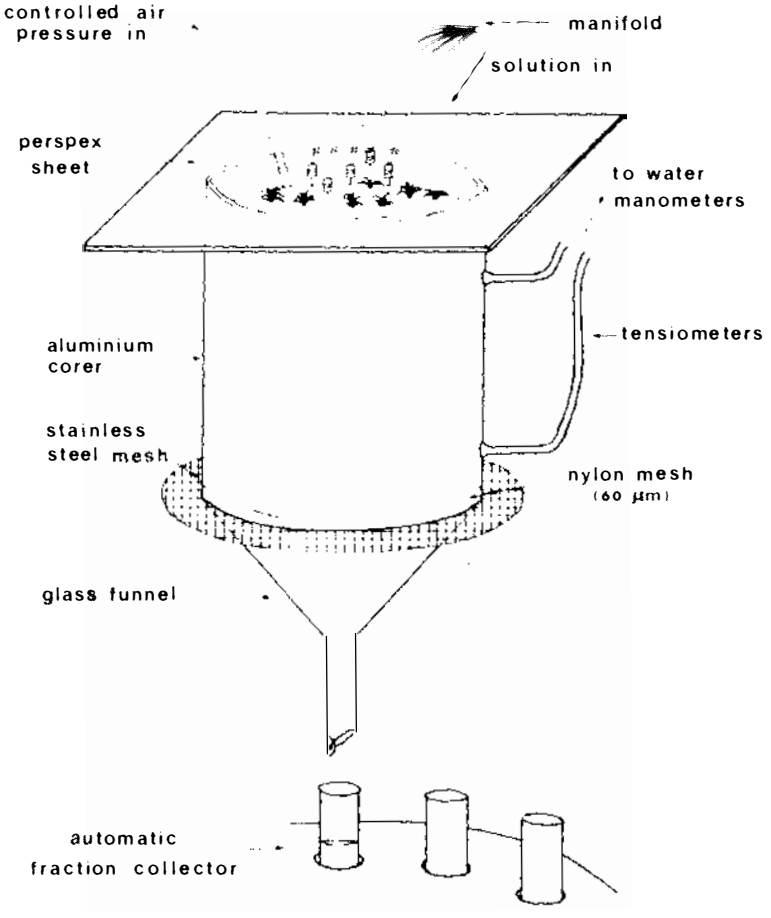

Fig. 4.1 General experimental set-up for miscible displacement study.

diameter and 170 mm long with a bevelled cutting edge, were forced into the soil to the desired depth. The wall thickness of the cores was 2.5 mm, giving an area ratio[1] of 0.07, and the corer could then be defined as a thin wall sampler (area ratio less than 0.2, Loveday, 1974). Soil water content when the cores were taken was approximately at field capacity. To minimise disturbance of soil structure, excavation of the soil cores was carefully made by removing the soil around each core to slightly deeper than the soil core depth and then breaking off the soil core. The excess soil was removed from the base of the core by gently chipping off the aggregates along the natural fracture planes when the soil was partly dry, to prevent smearing and so sealing off water conducting pores.

A fine nylon mesh with an effective pore diameter of 60 μm was used to seal the bottom of the cores. It was found more satisfactory than a porous plate, as it had a higher permeability and a considerably smaller pore volume. The pore volume of a fritted-glass plate of porosity 3 and 4.6 mm thick was found to be 0.14 ml/cm^2 which would be approximately 2% of the pore volume of the soil core used in this experiment. The use of such a plate would tend to mask the actual solute breakthrough from the soil core, especially if preferential flow occurs. The nylon mesh was placed across the column base and sealed to the edge of the core using silicone rubber sealant. Tensiometers with water manometers were installed and sealed into the soil core, 25 mm from both ends. Fritted glass filter sticks, 10 mm in diameter, were employed as the tensiometer sensors.

4.3.2 Saturated Flow Experiment

Soil columns were initially saturated with a solution containing 109 μg/ml potassium nitrate (KNO_3) and 100 μg/ml sodium azide, and then leached with the same solution which was supplied by a peristaltic pump. A head of approximately 10 mm was maintained on the soil surface. When the flux was constant and the hydraulic gradient was approximately unity as indicated by the tensiometers, the influent solution containing 100 μg/ml chloride as potassium chloride, 20 μg/ml phosphorus as potassium dihydrogen phosphate and 100 μg/ml sodium azide was applied to the soil as soon as the previous solution had disappeared from the soil surface.

---

[1] area ratio = $\frac{\text{area of annulus of displaced soil}}{\text{area of the sample at the cutting edge}}$

The effluent solution was collected at appropriate time intervals using an automatic fraction collector until approximately 2 pore volumes of the effluent were obtained. The effluent aliquots were analysed for chloride and phosphorus using a specific ion electrode and the Murphy and Riley method (1962), respectively.

Methylene blue dye solution (0.1% by weight aqueous solution) was subsequently applied to the soil core and leached for approximately 2 pore volumes. The saturated soil cores were then weighed to allow the pore volume to be determined later.

4.3.3 Unsaturated Flow Experiment

Desaturation of the soil core was then achieved by applying a positive air pressure to the closed chamber above the soil surface and reducing the inflow rate. The air pressure was maintained at 0.02 bar (200 ± 10 mm of water) and the corresponding pressure potentials inside the soil cores as indicated by the tensiometers were - 200 ± 10 mm of water at both ends. When a new steady state had been reached, the influent solution was changed to a solution containing 500 µg/ml of bromide as potassium bromide (KBr), 100 µg/ml sodium azide and 1% by weight rhodamine B dye. This solution was introduced into the soil cores through a manifold with 5 small outlets which allowed it to be fairly uniformly distributed over the soil surface. Effluent aliquots were collected and analysed for bromide until 2 pore volumes were obtained. No rhodamine B dye was visible in any of the aliquots.

At the conclusion of the experiment, the unsaturated soil cores were weighed and then oven-dried to constant mass at 105C. The saturated and unsaturated liquid-filled pore volumes were determined gravimetrically from the wet and dry mass and the density of water.

4.4 RESULTS AND DISCUSSION

4.4.1 Saturated Flow Experiment

Physical data for the duplicate soil cores are given in Table 4.1. Breakthrough curves for chloride and phosphorus obtained from the saturated soil cores are presented in Fig. 4.2. Both chloride and

Table 4.1 Physical data for saturated and unsaturated flow.

	Saturated Flow			Unsaturated Flow			
	K (10^{-5} m s^{-1})	θ	Time for one pore volume (hr)	K (10^{-7} m s^{-1})	θ	Time for one pore volume (hr)	E (10^{-8} m^2 s^{-1})
Core I	2.44	0.562	0.90	1.03	0.535	215	1.80
Core II	1.67	0.558	1.3	1.56	0.531	137	0.58

K = hydraulic conductivity

θ = volumetric water content

E = dispersion coefficient

phosphorus appeared in the effluent almost immediately after application to the soil surface of both cores, indicating very pronounced preferential movement of solutes occurring during the displacement process. The breakthrough curves obtained are similar to the ones obtained from small "undisturbed" soil cores (54 mm in diameter and 60 mm long) containing a worm channel by Kanchanasut et al. (1978) and from the artificial soil cores containing a channel or slit described in Chapter 3 (section 3.5) using the same soil. In Fig. 4.2, breakthrough curves for the duplicate cores are slightly different; C_e/C_i of chloride and phosphorus was 0.6 and 0.42 at 0.1 pore volume respectively for core I with an hydraulic conductivity of 2.44×10^{-5} m s^{-1}, while the corresponding values were 0.4 and 0.14 for core II with the slightly slower hydraulic conductivity of 1.67×10^{-5} m s^{-1}. The relatively large size soil cores used in this experiment provided a relatively narrow range of measured hydraulic conductivity values. The mean and standard error for 5 cores was $(2.42 \pm 0.5) \times 10^{-5}$ m s^{-1}. For smaller, wax coated cores 76 mm in diameter and length collected at the same site, Corker (1977) found lower, but more variable conductivity values. His values were $(1.5 \pm 1.14) \times 10^{-5}$ m s^{-1} for 10 core samples obtained from 0-75 mm depth and $(9.44 \pm 3.3) \times 10^{-6}$ m s^{-1} for 5 core samples obtained from 100-175 mm depth.

The differences in the measured hydraulic conductivity values could be due to differences in field water status and soil organism activities when core samples were taken, rather than the different core volumes. Also in small soil cores, compression during sampling is more likely.

Methylene blue dye, which was employed to show the dominant flow paths, revealed that the movement of solutes predominantly occurred in the large pores consisting of worm channels, decayed root channels, the space between roots and the soil matrix, and fracture planes. Cross-sections of one of the soil cores are shown in Fig. 4.3. Blue-stained worm channels are obvious, particularly near the soil surface. Blue-stained fracture planes, roots and worm channels were observed in vertical sections of the soil core (Fig. 4.4). The evidence from Fig. 4.4 indicates that the movement occurred in large interconnected pores of all types. Worm channels did not necessarily have to reach the surface to be effective in conducting water and solutes, provided

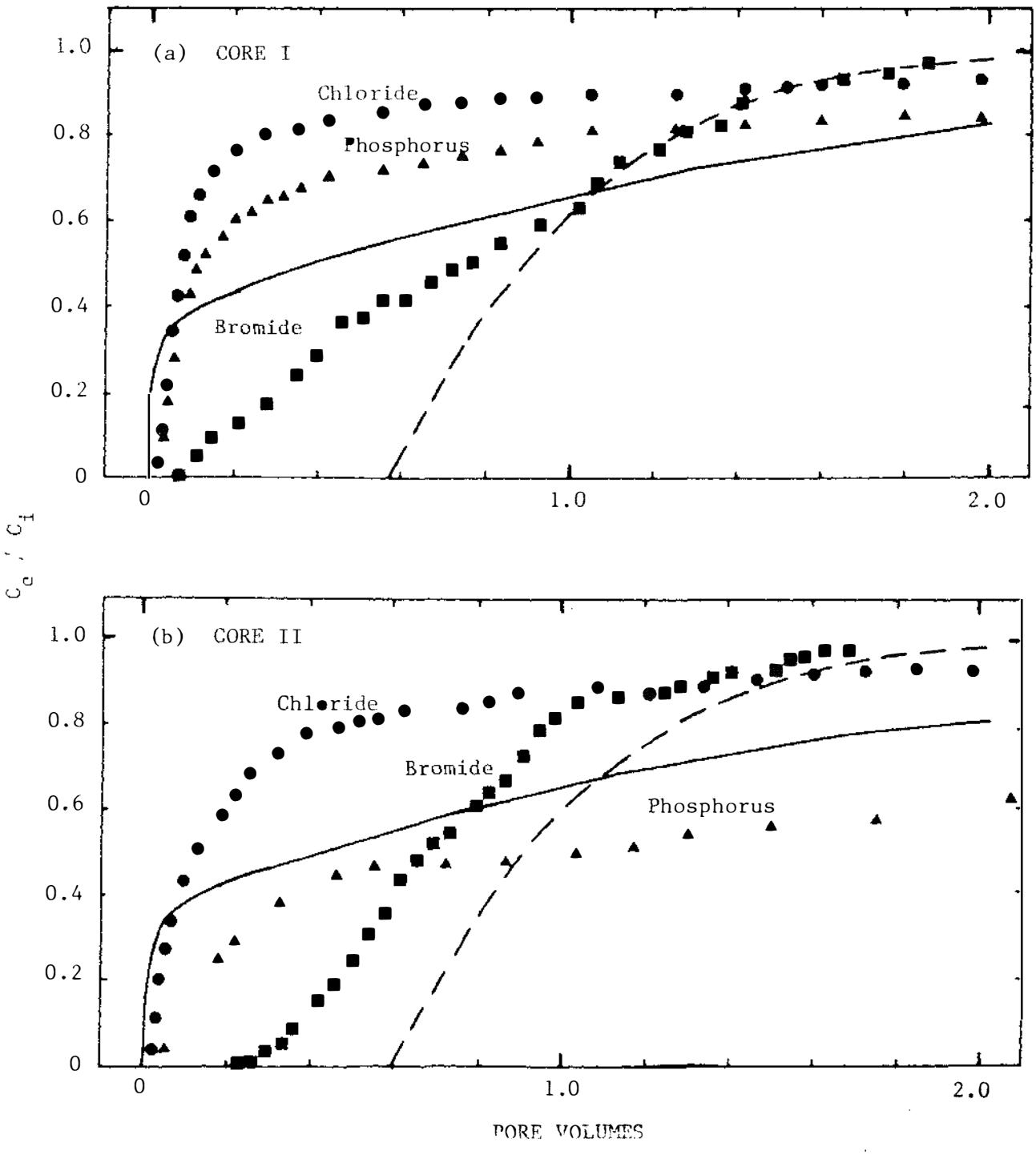

Fig. 4.2 Breakthrough data for 'undisturbed' soil cores: chloride (●) and phosphorus (▲) for saturated flow, and bromide (■) for unsaturated flow at -200 mm pressure potential. Calculated breakthrough curves for bromide are presented, assuming channel diameter of 0.15 mm (——) and 0.1 mm (— —). Duplicate cores (a) and (b).

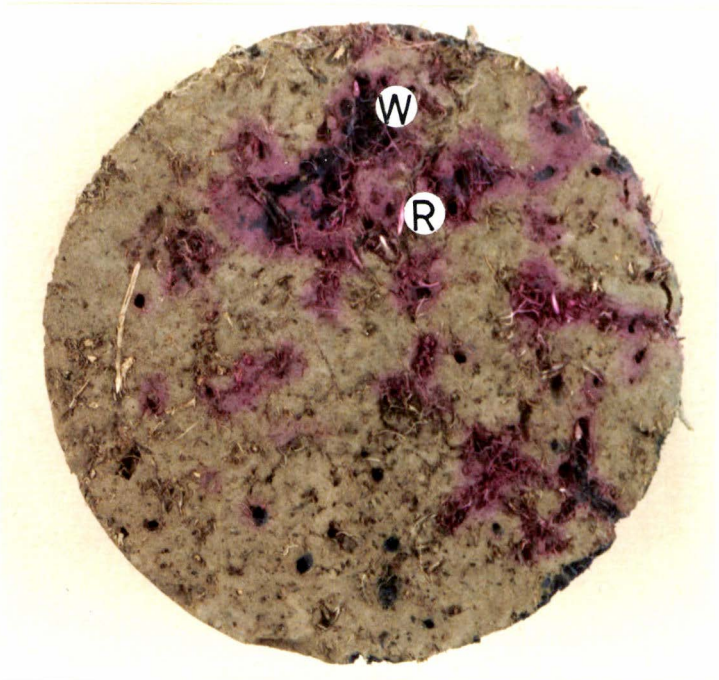

(a)

20 mm below the soil surface

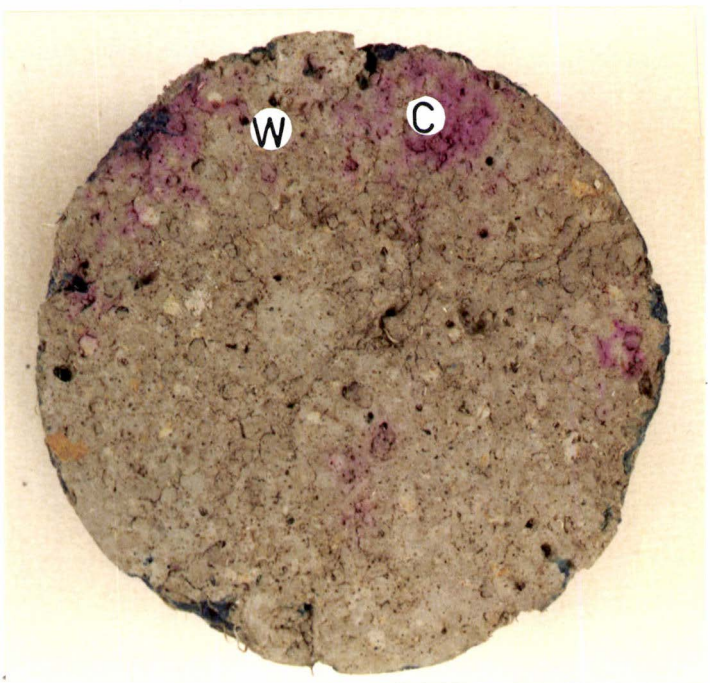

(b)

20 mm above the bottom end of the soil core

Fig. 4.3 Cross sections 143 mm in diameter of a soil core. The blue colour indicates the dominant pathways for saturated flow and the pink colour indicates the dominant pathways for unsaturated flow at -200 mm pressure potential. W = worm channel, R = root channel, C = planar crack.

(a)

20 mm below
the soil surface

20 mm

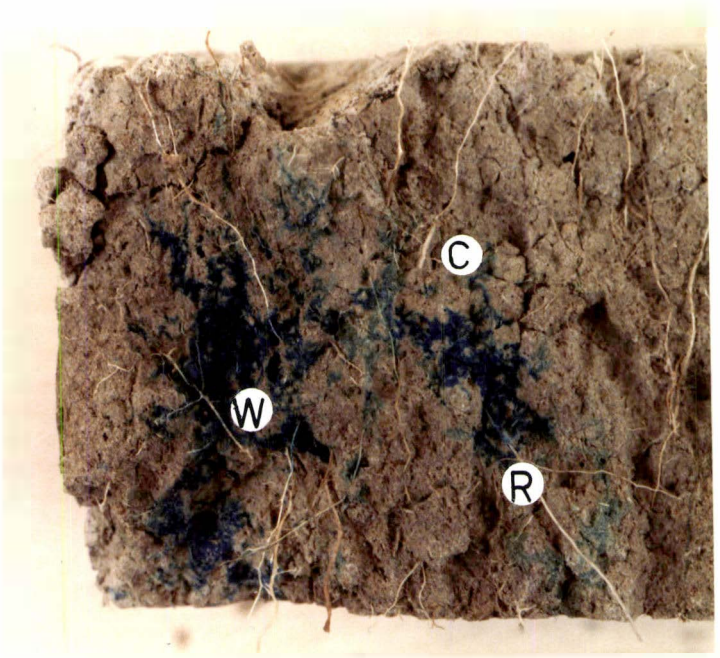

(b)

20 mm above the
bottom end of
the soil core

20 mm

Fig. 4.4 Vertical sections of a soil core. The blue colour indicates the dominant pathways of saturated flow and the pink colour indicates the dominant pathways of unsaturated flow at -200 mm pressure potential.
W = worm channel, R = root channel, C = planar crack.

they were connected with other somewhat smaller conducting channels, planar cracks and/or roots which did reach the surface. The size of worm channels varied; the largest size observed near the soil surface was 3 mm and near the bottom of the core was 2 mm. Only a few worm channels near the bottom end of the soil core were blue-stained.

If a single vertical cylindrical channel of 1 mm in diameter went from the soil surface to the bottom of the soil core, the hydraulic conductivity due to that channel alone calculated from the Hagen-Poiseuille equation (Appendix D) would have been 10 times greater than the value measured, so there were obviously no continuous vertical worm channels through the cores. Some conducting channels were cut off by the core-wall, causing blue staining on the side of the soil core, but there was no indication of solution leaking down between the soil and the corer. Due to the very strong adsorption of methylene blue by soil, the colour observed only shows the pathways of highly preferential solute movement. Only those channels large enough for the viscous flow of solute in them to be greater than the transient diffusion into the surrounding soil will be stained to any depth. The pathways of phosphorus movement, which is also very strongly adsorbed, would be expected to be similar to methylene blue. The movement of non-adsorbed ions such as chloride, would be expected to occur through a larger soil volume than that indicated by methylene blue staining.

4.4.2 Unsaturated Flow Experiment

Breakthrough data for bromide from the unsaturated soil cores at -200 mm pressure potential are shown in Fig. 4.2, along with the saturated flow data discussed above. Note that pore volumes were determined from the liquid-filled pore volumes. The unsaturated hydraulic conductivities and volumetric water contents for both cores are given in Table 4.1. The -200 mm pressure potential in the soil cores implies that cylindrical channels of minimum diameter 0.15 mm, and planar cracks of minimum width 0.07 mm, would be air-filled and so ineffective in conducting water or solutes. The applied bromide solution would have to move through pores of smaller size. Scotter (1978), assuming a very idealized soil pore geometry, concluded that solute movement would not be preferential in soil when the pressure

potential is less than -200 mm (-0.02 bar). The experimental data are in fact similar to the classical "S-shaped"breakthrough curves, often reported in the literature (e.g. Nielsen and Biggar, 1962) and are quite different to the saturated breakthrough curves for the same soil cores. However, the bromide appeared in the effluent earlier than expected from "classical theory", the relative concentration reaching 0.5 after 0.8 and 0.7 pore volume had flowed through the duplicate cores, rather than after one pore volume. The possible reasons for this are discussed later.

Rhodamine B dye was used to mark the preferential pathways in the unsaturated soil cores. Fig. 4.3 shows the pink colour is concentrated in certain areas of the soil core cross-section, suggesting some preferential movement. However the breakthrough data indicate movement of the bromide solution took place over a much wider area than that showing the pink colour of rhodamine B dye, which is a very strongly adsorbed substance. The method of solution application on the natural soil surface, using a manifold of 5 point sources, may have been a factor inducing the non-uniformity of pink colour near the soil surface. However, both Fig. 4.3a and Fig. 4.4a show the pink colour around the blue-walled larger channels, suggesting the movement of rhodamine B dye occurred to some extent in the same pathways as methylene blue. Such flow may perhaps be explained by the effect of short pore constrictions or pore necks near the surface, which allow some of the larger pores to remain water-filled and so still able to conduct liquid in the unsaturated soil.

To investigate this possibility, the Hagen-Poiseuille equation was solved for gravity-induced flow of liquid through a vertical cylindrical channel with a short constriction at the top. For example, if a constriction 0.15 mm in diameter and 2 mm long is connected to a 3 mm in diameter channel 148 mm long, a flow rate of 9.17×10^{-8} m s^{-1} will result. This is 75 times greater than the flow conducted by a uniform channel 0.15 mm in diameter, however both channels would drain at a pressure potential of -200 mm. (Details are given in Appendix D). This type of pore geometry is probably one of the factors allowing some preferential solute movement to occur in unsaturated soil.

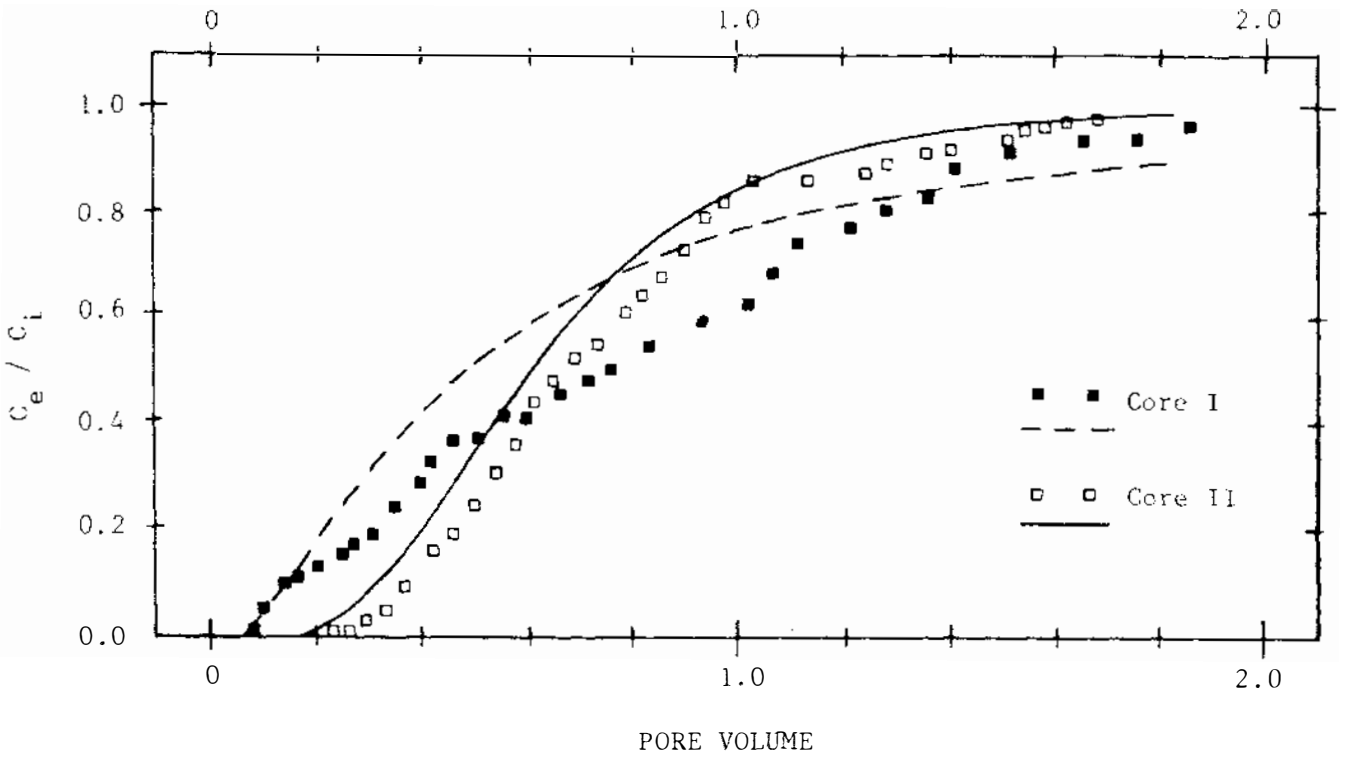

Fig. 4.5 Unsaturated breakthrough data for bromide (■ , □) and the corresponding predicted curves (- - -, ——) obtained from a convective-dispersive model.

Other possibilities that might cause unsaturated flow to occur in the adjacent pathways to saturated flow, are associations of large and small pores. Plant roots have been observed to grow and extend preferentially into the places where soil is less compact, such as in the old worm channels, and planar cracks (Scott-Russell, 1977), thus larger and smaller preferential channels may tend to occur together.

Anion exclusion might be another possible reason for early breakthrough. Bromide exclusion has been observed by Smith and David (1974) in soil columns with high cation exchange capacity. The soil properties of Tokomaru silt loam given in Appendix A do not suggest the soil would cause much anion exclusion however.

4.4.3 Computations

4.4.3.1 Convective-dispersive model

Unsaturated flow of bromide in the undisturbed soil cores was fitted to the convective-dispersive equation (1.1) using the method proposed by Rose and Passioura (1971a). This equation assumes uniform flow occurring through the soil and that the average pore-water velocity represents the flow velocity in the porous medium. An adjustment was made to account for displacement to the left of the breakthrough curves, as discussed earlier in Section 2.4.4.

The resulting predicted curves shown in Fig. 4.5 are in approximate agreement with the experimental data. The Brenner numbers obtained from solving equation (7) given by Rose and Passioura (1971) were 1.6 and 7.4 for core I and II respectively. However, their procedure is strictly valid only for Brenner numbers ranging from 16-640. The deviation from a straight line when the relative concentration of the effluent was plotted against ln (V/V_o) on probability paper was indicated by correlation coefficients of 0.973 and 0.997 for core I and core II respectively. Such deviations, particularly for core I, may indicate non-uniform flow occurring in the soil core. The experimental results discussed earlier in Section 4.4.2 suggested some preferential flow and/or anion exclusion occurred during displacement through the soil cores.

The calculated dispersion coefficients for both cores are given in Table 4.1. These values, however, are somewhat in error, for the reasons discussed above.

4.4.3.2 Viscous flow with lateral diffusion model

The computation method developed by Scotter (1978) for predicting the movement of solute through uniform vertical cylindrical channels was also employed. His theory and the CSMP computer programme used, are given in detail in Appendix C. The two channel diameters assumed were 0.15 and 0.1 mm, which would be drained at -200 and -300 mm pressure potential respectively. The molecular diffusion coefficient of bromide in soil was taken as $7.5 \times 10^{-10} m^2 s^{-1}$ (Robinson and Stokes, 1959) assuming a tortuosity-transmission factor of 0.4 (Scotter, 1978). The number of channels, and the spacing between them needed to give the measured unsaturated hydraulic conductivity values, are given in Table 4.2. A uniform channel spacing is assumed. The computed breakthrough curves are shown together with the experimental data in Fig. 4.2.

Table 4.2 Channel sizes assumed and the spacing between them.

Hydraulic conductivity ($m\ s^{-1}$)	Channel diameter (mm)	Spacing between channels (mm)	Number of channels $/m^2$
1.56×10^{-7}	0.1	7.0	6465
	0.15	15.8	1277
1.03×10^{-7}	0.1	8.6	4271
	0.15	19.3	844

The actual geometry of the pores responsible for most of the flow in the unsaturated soil is of course much more complex than that assumed in the simple model. Thus close agreement between the measured and the calculated breakthrough curves cannot be expected. However, the computed curves do show how sensitive dispersion is to small differences in the size of the conducting pores in soil with the same hydraulic conductivity. This makes the differences between the results for the duplicate cores more understandable.

For approximately the first pore volume, the computed curves envelope the experimental curves, but after that the experimental relative concentration values tend to be higher than the computed ones. This could be due in part at least to the non-uniform channel diameter referred to earlier and the random, or even clumped, distribution of the larger conducting channels in the soil, rather than the regular shaped channels and uniform distribution assumed in the computations. The results of a random or clumped distribution would be for certain sections of the cores to more quickly approach concentration equilibrium with the percolating solution, causing higher relative concentration values in the effluent at intermediate times than would be the case with a uniform spacing.

4.5 GENERAL DISCUSSION

The experimental set-up used in this study allowed saturated and unsaturated miscible displacement experiments to be conducted on the same core. Published laboratory studies of unsaturated miscible displacement have usually involved placing disturbed soil, or in a few cases a soil core, between two porous plates. The problems of contact between the soil and the plates and dispersion within the plates then arise. Here the use of gravity-induced flow, with no porous material on top of the core, and nylon mesh at the base, virtually eliminated these problems. Also the experimental set-up and the sampling procedure, minimized disturbance of pore continuity at both ends of the core. The precautions taken would seem to be necessary if realistic breakthrough data are to be obtained, particularly if any preferential flow occurs in soil.

4.6 CONCLUSIONS

1. Under saturated conditions, both chloride and phosphorus moved preferentially through 2.4 litre soil cores from the A horizon of a Fragiaqualf under permanent pasture.

2. Methylene blue dye, which was used to mark the pathways of saturated flow, indicated the movement predominantly occurred in the larger soil pores consisting of worm channels, decayed root channels, the spaces between roots and the soil matrix, and natural fracture

planes. Networks of interconnected pores of different types seemed to provide the flow paths, rather than flow down a single channel.

3. Under unsaturated conditions, when -0.02 bar (-200 mm of water) pressure potential was maintained within the soil cores during miscible displacement, bromide movement was more uniform, the breakthrough curves tending toward the classical "S-shape". However, the flow was still to some extent preferential.

4. The pathways of preferential movement in the unsaturated soil were visually indicated by rhodamine B dye. The rhodamine B dye staining around the large blue-walled channels indicated the preferential movement tended to occur along the same pathways as saturated flow. It is likely short constrictions near the top of larger channels keeps some channels from draining, and so they remain as preferential conducting pathways in unsaturated soil.

5. The colour observed from both dyes only shows the preferential pathways of water and solute movement, due to the strong adsorption of dye used by the soil.

6. Computed breakthrough curves for soil containing uniformly spaced, vertical, cylindrical channels 0.1 and 0.15 mm in diameter enveloped the experimental unsaturated miscible displacement data up to nearly one pore volume, and showed how sensitive the breakthrough curves are to small changes in channel size within this size range.

CHAPTER 5

WATER AND ANION MOVEMENT TO MOLE DRAINS

5.1 INTRODUCTION

Mole-tile drainage systems are widely used to remove excess water from the root zone in New Zealand (Hudson et al., 1962; Bowler, 1980). In the poorly drained Tokomaru silt loam, where a compact silt loam fragipan exists below 780 mm depth, mole-tile drains are often installed in the clay loam B horizon to alleviate waterlogging problems. Mole-tile drainage systems have often been found to remain effective over a fairly long period of time. Under favourable conditions, they may remain operative for 10 to 25 years under pasture (Bowler, 1980). Mole drainage can greatly enhance the hydraulic conductivity of the B horizon, as Scotter et al. (1979a) showed. They reported peak drainage flows equivalent to 25 mm/day water movement to the soil, while *in situ* saturated hydraulic conductivity measurements in the B horizon at adjacent undrained sites ranged from 0.02 to 0.6 mm/day.

Unlike the flow net of drainage water to the drain pipe in a sand tank or in homogeneous soil, in which the streamlines are regular and perpendicular to equipotential lines (Kirkham and Powers, 1972), the flow of water to mole drains is believed to occur mostly along the cracks caused by the passage of the mole plough (Hudson et al., 1962; Bowler, 1980). Bowler (1980) has described the action of the mole plough in the soil. When the plough is being pulled through the soil, its movement is accompanied by heaving, which causes cracking extending to about 0.3 m each side of the plough and may reach the surface in pasture land. The cracks created by the plough occur largely along the natural planes of weakness. In the summer following the pulling, the cracks widen due to shrinkage, providing gaps for plant roots to penetrate deeper into the soil profile. Scotter et al. (1979a) observed a lucerne (*Medicago sativa* L.) root, and the other fine roots, growing in the mole-drains and where the slit left by the mole plough had been 18 months earlier in Tokomaru silt loam. As such roots shrink and decay, the remaining cavities could provide pathways for rapid water movement into the mole drains. Scotter et al. (1979a) also refer briefly to dye movement studies indicating preferential flow through pathways directly above the mole drains, often involving structural cracks, and worm and root channels. The disturbance caused by the mole plough appeared to allow roots, humus and worms to better penetrate the B horizon above the mole.

Mole-tile discharge as a percentage of rainfall is greatest when the soil above the drains is at field capacity or wetter prior to a rainfall event. However, even if the soil is initially quite dry, the drains can still sometimes flow. Bowler (1980) pointed out that the accentuated soil cracking associated with moling and summer drying could cause flow to occur under a rainfall intensity of 30 mm in 8 hours, while an intensity of 10 mm in 10-12 hours would cause flow only when the soil above the moles had rewet to field capacity.

Significant losses of applied fertilizer in the mole-tile drainage from Tokomaru silt loam soil have been reported by Turner et al. (1976), Sharpley and Syers (1979a) and Gandar and Gregg (1979). No fixed pattern of nitrogen and phosphorus leaching was observed by Turner et al. (1976), but a seasonal trend in the concentration of the drainage water appeared, with the highest concentration in the early drainage events, then rapidly decreasing concentration during successive flow events. The high concentrations observed in early drainage events were probably due to the rapid leaching of nutrients already present in or adjacent to the conducting channels. However, the results quoted were obtained by intermittent sampling of the discharge from 0.125 ha plots. Nearby, Sharpley and Syers (1979a) found mole-tile drains contributed 27% of the stream flow in a small catchment, and 22% of the dissolved inorganic phosphate in the stream flow.

Published research related to mole-tile drainage has reported water and nutrient yields from areas of at least 1000 m^2 (Macgregor et al., 1975; Rennes et al., 1976; Turner et al., 1976; Sharpley and Syers, 1979a; Gandar and Gregg, 1979). However no one appears to have studied the behaviour of an individual mole drain, and the soil it is in, on a smaller scale, or to have looked in detail at the actual flow paths in the soil from the surface to the mole. To understand the large scale results, smaller scale investigation is necessary and such an investigation is described in this Chapter.

5.2 OBJECTIVES

The experiment described aimed to study the flow paths in a mole-tile drained soil profile, and the movement of sorbed and non-sorbed anions from the soil surface to the drainage system.

5.3 MATERIALS AND METHODS

The field experiment was conducted in the area near to where the undisturbed soil cores described in Chapter 4 were collected (Section 4.3). Tokomaru silt loam is classified as an Aeric Fragiaqualf (Soil Survey Staff, 1975) and as a gleyed yellow-grey earth (New Zealand Soil Bureau Staff, 1963). The soil profile has been described in detail by Pollok (1975), and his description is given in Appendix A. At the site, the soil consists of a silt loam A horizon extending to approximately 250 mm, a clay loam B horizon to 780 mm, then a very compact silt loam fragipan C horizon extending to 1100 mm and underlain by a somewhat less compact silt loam (Scotter et al., 1979a). The experimental area was growing ryegrass-white clover pasture and had been mole-tile drained approximately 6 years prior to the commencement of this study. The mole drains were pulled at 2 m spacing in the B horizon at approximately 450 mm depth on a gradient of 1%. The tile drains were installed perpendicular to the moles at approximately 750 mm depth on a minimum gradient of 0.4%.

The general experimental set-up for this study is illustrated in Fig. 5.1. An infiltrometer ring, 380 mm in diameter, was installed to approximately 100 mm depth above a mole line. The influent solution was ponded in the ring, and the effluent, which percolated through the soil profile, was collected from the mole in a pit located adjacent to the infiltrometer ring.

The experiment was carried during late autumn and winter when the soil was at 'field capacity'. It was conducted in a similar manner to the laboratory experiment using saturated soil columns. The influent solution, containing 100 µg/ml chloride as potassium chloride and 40 µg/ml phosphorus as potassium dihydrogen phosphate, was ponded in the infiltrometer ring at a nearly constant head of 20-25 mm above the soil surface. The effluent solution was collected manually at 0.5 or

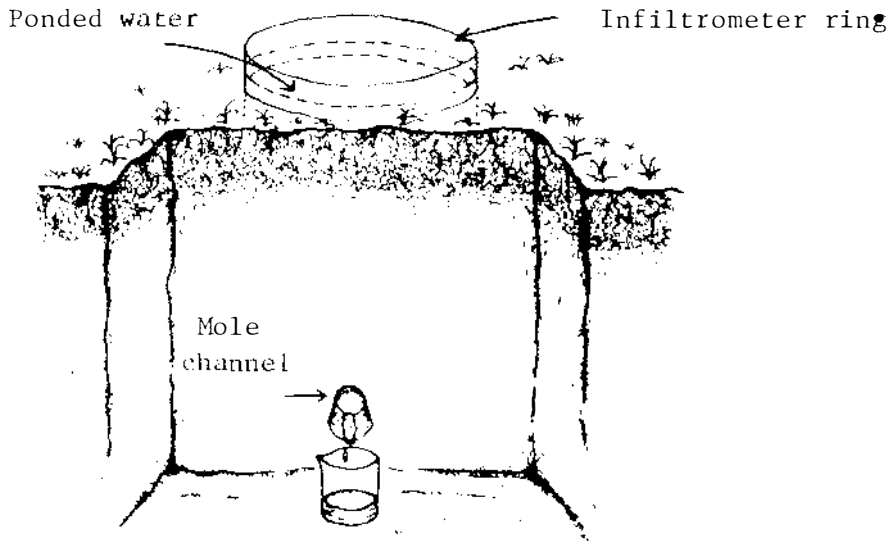

Fig. 5.1 Experimental set-up for the miscible displacement experiment above the mole drain. The infiltrometer ring was 380 mm in diameter and the mole channel located at 400 mm depth.

1 minute time intervals until approximately one pore volume had passed through the soil above the mole. To prevent drainage from sources other than that applied to the infiltrometer ring, the experiment was carried out on a fine day when no natural mole-tile drainage was occurring. The soil surrounding infiltrometer ring was wet at the start of the experiment to minimize lateral flow. Water was then ponded in the ring until the infiltration rate and the mole drain flow were nearly equal. At this stage, water movement was assumed to occur within the soil cylinder below the ring to the mole depth, from which the pore volume was estimated. The ponded water was then replaced with the chloride and phosphorus solution.

At the end of the experiment, approximately one pore volume of 0.1% methylene blue dye solution was applied to the soil. The soil was allowed to drain for 2 days, then the profile was exposed and the dye movement pathways were observed.

5.4 RESULTS AND DISCUSSION

Breakthrough data showing the chloride and phosphorus concentration in the effluent from the mole channel are presented in Fig. 5.2. Both chloride and phosphorus appeared in the mole effluent almost immediately after application to the soil surface, indicating highly pronounced preferential flow occurred in the saturated soil above the mole. During Experiment I, which was conducted in late autumn (15 April, 1979), the steady state infiltration rate was 6.75×10^{-5} m s^{-1}. The effluent to influent solution ratio (C_e/C_i) of both anions rose quickly to approximately 0.8 after only 5 minutes or 0.1 pore volumes of the solution had been applied to the soil, but subsequently continued to rise only very slowly.

Both chloride and phosphorus appeared later in absolute time when the experiment was repeated at an adjacent site at the end of winter (28 August, 1979) (Experiment II). The infiltrability observed (6.39×10^{-6} m s^{-1}) was an order of magnitude less than in Experiment I. Preferential movement of both anions was however still very pronounced. C_e/C_i reached 0.49 for chloride and 0.27 for phosphorus within 62 minutes or 0.1 pore volume of the application of the ions to the surface. In both experiments, the concentration of phosphorus increased more slowly

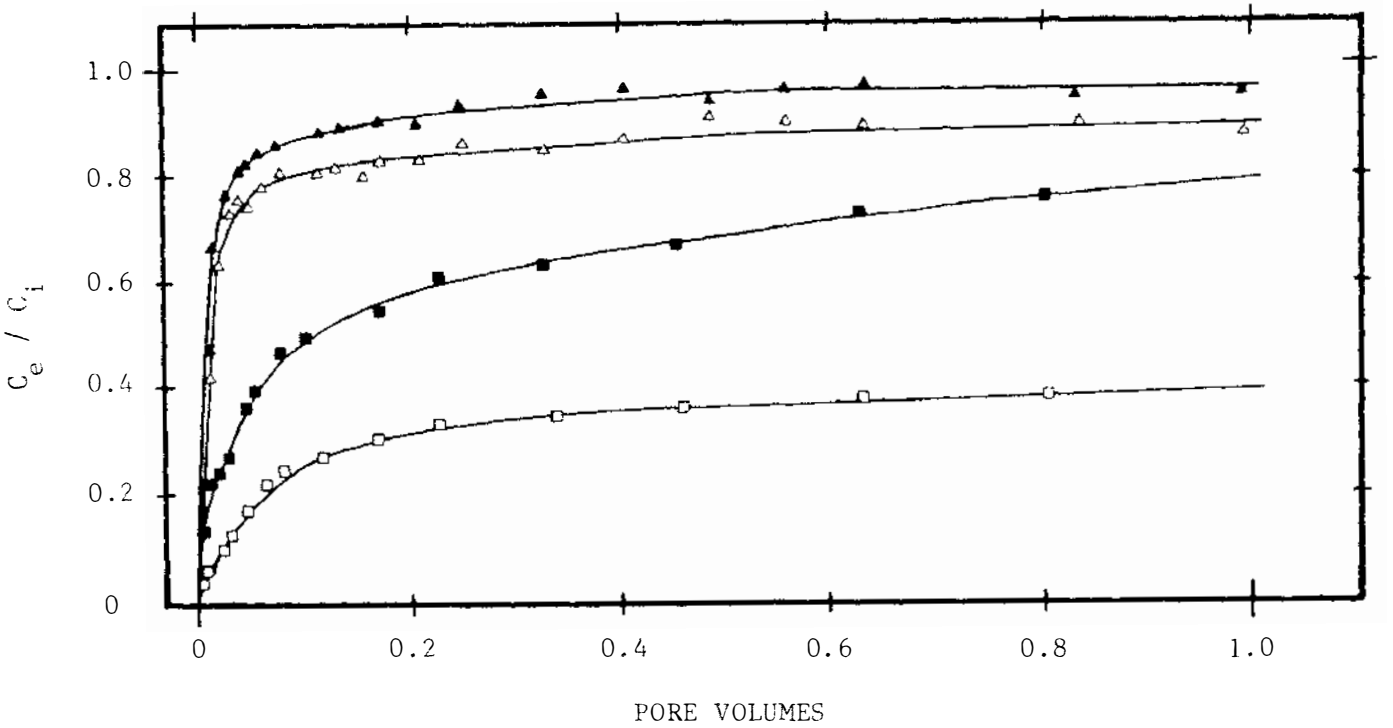

Fig. 5.2 Breakthrough data for saturated soil profile above the mole drain; chloride (▲—▲) and phosphorus (△—△) for Experiment I with infiltration rate of 6.75×10^{-5} m s^{-1}, and chloride (■—■) and phosphorus (□—□) for Experiment II with infiltration rate of 6.67×10^{-6} m s^{-1}. The curves have been visually fitted to the data points. Times corresponding to one pore volume were 51 minutes and 9.5 hours for Experiment I and II, respectively. C_e/C_i is the ratio of effluent to influent concentration.

than chloride. The curves shown are similar to those obtained from the soil columns containing artificial channels or planar cracks (Section 4.4), the saturated soil cores (Section 4.4.1), and those predicted by the simple preferential flow theory proposed by Scotter (1978) (Appendix C.1).

It was not possible to quantify the size and number of the conducting channels from the breakthrough data. However, it can be inferred that relatively large continuous channels were responsible for most of the flow in experiment I, while smaller or fewer large channels were effective during experiment II, which showed less pronounced preferential flow.

The application of methylene blue to the soil after experiment II showed that the dye solution moved into the soil through large pores, such as gaps between roots and the surrounding soil, decayed root channels, worm channels, soil cracks and the incipient fracture planes between structural units. Grass root channels and worm channels appeared to be the major pathways for water intake into the soil profile. Relatively fewer blue-stained roots and worm channels were observed in the subsurface horizon than in the surface horizon. Fig. 5.3 shows some of the preferential pathways observed in the soil profile. Some conducting worm channels extended from the soil surface nearly to mole depth. Grass roots were very extensive particularly near the soil surface, and extended down to mole depth and beyond. Some roots were found penetrating the mole cavity itself (Fig. 5.4), and also in old worm channels. The methylene blue-staining tended to be concentrated in the area directly above the mole where the soil had been disturbed at the time the mole was pulled (Figs.5.4a and b). This was also observed in an earlier pilot study described by Scotter et al. (1979).

Staining of large fracture planes was also observed quite commonly. Fig. 5.5a shows such a blue stained natural fracture plane with associated plant roots and worm channels. The presence of preferential root growth between soil structural units would provide continuous channels for rapid water movement as discussed earlier. Pollok (1975) and Soil Survey Staff (1975) observed extensive root growth between the structural soil units in the fragipan, and suggested also that the cavities left by these

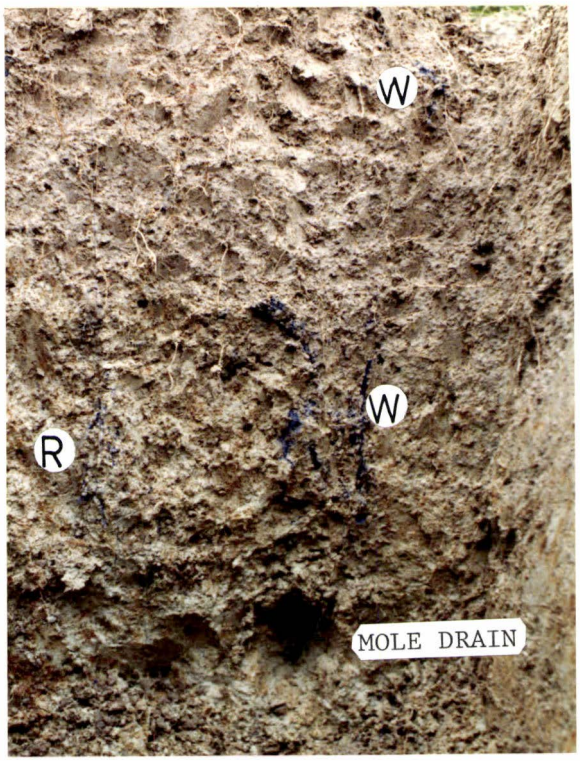

(a)

Preferential pathways in the soil profile directly above the mole.

100 mm

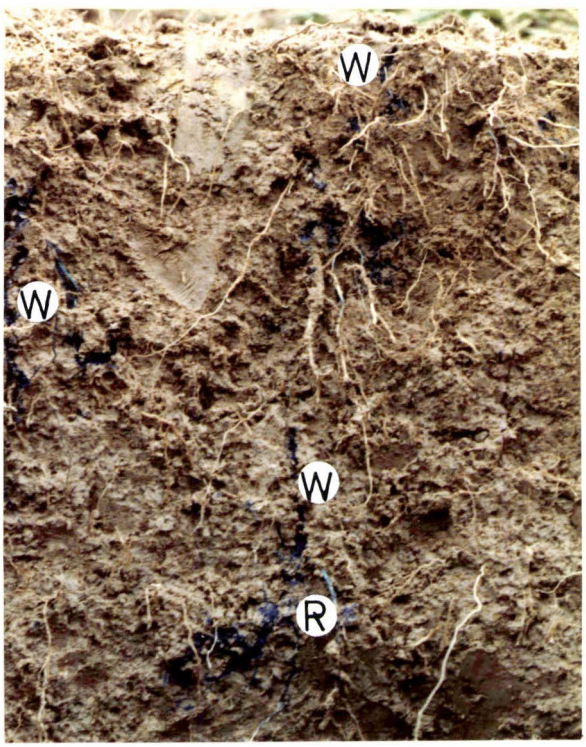

(b)

Conducting worm channels and root channels.

50 mm

Fig. 5.3 Preferential pathways observed in the soil profile above the mole drain, as indicated by methylene blue staining. W = worm channel, R = root channel.

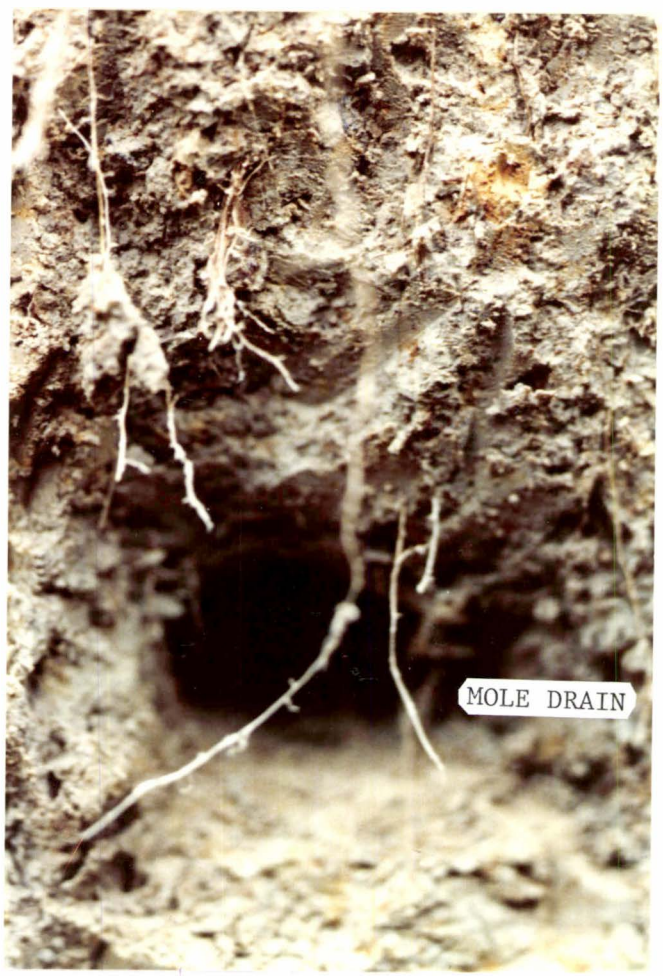

Fig. 5.4 Mole drain at 400 mm profile depth in Tokomaru silt loam soil in Dairy Farm No.4 near Massey University. Grass roots penetrating into the mole were commonly observed.

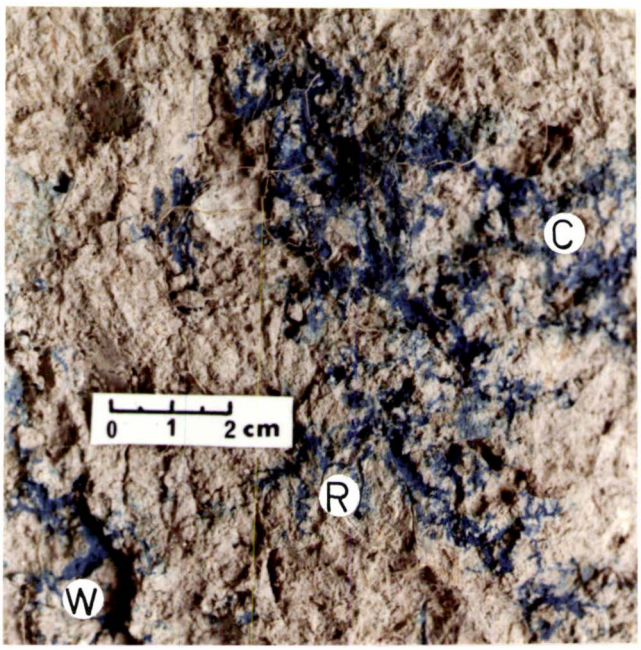

(a)

Vertical view of conducting channels in a natural fracture plane.

20 mm

(b)

Cross-section view of conducting worm channels and the interconnected cracks.

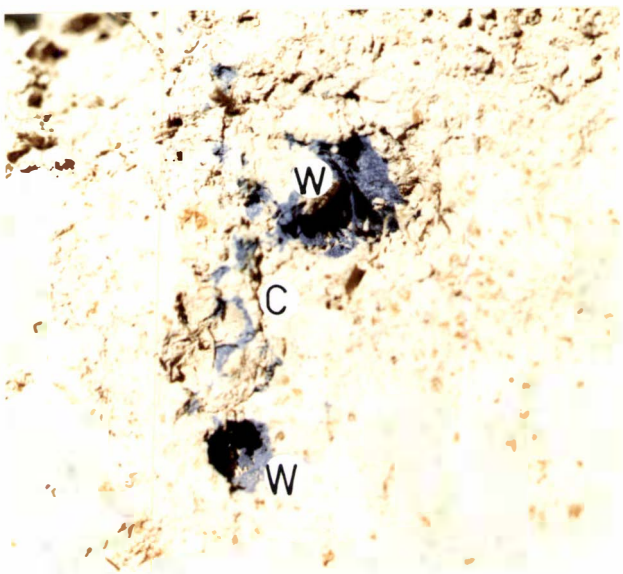

20 mm

Fig. 5.5 Preferential pathways observed in the soil profile.
W = worm channel, R = root channel, C = planar crack.

roots would allow some water to move through the fragipan. Preferential flow through a combination of conducting worm channels and cracks is shown in Fig. 5.5b.

The conducting pores in the soil profile were usually a combination of grass root channels with worm channels (Figs.5.3a and b), worm channels with cracks (Fig. 5.5b) or a combination of root channels, worm channels and cracks (Fig. 5.5a). The size and frequency of these channels presumably vary markedly with season, due to root and worm activity and structural cracking induced by drying (Corker, 1977; Bowler, 1980). The largest size of the conducting worm channel observed during this experiment was approximately 3 mm in diameter. The width of soil cracks was not measured, but they were probably wider in autumn when experiment I was conducted, due to shrinkage during summer of clay minerals and organic matter.

The results of this experiment would not be necessarily apply under natural rainfall. The hydraulic conductivities observed (243 and 23 mm/hour) were considerably higher than common rainfall intensities. Thus, with effective mole-tile drainage, surface ponding is only observed at this site after sustained, heavy rain. However, the results support and explain the observation made by Macgregor and Gregg on the same site, and reported by Kanchanasut et al. (1978). MacGregor found urea and coliforms in the mole-tile drainage less than 2 hours after the spray application of dairy-shed waste at 10 mm hr^{-1} in early spring, when the soil was at field capacity. Gregg found that when superphosphate was applied to the soil surface, the drainage discharge caused by 10 mm of rainfall the following night showed a 10 fold increase (from 0.1 to 1.0 µg/ml) in dissolved inorganic phosphate over the preceding drainage event.

5.5 PRACTICAL IMPLICATIONS

The results presented in this chapter suggest a number of practical implications. Firstly, if any effluent is applied to mole-tile drained soils under ponded conditions, virtually untreated effluent can appear in the drainage system within minutes. Whether or not the pollutants in the effluent are capable of absorption by, or reaction with, the soil matrix is of little importance, as the effluent 'sees' very little of the soil in its travel along preferential pathways.

Secondly, the drainage from heavy rainfall inducing ponding may result in relatively little leaching from the soil matrix, as the preferential flow pattern will allow for little interaction with the soil solution. In general, drainage from light or intermittent rain could be expected to leach more nutrients than the same amount of drainage from heavy rain.

Thirdly, as biologically induced channels appear responsible for most of the flow to the mole drains, it would seem important to maintain good growth and a high worm population for moles to remain effective. Fewer roots and worm channels, as well as compaction due to wheel traffic, could be responsible for any observed deterioration in soil permeability and mole drain performance when a change in land use from pasture to cropping occurs. Conversely, improved pasture growth, however induced, is likely to enhance mole drain performance.

5.6 CONCLUSIONS

(1) The observed breakthrough data for chloride and phosphorus indicate that most of the solute movement occurred preferentially through the saturated soil profile to the mole drains. More pronounced preferential flow was observed in late autumn than in late winter.

(2) Dye tracer studies indicated the pathways which conducted water preferentially were mostly directly above the mole drain, close to where the mole blade had been earlier. The effective conducting pathways include worm channels, root channels, and soil cracks. Any particular preferential flow path from the soil surface to the mole was usually a combination of at least two of these pathways.

(3) Grass roots and worm channels were the most evident pathways near the soil surface, while soil cracks were the most evident conducting pathways in the B horizon.

CHAPTER 6

BROMIDE LEACHING UNDER FIELD CONDITIONS

6.1 INTRODUCTION

Results from Chapter 5 indicate that when water was ponded on pasture, it moved preferentially through the soil below and reached the mole drains in minutes, without displacing most of the solution in the soil matrix. Therefore, little leaching of surface applied fertilizer from that soil would be expected, while applied effluent would move straight through. However, with pasture and an effective mole drain system, ponding is unlikely under natural rainfall conditions. In contrast, localised ponding may occur under natural rainfall on a cultivated soil, due to slower saturated hydraulic conductivity induced by repeated tillage, which breaks down soil structure and biopores (such as worm channels and root channels) near the surface and also may induce a compacted layer or plough pan. This chapter looks at leaching of bromide under ponded conditions in mole-drained soil profiles under pasture and crops, and under natural rainfall in soil under pasture.

Fig. 6.1 illustrates various possible leaching patterns for a slug of solute initially at the soil surface. Curve (b) shows "piston flow" when there is only convection, with negligible dispersion. If dispersion occurs, "classical" theory predicts a distribution shown as curve (d) on the Figure, which is the solution of equation (1.5). However several studies have shown that under natural rainfall the leaching of surface applied solutes can result in an asymmetrical vertical distribution of solutes with a "leading tail" (Olsen et al., 1970; Bosewell and Anderson, 1970; Cassel, 1971; Wild, 1972; Kissel et al., 1973; Burns, 1974; Wild and Babiker, 1976; Cameron et al., 1979) (Fig. 6.1, curve (c)). However leaching surface applied solutes in packed soil columns of sand or disturbed soil does result in a normal distribution, as would be expected from convective-dispersive theory (Biggar and Nielsen, 1962; Levin, 1964; Corey et al., 1967; Evans and Levin, 1969; Ghuma et al., 1975; Kirda et al., 1973) (Fig. 6.1, curve (d)). The peaks of concentration in natural soil profiles have often been observed at shallower depths than expected. For example, Wild and Babiker (1976) observed the peak of nitrate and chloride concentration at approximately half the expected depth, with tailing to at least 800 mm depth after 50 mm of water was applied (Fig. 6.1, curve (c)).

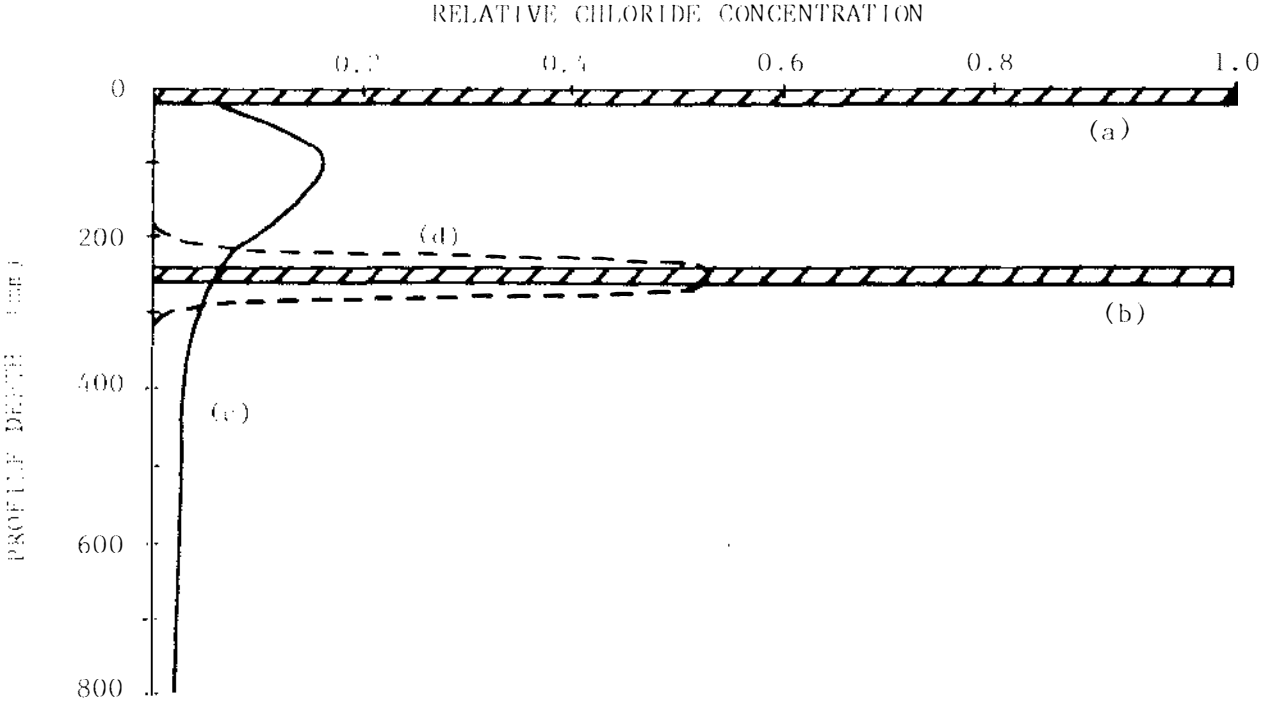

Fig. 6.1 Distribution of surface applied chloride after leaching with 50 mm of water:

(a) Initial distribution,

(b) Piston flow displacement,

(c) Observed field chloride displacement under intermittent irrigation of bare soil (Wild and Babiker, 1976),

(d) Calculated curve following convective-dispersive theory (Gardner, 1965; and equation (1.5)), assuming $D = 8.3 \times 10^{-9}$ m^2 s^{-1}, $C_0 = 1.0$, and $z_0 = 25$ mm. Field values for θ and v were used (0.2 and 2.2×10^{-7} m s^{-1} respectively, as found by Wild and Babiker, 1976).

Such asymmetrical distribution patterns of solutes in the soil profile suggest uneven downward movement of water, including preferential flow down large channels and cracks (Wild, 1972; Rao et al., 1974; Wild and Babiker, 1976; Cameron et al., 1979; Shuford et al., 1977). Similar asymmetrical distribution patterns with a "leading tail" have been obtained for chloride and tritiated water movement into soil, as reported by Quisenberry and Phillips (1976), Blake et al. (1973), and Quisenberry and Phillips (1978).

Many attempts have been made to predict solute movement in the soil profile using convective-dispersive theory, both under steady-state conditions (Gardner, 1965), and under unsteady-state conditions (Bresler and Hanks, 1969; Warrick et al., 1971; Shuford et al., 1977). Gardner (1965) used an equation derived by Day (1956) (equation 1.5) to predict nitrate leaching under natural rainfall, assuming a constant flow velocity and dispersion coefficient. He found the equation adequately described the leaching in a bare, uniform soil, using data published by Wetselaar (1962). However, Gardner perceptively commented that if the soil is inhomogeneous with a few channels carrying most of water downward, then it would be difficult to apply the convective-dispersive theory to a natural soil profile. Bresler and Hanks (1969) and Warrick et al. (1971) developed equations using a time dependent water flow velocity and dispersion coefficient to describe chloride movement in the soil profile. They observed solute moved deeper in the field than the theory predicted. The greater leaching depth was attributed to the influence of large pores, and cracks.

Biggar and Nielsen (1967) suggested that leaching soil at water contents below saturation could produce more efficient leaching, and thereby reduce the amount of water required to move undesirable salts from the soil profile. They also suggested that leaching by rainfall is often more efficient than by ponding. A number of field experiment have indicated that leaching by intermittent ponding or sprinkling is more effective than leaching by continuous ponding (Biggar and Nielsen, 1967; Miller et al., 1965; Talsma, 1967; Oster et al., 1972; Wilson et al., 1961). This is because under intermittent water application or light rainfall, leaching occurs in unsaturated soil at a slow rate which allows greater exchange by diffusion of solutes between regions of varying velocity. The differences in solute movement under saturated

and unsaturated flow conditions in the soil cores of Tokomaru silt loam have been discussed in Chapter 4. Desaturation of the soil to -200 mm pressure potential resulted in much more uniform miscible displacement than under saturated conditions when flow was very preferential. This suggests even a small change in pressure potential from 0 to -200 mm would lead to more efficient leaching.

6.2 OBJECTIVES

The experiment described in this chapter aimed to study the leaching patterns of bromide in mole-drained Tokomaru silt loam under field conditions, as affected by the methods of water application (i.e. continuous ponding and winter rainfall), and to interpret the results in terms of the experiments and theory already outlined.

6.3 MATERIALS AND METHODS

6.3.1 Experimental Design

Two water application methods were employed to leach bromide in the field. They were:

1. Continuous ponding
2. Natural rainfall.

6.3.1.1 Continuous ponding experiment

A double ring infiltrometer was employed in this experiment. An outer-ring, 780 mm in diameter, was used to provide a buffer area around the inner-ring which was 380 mm in diameter. Before ponding, 2 mm of 5000 µg/ml bromide solution as calcium bromide ($CaBr_2.H_2O$) was applied to the soil surface in both rings as a fine spray. The quantity of bromide solution used was arbitrarily chosen to be large enough to apply uniformly, but little enough so it remained initially near the soil surface. Five soil core samples were taken from the outer-ring to establish the initial bromide distribution, using an open-sided soil corer with a cutting diameter of 18 mm and an outside diameter of 25 mm. Then 50 mm of water was ponded in both inner and

outer rings and the infiltration rate was measured for a period of 1 hour. After the ponded water had disappeared from the soil surface, which took place after 20 to 44 hours, 13 soil cores were removed from inside the inner-ring. The cores were sectioned and bromide content determined, as described in Section 6.3.2.

The ponding experiment was conducted at two locations. The soil at both sites was Tokomaru silt loam, but different management practices had been imposed. One set of experiments was conducted in the same area as the anion movement to a mole experiment (Section 5.3), which was under permanent pasture. The other site was approximately 1 km away on the Tiritea Research Area, and had been cultivated and double-cropped continuously with winter oats, and summer maize or barley for five years. The experiments were conducted during winter of 1979 when the oat crop was approximately 300 mm high.

6.3.1.2 Natural rainfall experiment

This experiment was conducted also during winter of 1979, in the same area as the continuous ponding experiment under pasture. During this time evapotranspiration was small relative to the rainfall. The plot dimension were 1.6 x 5.0 m with a surrounding 0.2 m buffer area. The plot was divided into 6 sub-plots, giving randomly arranged duplicate subplots for sampling at three different times. Each subplot was 0.5 x 1.6 m and lay across the mole line.

The same depth and concentration of bromide solution as used in the previous experiment was applied. Application of solution to the soil surface was carefully made using a watering-can, so that bromide would be distributed as uniformly as possible on the plot and the surrounding buffer area. The initial bromide distribution was measured by soil sampling on the day after application. Twenty five soil cores were randomly removed from each of two sub-plots to 50 mm depth and sectioned. The bromide concentration in each segment was determined in the laboratory as described in Section 6.3.2.

The resulting bromide distribution in the soil profile was measured twice, after 46 mm, and again after 182 mm of rainfall in excess of evapotranspiration had infiltrated into the soil profile. Soil samples were taken in the manner described previously in Section 6.3.1.1.

Twenty cores were removed randomly from each of the two sub-plots to 300 and 600 mm depth, after 46 and 182 mm excess rainfall, respectively.

The excess rainfall was obtained as the difference between the rainfall and the evapotranspiration. Surface run-off in the flat mole-tile drained pasture area was assumed negligible. Evapotranspiration was estimated using Priestley and Taylor's method (1972) as described by Scotter et al. (1979b). The rainfall data and estimated evapotranspiration during the period of experimentation are presented in Fig. 6.2.

6.3.2 Bromide Retention by Soil

Bromide adsorption by soil was investigated using undisturbed soil cores. Cores 20 mm deep and 73 mm in diameter, taken from 0-20 mm and 100-120 mm profile depths, were used. The cores were placed in individual beakers and 8.4 ml (equivalent to 2 mm depth) of 5000 µg/ml bromide solution was dripped onto the surface of the soil uniformly. The samples were then left at room temperature in closed beakers for equilibration. After 18 hours, the samples were oven-dried, extracted with 500 ml distilled water and analysed for bromide.

6.3.3 Bromide Retention by Plants

To analyse bromide retention by the pasture, the aerial parts of all plants growing in both sub-plots were removed after the soil had been leached by 182 mm of excess rainfall, and analysed for bromide, as described in the following section.

6.3.4 Bromide Determination

6.3.4.1 Soil samples

Soil samples obtained from the field were weighed, oven-dried at 105C for 12-24 hours, weighed again, and the gravimetric water content determined. Bromide was then extracted from the oven-dried samples by distilled water with 2% by volume ISA (Ionic Strength Adjuster, 5 M sodium nitrate), using a soil: water ratio of approximately 1:5. Aggregates were broken down and the suspension left at room temperature

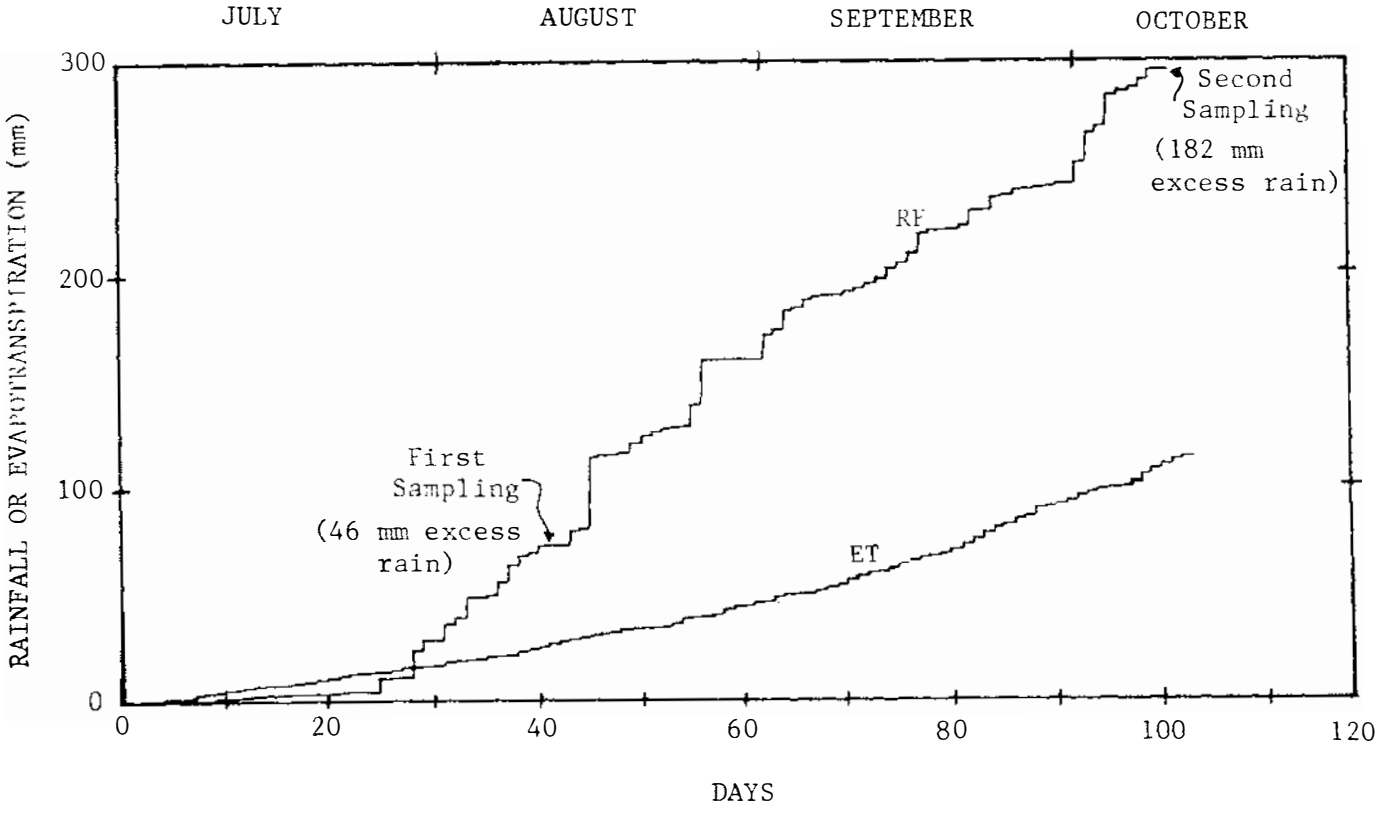

Fig. 6.2 Daily rainfall (RF) and evapotranspiration (ET) data during experiment in 1979.

for about 3 hours, with occasionally stirring. A bromide selective electrode (Orion Solid state bromide electrode) and reference electrode, connected to a meter (Orion Research Microprocessor Ionalyzer 901) were used to measure bromide concentration. The electrodes were immersed into the clear supernatant above the soil suspension. The reading was recorded when the number displayed had stabilised, usually after 1 minutes. A similar procedure for bromide extraction and measurement in soil was found satisfactorily by Abdalla and Lear (1975).

6.3.4.2 Plant tissues

To determine bromide in plant tissues, plant samples were oven-dried at 105C for 15 hours, then ground finely. One gram of dried plant sample was mixed with 50 ml distilled water containing 2% of ISA solution in a plastic container with a tightly fitted lid. The samples were thoroughly shaken and then placed in an ultrasonic bath for 10 minutes. The supernatant was then filtered and bromide determination was made on the filtrate using the bromide selective electrode. The methods of extraction and measurement were, in general, the same as those proposed by Abdalla and Lear (1975).

6.3.5 Leaching of Dye under Natural Rainfall

Rhodamine B dye was employed to mark the pathways of preferential movement under natural rainfall conditions, especially near the soil surface. Two rings, 143 mm in diameter, were pushed into the soil to 150 mm depth and then 5 mm of 1% rhodamine B dye in aqueous solution was ponded on the soil surface. Later, after receiving 65 mm of excess rainfall, the rings and soil enclosed were removed and brought to the laboratory. The soil cores were sectioned vertically at field moisture content and the dye pattern observed. This experiment was conducted during November and December when the soil was somewhat drier than field capacity most of the time. Most of the dye movement probably occurred on two individual days when 27 mm and 58 mm of rain fell. However, ponding probably did not occur, due to the relatively dry antecedent water contents.

6.3.6 Soil Bulk Density

Six soil cores, 50 mm long and 50 mm in diameter were taken from each profile depth to measure bulk density, using techniques described by Loveday (1974). Bulk densities at the two locations are shown in Fig. 6.3.

6.4 RESULTS AND DISCUSSION

6.4.1 Continuous Ponding Experiment

As already indicated, this experiment was conducted at two locations, one under permanent pasture and the other under cultivation. Fig. 6.4 shows the results of three replicates (a, b, and c) obtained from the location under pasture and Fig. 6.5 shows the results of 2 replicates (a and b) from the location under cultivation. Data presented in the figures are the mean values, the individual bromide concentration measurements are given in Appendix E.

6.4.1.1 Pre-leaching measurement

The bromide found in samples taken approximately 3 hours after application to the soil surface had moved deeper into the soil profile than expected. The 2 mm of bromide solution applied would have been uniformly distributed within the top 4 mm if the movement had occurred as piston flow, assuming a saturated volumetric water content of 0.5. While the concentration of bromide observed was highest in the top 10 mm, a significant amount of bromide was found below this depth. However nearly all of the bromide remained in the top 50 mm, as shown in Fig. 6.4 and Fig, 6.5. Table 6.1, giving the recovery percentages of applied bromide, indicates only small amounts of bromide being recovered below 50 mm depth. However, relatively low recovery percentages (averaging 46%) were observed at both locations. The possible reasons for this will be discussed later in Section 6.4.5.

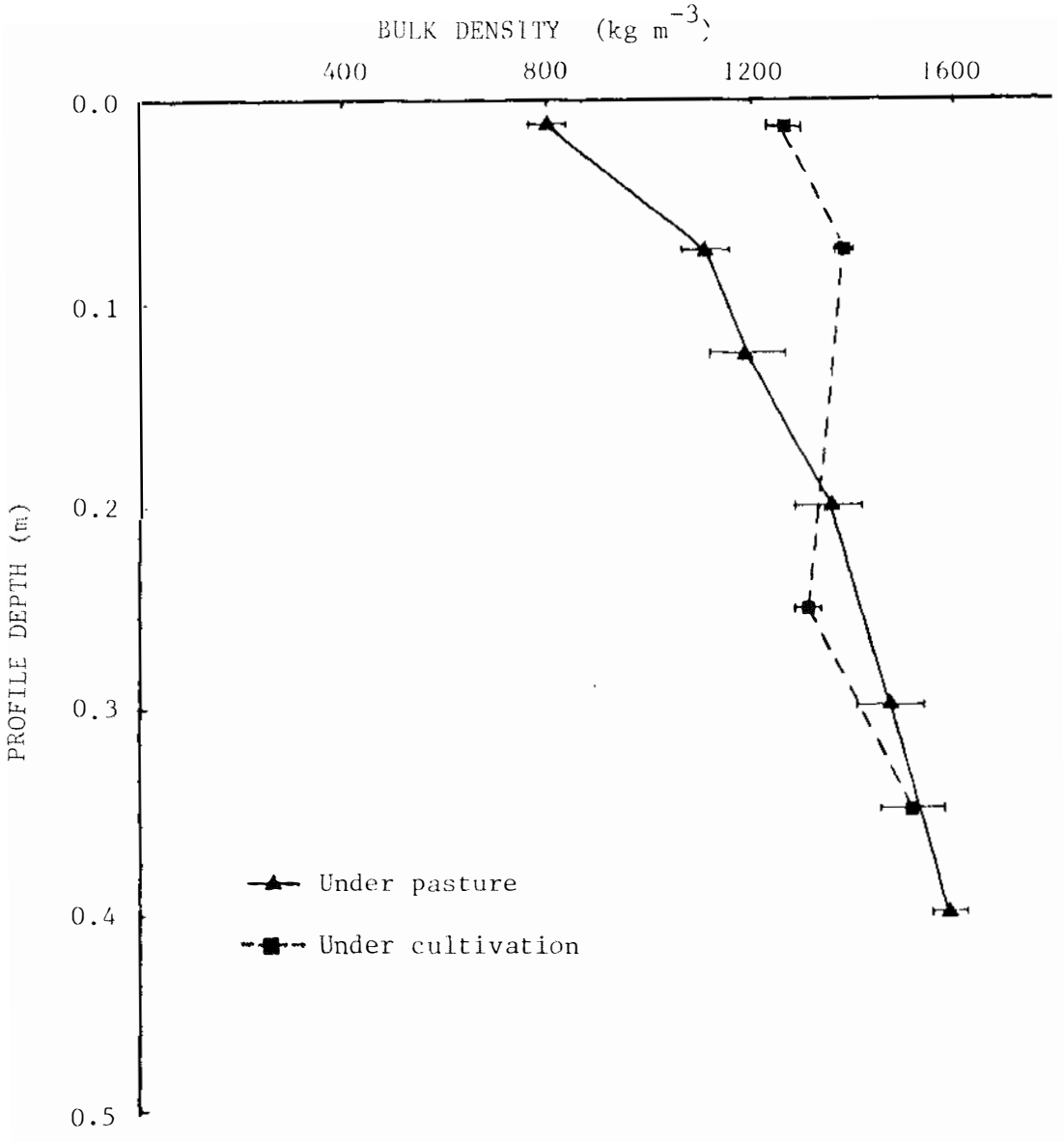

Fig. 6.3 Soil bulk density distribution in the soil profiles under pasture and cultivation (means and standard deviations of 6 replicates at each depth).

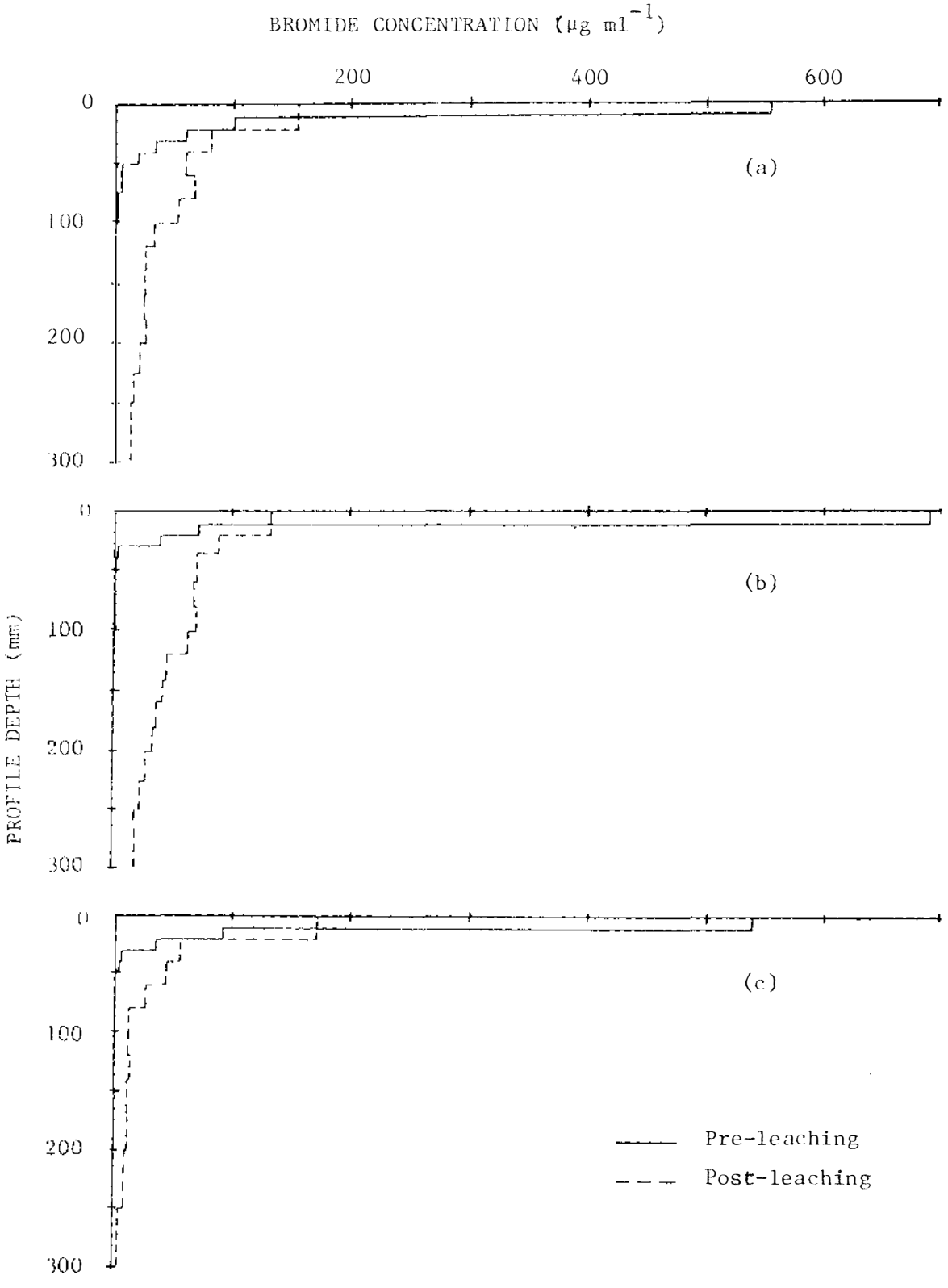

Fig. 6.4 Bromide distribution in the soil profile before and after ponding 50 mm of water on the soil surface in continuous pasture growing area. The concentration of bromide before ponding was the average of 5 core samples, and after ponding was the average of 13 core samples.

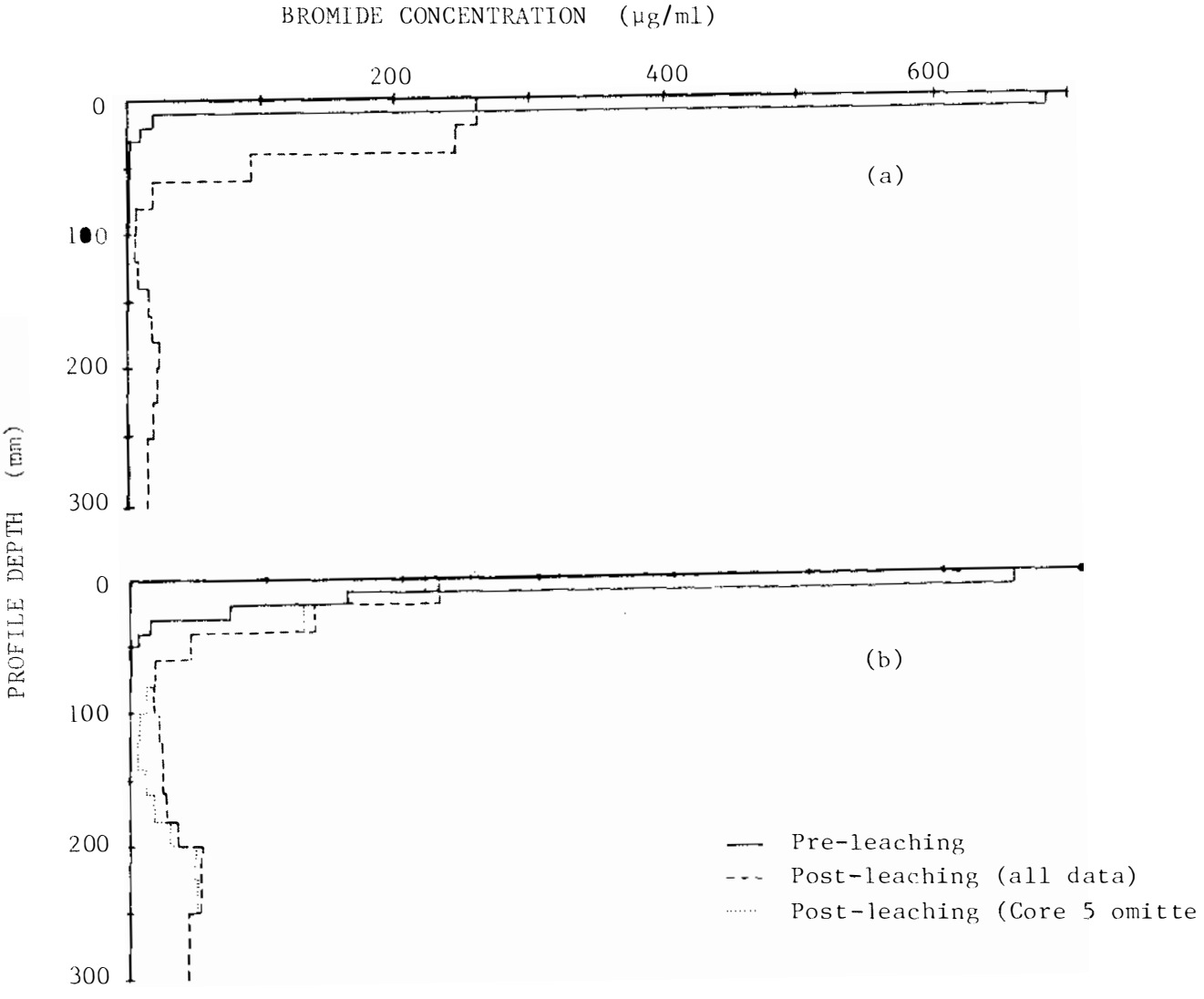

Fig. 6.5 Bromide distribution in the soil profile before and after ponding 50 mm of water on the soil surface in the cultivated area. Each measurement before ponding was the average of 5 core samples, and after ponding was the average of 13 core samples.

Table 6.1 Recovery percentages of applied bromide from the soil profiles.

Experiments	Depth (mm)			
	0-50	0-100	0-300	0-600
Surface ponding				
Under pasture:				
(a) Pre-leaching	48	49	-	-
Post-leaching	31	36	46	-
(b) Pre-leaching	43	43	-	-
Post-leaching	32	48	78	-
(c) Pre-leaching	40	40	-	-
Post-leaching	35	47	66	-
Under cultivation:				
(a) Pre-leaching	40	40	-	-
Post-leaching	62	66	84	-
(b) Pre-leaching	57	57	-	-
Post-leaching	41	87	86	-
Natural Rainfall				
Pre-leaching	31	-	-	-
After 46 mm excess rainfall	15	24	59	-
After 182 mm excess rainfall	10	13	-	41

6.4.1.2 Post-leaching measurements

The results obtained in Chapter 4 (Section 4.4.1) indicated that, under saturated flow, the movement of chloride and phosphorus occurred preferentially through undisturbed soil cores from 0-150 mm depth. Thus the movement of bromide in a natural soil profile of the same soil under ponded conditions might also be expected to be preferential. The results show ponding of 50 mm of water caused bromide to move to at least 300 mm depth in all experiments (Fig. 6.4 and 6.5). If leaching had occurred as piston flow, and a volumetric water content of 0.5 assumed, the ponded water would have leached the bromide as a narrow band to approximately 100 mm depth (Fig. 6.1, curve (b)). If leaching had occurred in the way described by the commonly used convective-dispersive equation (Gardner, 1965), the peak of bromide concentration would have appeared near 100 mm depth with a symmetrical "bell-shaped" concentration distribution (Fig. 6.1, curve (d)).

In contrast with the above however, a relatively high concentration of bromide was observed remaining near the soil surface at both locations. The concentration of bromide was at a maximum in the top 20 mm in all experiments. The distributions of bromide under pasture obtained from the 3 replicates shown in Fig. 6.4 are similar, with an approximately exponential decrease with depth.

The distribution of bromide concentration in the cultivated soil profile was somewhat different. Fig. 6.5 shows the concentration of bromide decreased with depth from the soil surface to a minimum at 100-140 mm depth, then increased with a second peak of concentration appearing at 200-250 mm depth. In the layer where the concentration of bromide was at minimum, the soil bulk density was 1400 kg m^{-3}, higher than the soil above and below (Fig. 6.3). This layer of compaction was probably a plough pan. A larger variation in bromide concentration was observed in replicate samples taken from this layer than from other depths in the profile (Appendix E). The concentration ranged from 1 to 54 µg/ml in one experiment and 0 to 238 µg/ml in the other experiment. Only a few core samples contained a high bromide concentration. This suggests the movement had occurred through only a few larger channels or cracks in the compacted layer, perhaps in

association with plant roots. The few high concentration samples significantly increased the mean values. Fig 6.5b shows the mean concentration distribution for all 13 cores, and for 12 cores omitting the one containing an unusually high bromide concentration (Core 5, Table E.2, Appendix E). The two curves are quite different at around the depth of the compacted layer. The presence or absence of such cores also affects the recovery percentage. If only one more core like Core 5 had been included in the sampling, the recovery percentages of bromide obtained would have increased 10%.

Plant roots tend to grow preferentially into cracks in compacted soil, as discussed by Scott-Russell (1977) and found by Pollok (1975) in the fragipan of this soil. So cracks, roots, and solute flow might be expected to occur together. The distribution of the conducting pores in the soil profile under cultivation is probably somewhat similar to the distribution of plant roots illustrated by Taylor and Ashcroft (1972) in their Fig. 11.9. Their photograph shows root growth was abundant above and below, but sparse within a compact plough layer.

The second peak of bromide distribution appeared below the compacted layer in both replicates. This peak indicates the movement of bromide below the compacted layer occurred relatively uniformly. It is similar in shape to the bell-shaped distribution predicted by "classical" theory shown as curve (d) in Fig. 6.1. It is probable that the soil immediately below the compacted layer had a higher saturated hydraulic conductivity than the compacted layer itself, thus unsaturated flow conditions would always prevail there. As indicated in Chapter 4, preferential flow is much reduced under unsaturated flow conditions.

The "field capacity" volumetric water contents prior to, and after, leaching, are presented in Fig. 6.6. Also shown is the total porosity, calculated from the bulk and particle density using particle density data for this soil given by Scotter et al. (1979a). A number of interesting features are evident. Firstly both the total and the air-filled porosity are much higher under pasture than under cultivation. Secondly, when sampled the compacted layer was close to saturation, indicating only a small volume of macropores (> 0.06 mm diameter)

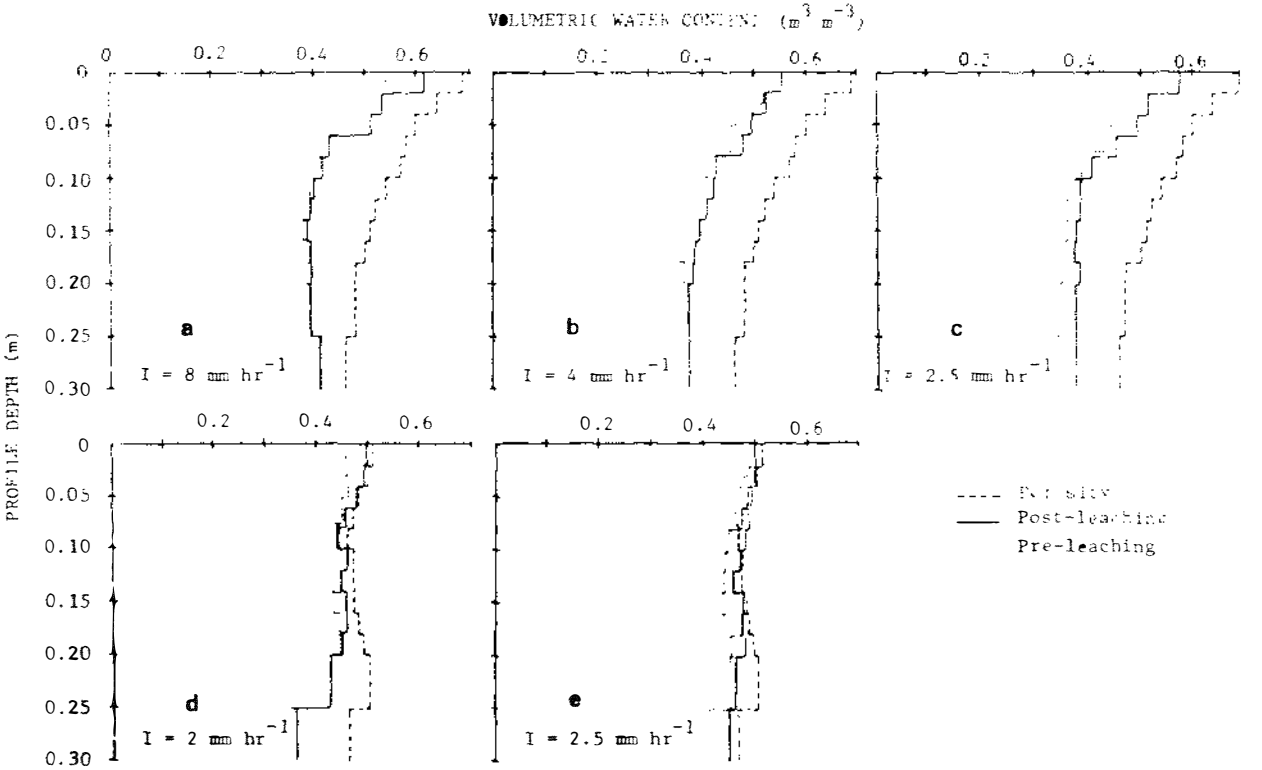

Fig. 6.6 Volumetric water content distribution in the soil profiles before and after ponding, and porosity. I = infiltration rate (mm/hr) in the first hour after ponding. Under pasture (a, b, and c) and under cultivation (d and e).

draining at "field capacity", while the soil below is unsaturated. In fact, a perched water-table was observed after ponding in one of the replicates. This supports the argument for the throttling effect of the compacted layer proposed above.

Surprisingly, the infiltration rates during the first hour of ponding into the cultivated and non-cultivated soil were fairly similar. This was perhaps due to a few very large pores or cracks, induced by the cultivation, compensating for the lower volume of macropores in the cultivated soil. The 50 mm of ponded water soaked in in less than 20 hours on two of the pasture plots, but took 2 days to soak into the third pasture plot and the two cultivated plots.

The bromide concentration remaining in the top 20 mm of soil was more than 240 µg/ml in the cultivated area, while appoximately 150 µg/ml was found in the pasture area. The finding of unleached bromide near the soil surface indicates preferential movement occurred during leaching. Leaching of bromide was less in the cultivated area, where the crop row spacing was 150 mm, than in the pasture area where pasture plants were more uniformly distributed on the soil surface. The conducting pores associated with plant roots in the cultivated area would have been widely spaced and also clumped within the rows. Bromide which was located between the crop rows would tend to move relatively slowly down the profile and would move even more slowly if this exposed soil had deteriorated in structure due to cultivation and rainfall impact. However the root-related conducting pores in the pasture area would be more closely spaced and uniformly distributed, which would allow bromide to be leached more effectively.

6.4.2 Natural Rainfall Experiments

The leaching of bromide under natural rainfall was under transient flow conditions. Fig. 6.7 shows the mean values of bromide concentration found in the soil profile.

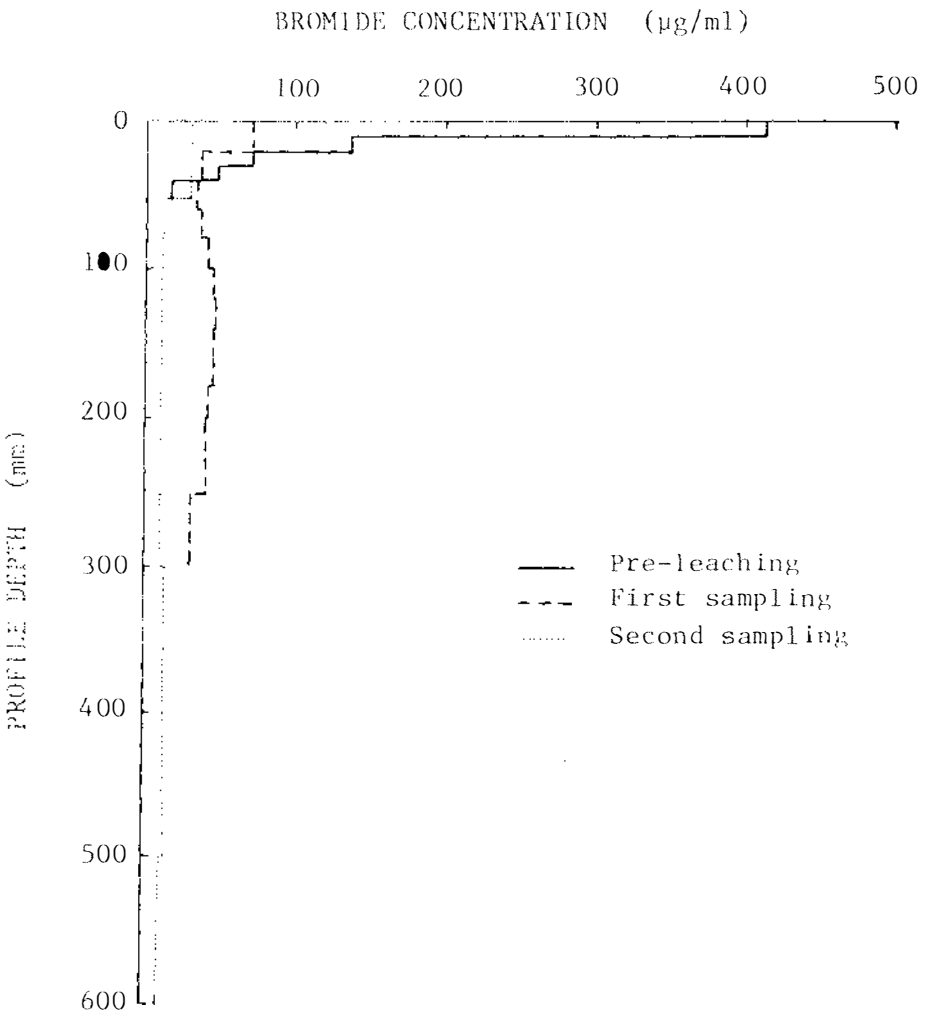

Fig. 6.7 Bromide distribution in the soil profile under natural rainfall in the continuous pasture growing area.

6.4.2.1 Pre-leaching measurements

The initial distribution of applied bromide was measured on the day after application when the soil water content was at "field capacity". The maximum concentration was in the top 10 mm segment, the concentration then decreased sharply in the succeeding depths. The average concentration was 42 µg/ml in the 40-50 mm depth segment, suggesting the movement of some bromide below this depth. This was probably one reason for the low recovery percentage of applied bromide in the top 50 mm depth. Some unusually high bromide concentrations were observed at 40-50 mm depth (218, 240, and 417 µg/ml), and variation of bromide concentration in the replicate samples was quite considerable. This will be discussed later in Section 6.4.3 and 6.4.5.

6.4.2.2 Post-leaching measurements

Distribution of bromide concentration with depth was measured after 46 mm and 182 mm of excess rainfall over evapotranspiration had infiltrated into the soil profile.

a. First sampling Daily rainfall records before the first sampling indicate rainfall was light and relatively uniformly distributed over that period (Fig. 6.2). The maximum daily rainfall during this period was 11 mm, probably not enough to cause saturation or surface run-off. Leaching of bromide thus probably occurred under unsaturated conditions most of the time. The movement under these conditions would be more uniform than under ponding conditions, as was shown in the laboratory experiment described in Chapter 4. The soil moisture profile at this sampling time is shown in Fig. 6.8. It indicates the water contents near the soil surface (0 to 50 mm depth) were slightly lower than under the ponded conditions (Fig. 6.6) while they were similar below 50 mm. However the water contents during leaching under natural rainfall would have varied from time to time, according to rainfall intensity and distribution.

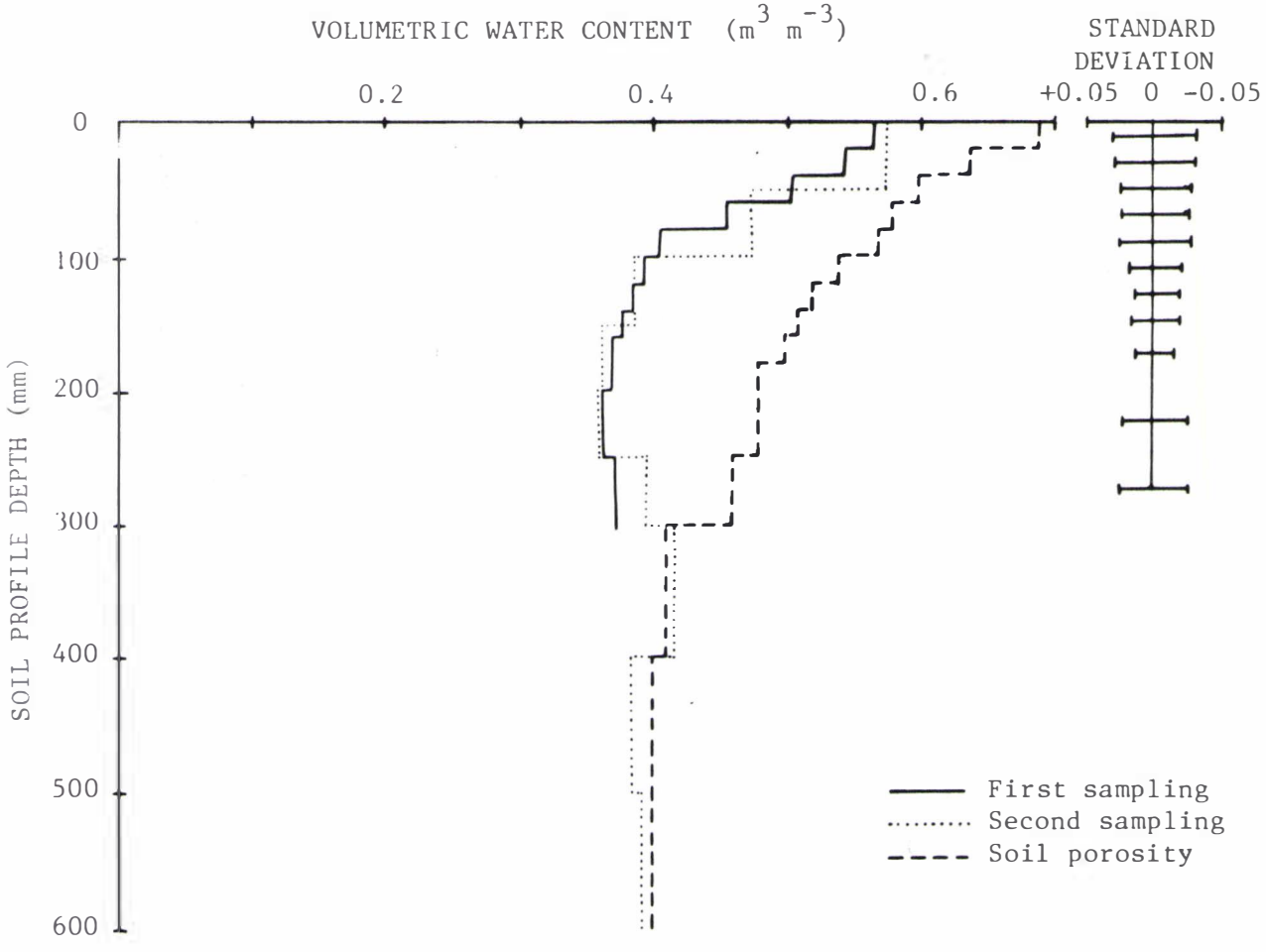

Fig. 6.8 Volumetric water content distribution in the soil profile under natural rainfall conditions at both sampling times (after 46 mm and 182 mm excess rainfall), and soil porosity. Means and standard deviations of 40 samples. The standard deviations refer to the first sampling. The site was under pasture.

The results however suggest preferential flow did occur to some extent, as indicated by the high concentration of bromide remaining in the top segment (Fig. 6.7). The average concentration of bromide in the top 20 mm was 71 µg/ml, which was the maximum throughout the profile. The average concentration in the succeeding depth dropped to 38 µg/ml, almost half of the above. Then the concentration increased slightly below this depth and a second peak of bromide concentration (47 µg/ml) appeared at about 130 mm depth. Such double peaks of concentration were also observed by Cameron et al. (1979) for nitrogen and chloride leaching in bare clay loam soil, and by Saffigna et al. (1977) in a sandy loam profile under potatoes. The 32 µg/ml average concentration measured at 250-300 mm depth suggests some bromide was leached below 300 mm depth.

The appearance of a second concentration peak, although a very flat one, suggests more uniform than preferential leaching, presumably due to unsaturated flow conditions. If the soil water content is approximately constant in time and space, simple leaching models predict the depth of the peak to be i/θ where i is the equivalent depth of water moving through the soil and θ is the volumetric water content (Gardner, 1965). Assuming water for evapotranspiration is removed from at or near the soil surface, i may be found as the excess of rainfall over evapotranspiration for the period in question. Dayananda et al. (1980) treat more complicated cases. Taking θ as 0.42 (the average value over the sampling depth, Fig. 6.8), and finding i from Fig. 6.2, the predicted depth of the concentration peak at the time of the first sampling is 110 mm, slightly shallower than the observed depth of 130 mm.

Bromide remaining in the top 50 mm of soil after leaching by natural rainfall was approximately half that remaining after leaching by a comparable amount of continuously ponded water, as indicated in Table 6.1. Higher efficiency of leaching by natural light rainfall rather than continuous ponding was also found by Wilson et al. (1961).

b. Second sampling There were a few heavy rainstorms between the first and second sampling, as indicated by the rainfall data in Fig. 6.2. The heavy rainfalls of 33 and 20 mm day^{-1} were probably large enough to cause mole discharge and localised surface ponding. Leaching of bromide would then be partly under saturated conditions, during which much of the flow would be preferentially through the larger channels. Some of the bromide apparently moved below 600 mm depth, and presumably some was carried away with the mole drains at 400 mm depth. The soil water content below 300 mm depth was near saturation (Fig. 6.8), indicating the moles were susceptible to drainage at that time. The total bromide recovered to the sampling depth was 41% (Table 6.1).

The first 46 mm of excess rainfall was much more effective in leaching bromide out of the surface soil than the next 136 mm, as can be seen from Fig. 6.7. The lighter rainfall events before the first sampling probably caused unsaturated and more uniform flow through the soil. Also the bromide remaining in the top 50 mm of soil after the first sampling was probably located within soil aggregates and in places removed from the flow pathways, and so was less prone to leaching.

After 182 mm of excess rainfall, the second peak of bromide concentration had moved to approximately 450 mm depth and flattened out almost completely. The simple leaching theory described above predicts a depth of 430 mm for the concentration peak at the time of the second sampling. Due to the presence of the mole drains at this depth, and the poor soil structure in the B horizon, the agreement between the observed and calculated depths is probably largely fortuitious.

6.4.3 Variability in Bromide Distribution

In this experiment, some unusually high bromide concentrations were found in several samples from every depth, as shown in Appendix E for the continuous ponding experiment, and in the histograms showing the frequency distribution of bromide in the soil profile for the experiment under natural rainfall in Fig. 6.9a. Presumably these samples included preferential pathways. Some cores tended to have high bromide concentration at all depths. However other cores had high values only at certain

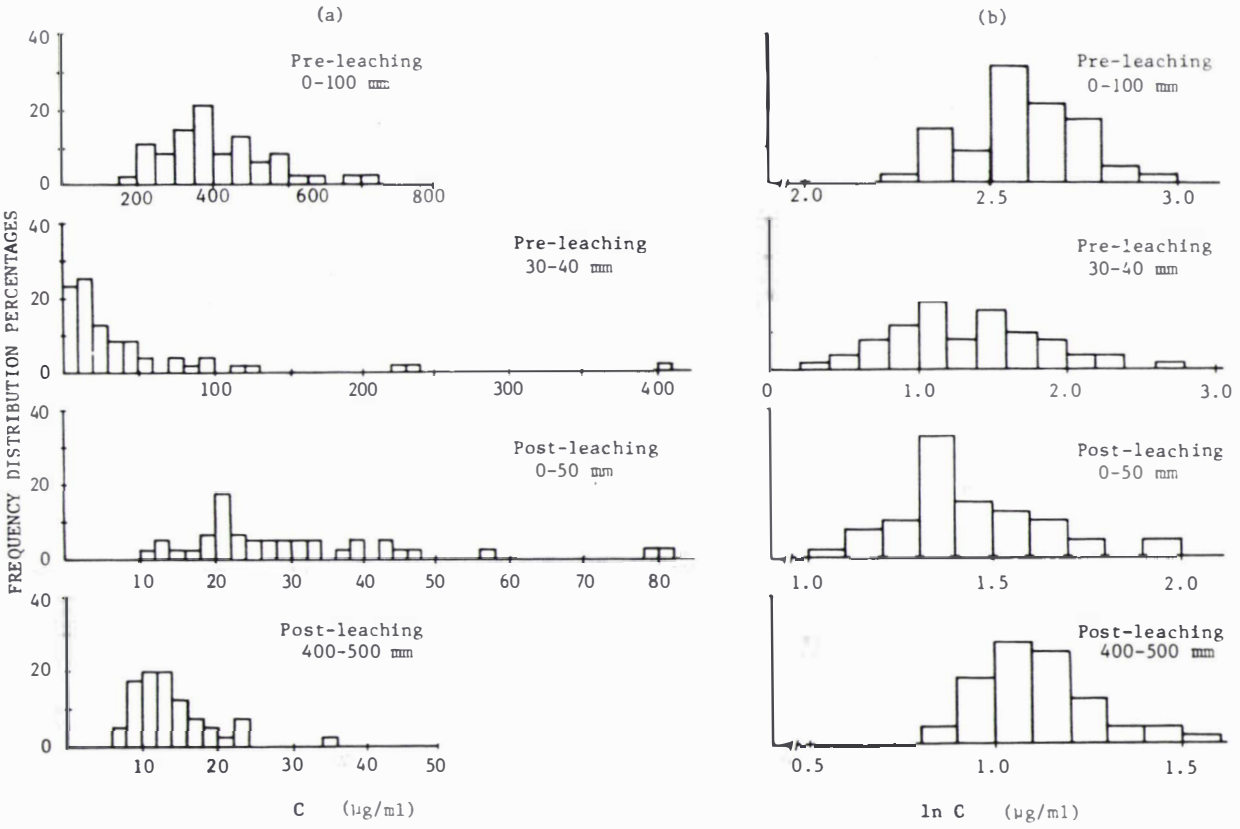

Fig. 6.9 Histograms showing frequency distributions of bromide concentration (C) in soil before and after leaching by 182 mm of excess rainfall.

(a) Frequency distribution of C,

(b) Frequency distribution of ln C.

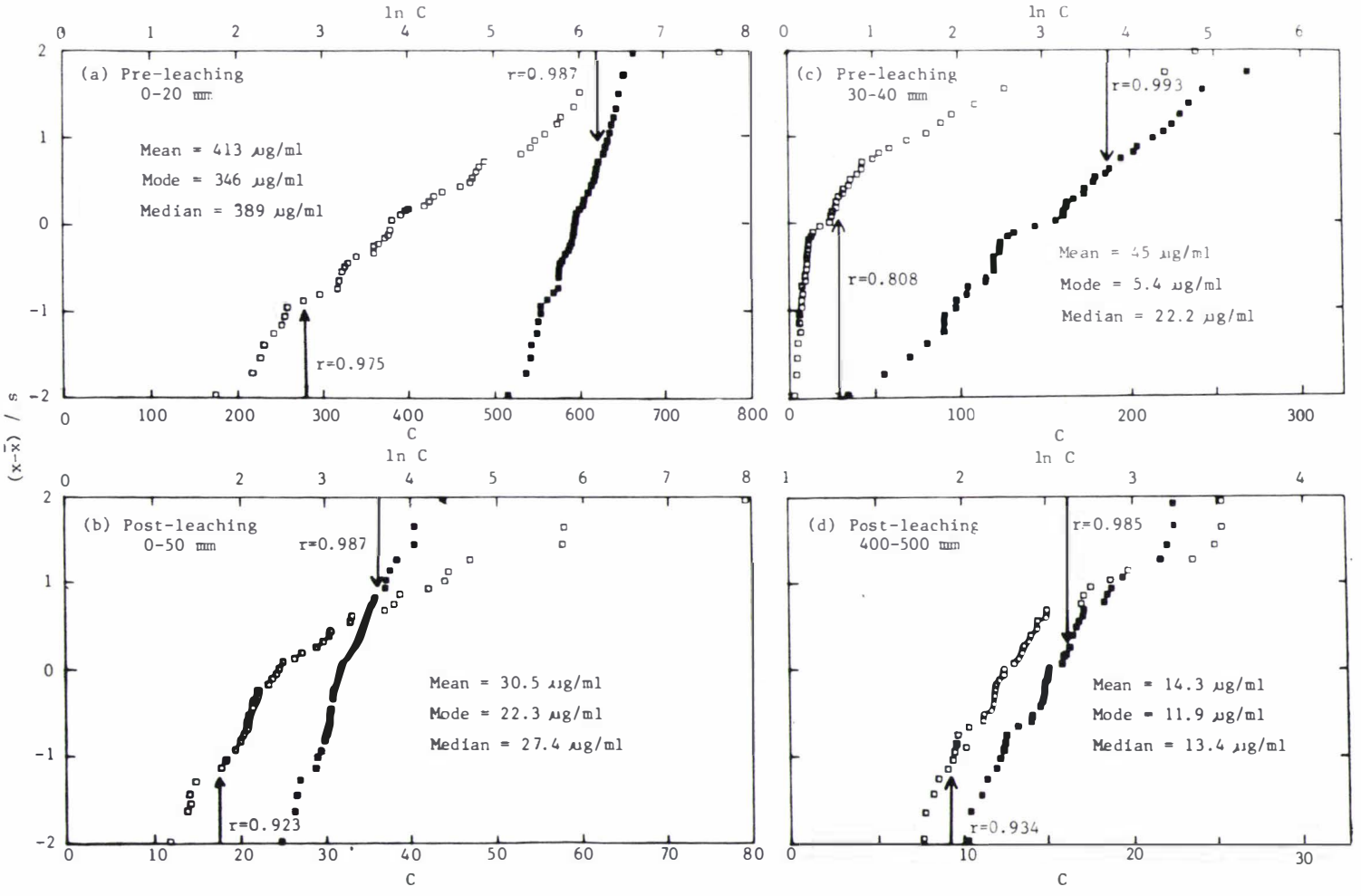

Fig. 6.10 Fractile diagrams showing the relationship of probability units $((x-\bar{x})/s)$ and bromide concentration in soil (C or ln C), where x=C (□) or ln C (■), $\bar{x}$ = mean values, s = standard deviation, and r = correlation coefficient. Post leaching data shown were after 182 mm excess rainfall.

depths, suggesting non-vertical preferential pathways had been intercepted.

The frequency distributions of bromide under natural rainfall were asymmetric, as seen from Fig. 6.9a. The frequency distributions in Fig. 6.9a were transformed to logarithmic distributions and these are shown in Fig. 6.9b. The histograms, each of which includes at least 40 measurements, indicate bromide concentration variability in the soil profile was more log-normally than normally distributed. Fractile diagrams, which have been used by Biggar and Nielsen (1976) as an indicator of normal or log-normal distribution, were also constructed. The details for construction of fractile diagrams, following Biggar and Nielsen's procedure, are given in Appendix F. Examples of fractile diagrams are shown in Fig. 6.10, with the corresponding linear correlation coefficient values (r). The probability units $((x - \bar{x})/s)$ were more linearly related to ln C than C, as indicated by the r values, also suggesting a log-normal distribution. The results of fractile diagram construction for observations under natural rainfall leaching, both pre-leaching and after 182 mm excess rainfall, given in Table F.1, indicate the r values for the relationships of probability units and ln C are consistently greater than the relationship with C.

The mean, mode, and median values, obtained from fractile diagrams and shown in Fig. 6.10 and Table F.1, are different. Mean values are higher than modal and median values in all cases. Data for the continuous ponding experiment are not presented as frequency distributions, as not enough replicates were taken to allow the data to be analysed this way.

The indicator of the variability in bromide concentration at any depth in the soil profile is given by the exponential of the standard deviation of ln C (written as exp s_L), and the coefficient of variation (C.V.), where C.V. = $100\ s_L/\bar{x}_L$, and $\bar{x}_L$ is the mean of ln C. The sixteenth and eighty-fourth percentiles of the log-normal distribution can be estimated as exp $(\bar{x}_L - s_L)$ and exp $(\bar{x}_L + s_L)$ respectively (Rokoski, 1972). The C.V. values for the ponded water experiments were calculated assuming log-normal distributions, and the values are shown in Table E.1 and E.2 in Appendix E. These C.V. values for the ponding experiments are much greater than for the experiment under natural rainfall

conditions (Appendix F), probably due to more preferential flow occurring under ponded conditions, and also perhaps less redistribution time being allowed before taking pre-leaching samples (3 hours compared to 24 hours in the natural rainfall experiment). The C.V. values tend to increase with soil depth, except under cultivation, where the C.V. is greatest at the depth of the compacted layer (Table E.2). In the natural rainfall experiment, the C.V. values for the first sampling (Table F.2) are smaller than for the second sampling (Table F.1). The smaller C.V. values for the first sampling are probably due to the light rainfall prior to sampling, while preferential flow induced by heavy rain would cause larger variabilities in the second sampling measurements.

Distributions of saturated hydraulic conductivity in the field have been observed to be log-normal by Mason et al. (1957), Rokoski (1972), Nielsen et al. (1973), and Baker (1978). Thus leaching, which is related to flow velocity, might be expected to result in log-normal distributions of solute concentration in the soil profile. Biggar and Nielsen (1976) and Van der Pol et al. (1979), presenting field leaching data in terms of flow velocities and dispersion coefficients, found these leaching parameters were log-normally distributed. Large variability in hydraulic conductivity data has been reported within a soil series. However the data have usually been obtained from a fairly large area, e.g. Nielsen et al. (1973) measured the soil hydraulic conductivity in twenty 6.5 m^2 plots distributed over 150 ha. The variability in bromide concentration reported here is on a much smaller scale, over 40 samples being taken from an area as small as 0.16 m^2. This raises interesting questions as to the scale of variability in the field. Perhaps the largest variability in soil occurs over distances related to parameters such as plant spacing, structure unit size, and the spacing between large biopores.

6.4.4 Leaching Flow Pathways under Natural Rainfall

Plant interception and stem flow, soil micro-relief or micro-depressions caused by animal pugging and large pores open to the soil surface, cause non-uniform entry of rain into the soil surface.

A subsidiary experiment was conducted to observe the leaching pathways under natural rainfall in the field, as described in Section 6.3.3. Rhodamine B dye was used as a tracer to mark the pathways. Fig. 6.11 shows the movement of dye tended to be concentrated in the area around and directly under the plant stems. The dye stain seems to be associated with roots (Fig. 6.11a and c), worm channels (Fig. 6.11b and c), and cracks (Fig. 6.11c). The accumulation of dye near the base of plants was probably caused by stem-flow, which had been initiated by the collection of rain by the aerial parts of a plant. The stem-flow would deliver it to the soil at the base of the plant, where it infiltrates in an amount considerably greater than in adjacent areas. Thus the interception of rain by foliage prevented water reaching the soil surface at some spots beneath the plants, but tended to funnel water straight down the stem into the soil. The reported examples of stem flow have usually referred to trees, large shrubs or large-leaved plants (Glover and Gwynne, 1962; Saffigna et al. 1976), however Glover et al. (1962) found that it was an important phenomenon in grassland. The intercepted water might also drip from the leaf tips directly to the soil, causing point sources of water infiltration.

Soil micro-relief or small depressions may cause localised surface ponding. Cameron et al. (1979) have discussed the effects of soil micro-relief on non-uniform leaching of chloride and nitrate into soil under natural rainfall. Surface run off into small depressions meant more infiltration, and so solutes moved deeper there than they did in the surrounding soil. Much variation in micro-relief was observed in the experimental area, as well as many small depressions caused by sheep pugging. Soil micro-depressions, in association with open channels to the soil surface, would cause non-uniform flow only if enough rain occurred to cause ponding in the hollows. However, if the whole surface was ponded, these depression areas might conduct water at a slower rate than the surrounding soil, due to lower saturated hydraulic conductivity of the compacted soil.

The non-uniformity of incoming water due to plants and micro-relief has often been neglected in leaching studies. Most experiments have been conducted in bare soil with a disturbed and levelled soil surface, such as reported by Wild and Babiker (1972), Wetselaar (1962), Miller et al. (1965), Biggar and Nielsen (1976), Van De Pol et al. (1977).

(a)

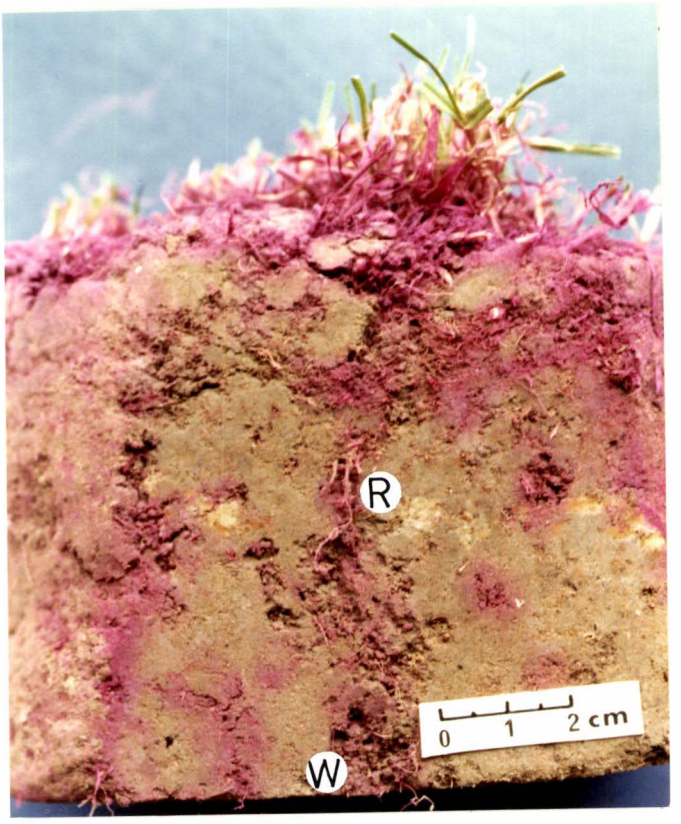

(b)

Fig. 6.11

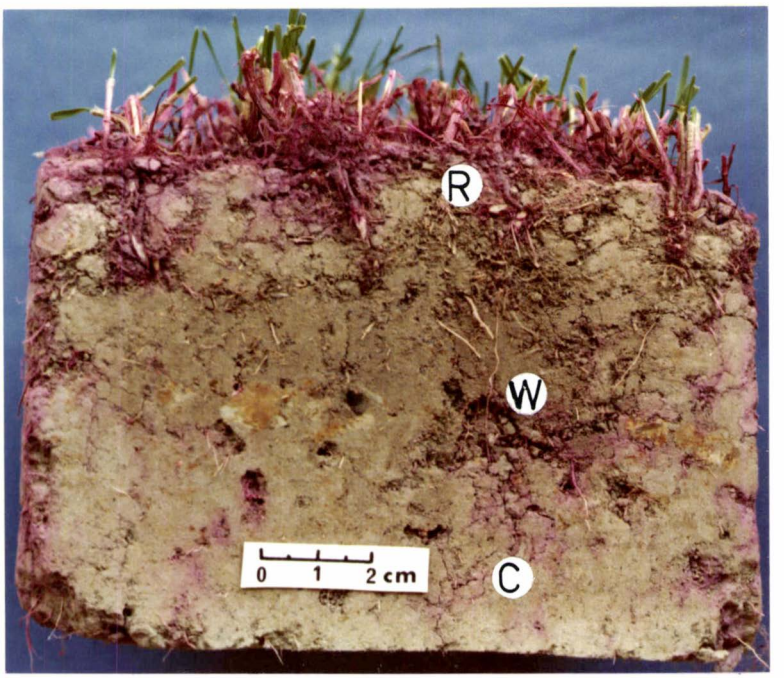

(c)

Fig. 6.11 Photographs indicating stem-flow responsible for non uniformity of water intake at the soil surface under natural rainfall.
W = worm channel, R = root, C = Crack

6.4.5 Possible Factors Tending to Cause Low Bromide Recovery Percentages

A relatively low recovery percentage of bromide, ranging from 40 to 86%, was obtained (Table 6.1). Some possible reasons for this are discussed below:-

a. Retention of bromide in soil Nearly complete recovery of applied bromide from soil was reported by Abdalla and Lear (1975), using water extraction and a bromide selective ion electrode for analysis. To check their results under the conditions in this study, the subsidiary laboratory experiment described in Section 6.3.2 was carried out. It investigated short-term (18 hour equilibration) bromide retention in soil under similar conditions in the field experiment. The results were 94% and 99% recovery from 0-20 mm and 100-120 mm core depths, respectively. The higher retention in the top layer was probably due to a higher organic matter content and so more anion adsorption, and/or plant uptake. Retention of bromide in soil in this experiment was therefore not a major factor.

b. Retention of bromide by plants Bromide uptake by plants was measured 99 days after its application to the soil surface. During this period 113 mm of evapotranspiration had occurred. The amounts of bromide measured from the two sub-plots were 13.5% and 11.5% of the applied amount. The rate of plant uptake was probably related to the transpiration rate and the amount of bromide available in soil. The amount of bromide uptake by plants at the time of the first sampling was probably much less, as only 27 mm of evapotranspiration had occurred by them.

c. Non-uniform bromide application Bromide solution was applied on the soil surface using a watering can at the start of the experiment under natural rainfall, and using an atomizer in the ponded water experiments. Several practice runs were made with the watering can prior to the actual application, in order to produce as uniform a distribution as possible. However, some non-uniformity of application in both experiments was unavoidable.

d. Retention of bromide on plants The concentration of bromide solution used was relatively high and the amount applied relatively low, so that the droplets of solution remaining on the plants would contain a significant amount of bromide which would not be recovered in the pre-leaching sampling.

e. Soil sampling method The soil corer used in this experiment was relatively small in comparison with the plant size and spacing. For ease of sampling, the soil samples tended not to include plant crowns and the soil directly under them. Thus, given the discussion in Section 6.4.4 concerning interception and stem flow, an unconcious bias probably occurred in the soil sampling, and this was probably the main reason for the low percentage recovery of bromide.

6.4.6 Computations

Leaching of solute from a thin surface layer into the soil profile beneath, under saturated conditions, was modelled numerically using CSMP. The computer programme used was similar to that used for modelling preferential solute movement by Scotter (1978) (see Appendix C.1) . The preferential flow was idealized as occurring in uniformly spaced, vertical, cylindrical channels. Viscous laminar flow, following the Hagen-Poiseulle equation, was assumed. An example of the computer programme for bromide leaching is given in Appendix C.4.

Bromide was assumed initially to be present only in the top 10 mm of the soil profile. Continuous leaching for 20 hours was simulated, and in that time 50 mm of leaching water had passed through the soil, assuming a saturated hydraulic conductivity of 6.94×10^{-7} m s^{-1} (i.e. the measured field infiltration rate of 2.5 mm hr^{-1}). During the leaching process, bromide in the soil matrix in the top 10 mm of soil diffused towards the channels, and was then translocated down into the profile with the viscous flow in the channels. Below 10 mm depth, bromide from the channels then diffused back into the surrounding soil matrix, due to the reversal in concentration gradient.

In the simulation of soil containing large channels, the viscous flow in the channels was much faster than the radial diffusion into or out of the surrounding soil. Thus relatively little bromide would be leached from the top 10 mm soil, but the small amount leached would penetrate quite deeply into the soil profile. The converse would hold for smaller channels.

The soil profile modelled was 300 mm deep and was divided into 6 layers of thickness 10, 10, 20, 40, 80 and 140 mm, the thickest layer being the deepest. The concentration of bromide in each soil layer, and in the effluent solution at 300 mm depth, were computed as a function of time. Three channel sizes were considered, with different spacings between them so as to give the same hydraulic conductivity. The channel sizes and related data are given in Table 6.2. The soil porosity assumed was 0.52, the average value pertaining in the field.

Table 6.2 Channel size and related data assuming hydraulic conductivity of 6.94×10^{-7} m s^{-1}

Diameter of channels (mm)	Maximum diffusion radius (mm)	Pressure potential to drain (mm)
0.10	2.81	-300
0.15	6.32	-200
0.20	13.28	-150

The results of the computations are shown in Figs. 6.12 and 6.13. The movement of solute through 0.2 mm diameter channels was found to be preferential by Scotter (1978), thus the shape of the concentration distribution curve appearing in Fig. 6.12 for the soil containing 0.2 mm channels is the result of leaching under preferential flow. A high concentration of bromide remains in the top 10 mm soil, and a negligibly small concentration, too low to appear on the graph, occurs in the profile below. Most of the bromide that is leached from the top layer moves below 300 mm depth. Fig. 6.13 shows the relative concentration (C/C_o)

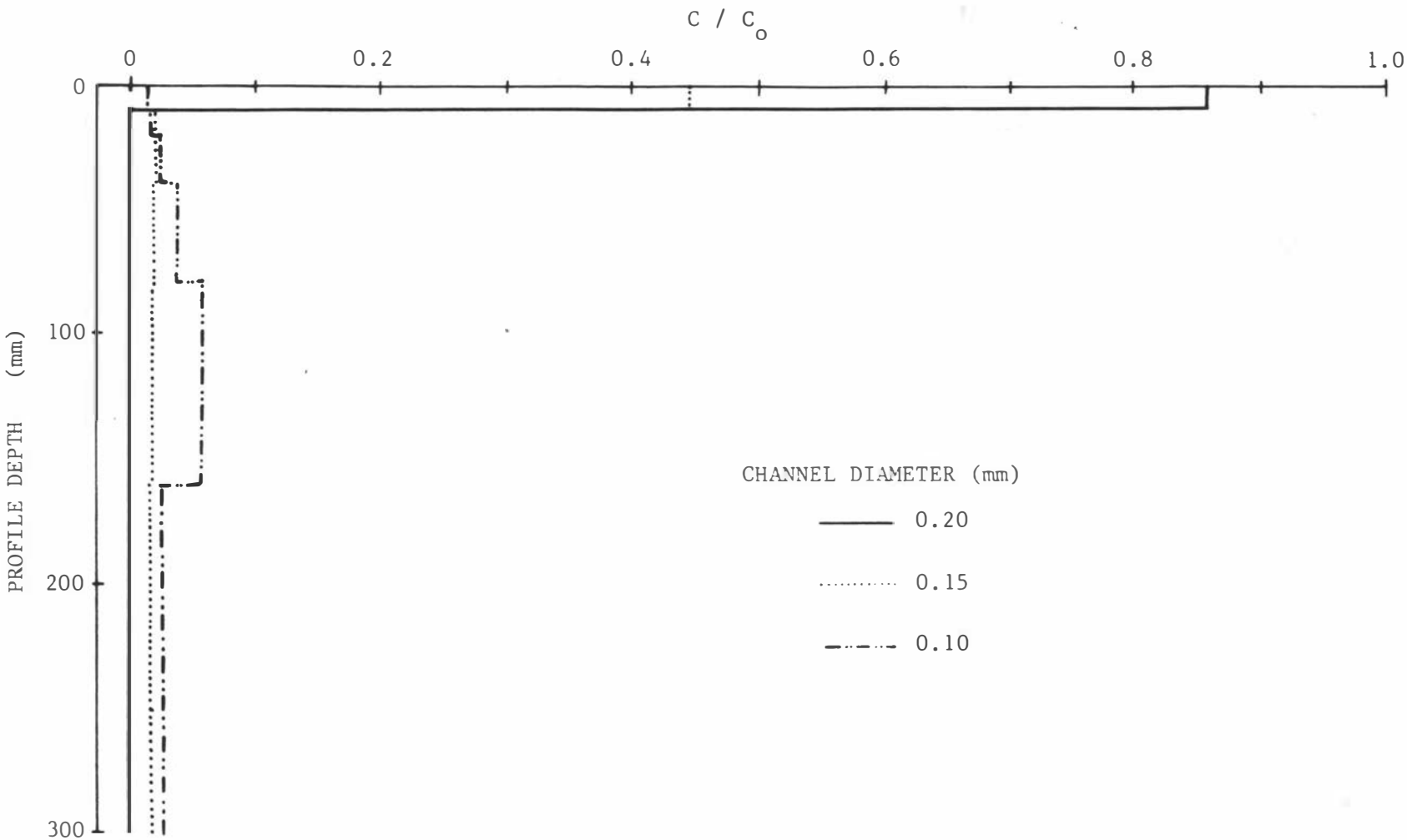

Fig. 6.12 Computed bromide concentration distribution after leaching in soil containing uniformly spaced, vertical, cylindrical channels. Initially the soil solution concentration (C) in the top 10 mm of soil was C_o.

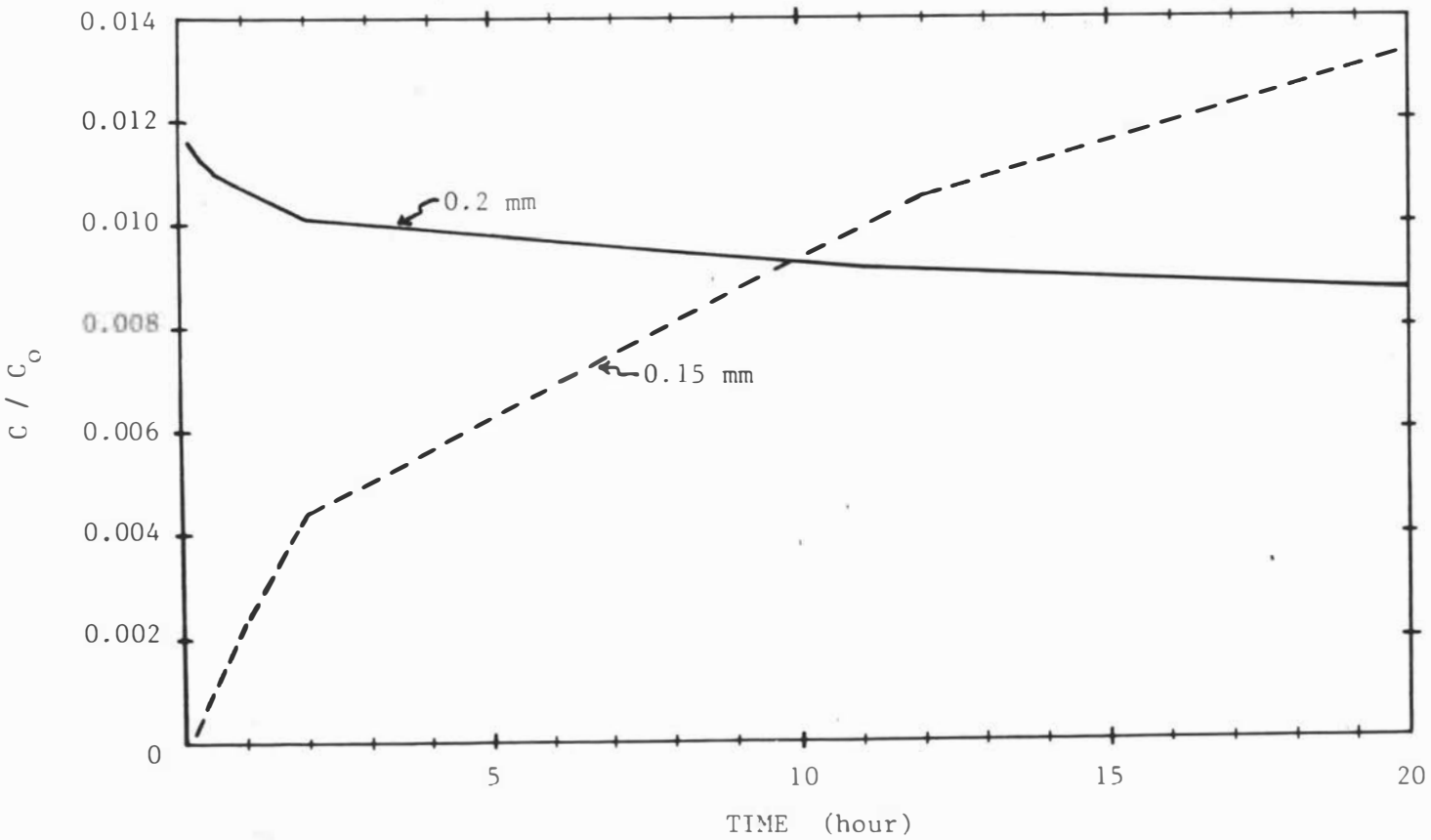

Fig. 6.13 Computed relative concentration of bromide leached from top 10 mm to below 300 mm depth in soil containing vertical cylindrical channels, 0.2 and 0.15 mm in diameter.

of bromide in the effluent increased quickly to 0.0116 after 10 minutes, and then dropped slowly to 0.009 after 20 hours. The total amount of bromide leached below 300 mm depth was 12% of the amount initially present in the top soil layer. In the field, continuous channels 0.2 mm in diameter or greater would constitute a "short circuit" to the mole-tile drainage system, but would cause relatively little leaching.

The concentration distribution of bromide in the soil containing 0.15 mm diameter channels indicates relatively less preferential flow occurring during leaching (Fig. 6.12). The concentration of bromide in the effluent increased steadily with time and reached 0.013 C/C_o after 20 hours (Fig. 6.13). Slightly less bromide was leached in this case, 9% of the initial amount moving below 300 depth.

No bromide moved below 300 mm depth in the soil with 0.1 mm channels, and the concentration distribution curve was effectively symmetrical with a distinct peak at approximately 120 mm depth (Fig. 6.12), which is similar to the classical distribution curve (curve (d) in Fig. 6.1). The relatively large segment thickness used below 200 mm depth in the numerical analysis caused the "bumpiness" in the distribution curve.

The ponded water leaching data in Figs. 6.4 and 6.5, with the high bromide concentration remaining at the surface, and the absence of a second peak lower in the soil profile, resemble more the curve for soil containing 0.15 mm diameter pores in Fig. 6.12 suggesting pores approximately this size were responsible for much of the flow. The natural rainfall leaching data in Fig. 6.7 shows lower concentrations at the surface, and a second concentration peak in the soil profile, resembling more the curves in Fig. 6.12 for a soil with 0.1 mm pores. This suggests the larger pores were drained and the pressure potential was less than -200 mm for much of the time in most of the soil profile under natural rainfall.

6.5 CONCLUSIONS

1. Some bromide was leached to 300 mm profile depth by both 50 mm of ponded water and 46 mm of excess rainfall in this experiment. Also preferential movement is indicated by the high concentration remaining unleached near the soil surface. About 31 to 62% of applied bromide remained in the top 50 mm of soil under ponded leaching conditions, while 15% remained under natural rainfall conditions.

2. Bromide was leached more effectively by natural rainfall than by continuous ponding, when the same amount of leaching water was used.

3. Large variability in bromide concentration in the replicate core samples was observed. Unusually high concentrations of bromide were found in some samples at all depths, which caused the frequency distribution to be log-normal rather than normal.

4. Interception and stem-flow, combined with the soil sampling technique used which inadvertently avoided sampling plant crowns and the soil directly under them, probably resulted in some bias in the sampling. The relatively low recovery percentages of the applied bromide (40 to 86%), particularly in the pre-leaching sampling, were probably largely due to this.

5. Plant uptake of bromide was probably small during the experiment involving leaching with ponded water. But approximately 10% of the applied bromide was taken up by plants by the end of the experiment under natural rainfall conditions.

6. Double peaks in bromide concentration were observed in the soil profiles under ponded water conditions in soil which had been cultivated, and under natural rainfall conditions in the pasture area. The second peak was probably the result of unsaturated, and so non-preferential flow. In the cultivated area this was probably brought about by the compacted layer throttling the flux into the soil beneath. Under natural rainfall conditions, unsaturated flow probably prevailed most of the time, due to the rainfall intensity being less than the saturated hydraulic conductivity.

7. No transport model seems to be able to describe quantitatively bromide movement in this experiment, particularly the effects of preferential flow. The results of the computations for bromide leaching in an idealized soil, containing uniformly spaced, vertical, cylindrical channels, indicated that bromide would be leached more effectively from soil where continuous channels 0.15 mm or larger were either absent, or air-filled and so ineffective. Such channels if uniform, would drain at -200 mm pressure potential.

8. A practical implication of the results is that soluble fertilizers applied to pasture or crops may not be as prone to leaching as is often thought. Interception, stem flow, and preferential flow in this soil may combine to leave a significant fraction of the applied fertilizer near the surface for a considerably period. On the other hand, preferential flow will leach some of the applied fertilizer more quickly below the root zone than would more uniform movement in the soil.

APPENDIX A

SOIL PROFILE DESCRIPTIONS AND PHYSICAL AND CHEMICAL DATA

Table A.1 Profile description of Tokomaru Silt Loam in Dairy Farm No.4, Massey University, Palmerston North (Pollok, 1975).

Horizon	Depth (cm)	Description
Ah1	0 to 10 ± 1	Silt loam; dark greyish brown (10 YR 4/2), with slight yellowish-red (5 YR 4/6, 5/6) mottling around grass roots; moderately developed fine and medium crumb structure; friable; considerable humus; numerous, fine grass roots; slightly imperfect internal drainage; moist; fairly distinct and even boundary.
Ah2	10 ± 1 to 20 ± 1	Silt loam; dark greyish brown (10 YR 4/2), with some yellowish-red (5 YR 4/6, 5/6) mottling around grass roots; moderately developed, medium crumb, cast granular and nutty structure; friable; moderate amount of humus; numerous, fine grass roots; some earthworms; some ironstone concretions; slightly imperfect internal drainage; moist; rather indistinct, slightly uneven boundary.
AB	20 ± 1 to 26 ± 2	Silt loam; greyish brown (2.5 Y 5/2), moderately settled yellowish-red (5 YR 4/6), dark reddish brown (2.5 YR 3/4) and dusky red (10 R 3/4) in a reticulate pattern; moderately to strongly developed, medium nutty structure; friable-firm; some humus; moderate number of grass roots; some earthworms; some ironstone concretions ca 6 mm in diameter; imperfect internal drainage; moist; rather indistinct, slightly uneven boundary.
Bg	26 ± 2 to 78 ± 5	Clay loam; light brownish grey (2.5 Y 6/2) and light olive grey (5 Y 6/2), with abundant, coarse, strong brown (7.5 YR 5/6) mottles arranged in a blotchy pattern, with greatest concentration towards the upper part of the horizon and sometimes developing into soft ironstone concretions; weakly to moderately developed, coarse blocky and prismatic structure; olive grey clay skins; very hard when dry, plastic and sticky when wet; some humus present in pipings from the horizon above and in the vicinity of old decaying bush roots; grass roots rare; no fauna seen; impeded internal drainage; wet; rather indistinct, somewhat uneven boundary due to weathering of the horizon beneath.
Cxg	78 ± 5 to 114 ± 3	Silt loam; colour of soil within peds light olive grey (5 Y 6/2), pale olive (5 Y 6/3) and strong brown (7.5 YR 5/6, 5/8) in a reticulated mottling pattern; colour of soil filling the cracks between peds uniform pale grey (5 Y 7/2), with a thin rusty brown band formed at the interface between crack and ped surface; strongly developed, very coarse polygonal structure (penta and hexa columnar and trapezocolumnar after Brewer, 1964) with the polygons varying from 15 to 40 cm in width and separated by large, mainly vertically oriented, soil-filled cracks 2-4 cm wide, both peds and cracks being continuous with the horizon beneath; thick clay skins; soil within peds compact and extremely hard when dry, moderately sticky and plastic when wet and dispersible in water (fragipan); virtually no humus within peds, but a little in the vicinity of decaying roots within the cracks; some old bush roots and a few more recent living roots within cracks, but virtually none within peds; no fauna seen; numerous pinhead Fe/Mn concretions within peds; impeded internal drainage, the main avenue for water movement being down the soil-filled cracks; moist; diffuse (imperceptibly merging) boundary.
Cwg1	114 ± 3 to 147 ± 1	Silt loam; colours as for horizon above, but with light olive grey (5 Y 6/2) now assuming predominance over strong brown (7.5 YR 5/6) in the mottling pattern within peds; structure, cracks and clay skins as in the horizon above; noticeable change in consistency, with the soil becoming less hard and compact and losing the properties of a fragipan; little if any humus; no roots; no fauna seen; pinhead concretions become darker in colour (black) and more manganiferous compared with the horizon above; imperfect internal drainage with the main avenue for water movement being down the soil-filled cracks between peds; moist; distinct, even boundary.

CONTINUED

Table A.1 (continued)

Horizon	Depth (cm)	Description
Cwg2	147 ± 1 to 157 ± 1	Silt loam; light olive grey (5 Y 6/2) to olive (5 Y 5/3), moderately mottled strong brown (7.5 YR 5/6, 5/8) in reticulate pattern; moderately developed, very coarse polygonal structure (penta and hexa columnar and trapezocolumnar after Brewer, 1964), with the soil-filled cracks between structural units tending to be finer and more widely spaced compared with the Cxg and Cwg1 horizons above; firm; no humus, roots or fauna; numerous dark grey and black Fe/Mn pinhead concretions; imperfect internal drainage; moist; overlies terrace gravels at depth.

Table A.2 Some Physical and Chemical Properties of Tokomaru Silt Loam (Pollok, 1975).

Table A.2.1 Particle Size Analysis

Horizon		Sample		Equivalent Spherical Diameter (mm)					
Symbol	Depth (cm)	Lab. No.	Depth (cm)	<0.002	0.006 to 0.002	0.02 to 0.006	0.06 to 0.02	0.2 to 0.06	2.0 to 0.2
				Cy	fSi	mSi	cseSi	fS	cseS
Ah1	0-8	4941	0-8	23.0	7.6	17.9	43.0	8.0	0.5
Ah2	8-20	4942	10-18	22.0	7.1	18.5	43.7	8.2	0.5
ABg	20-38	4943	23-33	23.8	7.4	18.0	41.2	8.7	0.9
Btg	38-76	4944	51-64	30.2	7.8	15.5	39.3	6.9	0.3
1Cxg	76-145	4945	97-127	18.4	4.8	16.3	46.6	12.7	1.2
1Cwg1	145-221	4946	168-198	18.0	6.4	15.0	45.9	13.1	1.6
2C	221-234	4947	221-229	8.9	6.2	17.8	26.5	22.0	18.6
1Cwg2	234-250+	4948	237-248	16.3	6.3	16.7	50.3	9.5	0.9

Table A 2.2 Chemical Analysis

Soil Horizon	pH		Cation Exchange Properties							Organic C and Total N		
	in water	in nKCl	meq/100 g soil						BS %	C %	N %	C/N
			Na	K	Ca	Mg	TEB	CEC				
Ah1	5.0	4.2	0.15	0.21	3.15	2.40	5.9	20.2	29	3.32	0.31	11
Ah2	4.9	4.1	0.05	0.18	3.15	2.12	5.5	18.0	31	2.08	0.28	7
ABg	5.3	4.4	0.16	0.12	2.55	2.58	5.4	13.8	39	1.98	0.14	14
Btg	5.0	3.6	0.49	0.31	1.35	3.28	5.4	16.0	34	0.83	0.15	6
1Cxg	5.1	3.4	0.99	0.15	2.00	3.90	7.0	12.9	54	0.12	0.04	3
1Cwg1	6.1	4.1	1.30	0.19	3.15	3.90	8.5	11.9	71	0.09	0.02	5
2C	6.3	4.6	0.76	0.08	1.80	2.70	5.3	5.4	98	0.03	0.01	3
1Cwg2	6.4	4.1	1.17	0.20	3.33	3.82	8.5	12.0	71	0.09	0.02	5

Table A.2.3 Clay Mineralogy

Soil Horizon	% Clay	Mica/Illite	Clay-vermiculite	Heat-collapsible 14 Å Clay	Clay-Chlorite	Interstratified Clay	Montmorillonite	Kaolinite	Halloysite	Allophane	Feldspar	Quartz	FeO(OH)
Ah1	23.0	+ + +	+ + +	+ +	-	+ + +	-	-	-	-	+	Tr?	Tr?
Ah2	22.0	+ + +	+ + +	+ +	-	+ + +	-	Tr	Tr	-	+	Tr?	+
ABg	23.8	+ + +	+ + +	+ +	-	+ + +	-	-	Tr?	-	+	+	+
Btg	30.2	+ + +	+ + +	+ +	-	+ + + +	-	Tr	Tr	-	+	Tr?	+ +
1Cxg	18.4	+ + + +	+ + +	+	-	-	Tr	-	Tr?	-	+	+	+
1Cwg1	18.0	+ + + +	+ + +	+	-	-	Tr	-	Tr?	-	+	Tr?	Tr
2C	8.9	+ + +	+ + +	+ +	-	-	Tr	-	+	-	+	+	Tr
1Cwg2	16.3	+ + + +	+ + +	+	-	-	+	-	Tr?	-	+	+	+

APPENDIX B

DIFFUSION OF SOLUTE INTO SPHERICAL SOIL AGGREGATES

Considering soil crumbs to be spherical, the diffusion of non-adsorbed solute into a soil crumb can be described by (Crank, 1956),

$$\frac{\partial C}{\partial t} = D_s \left(\frac{\partial^2 C}{\partial r^2} + \frac{2}{r} \frac{\partial C}{\partial r}\right) \qquad (B.1)$$

where C = solute concentration in soil solution ($M\ L^{-3}$)
t = time for diffusion (T)
D_s = diffusion coefficient of solute in soil ($L^2\ T^{-1}$)
r = radial distance from centre of sphere (L).

Assuming adsorption of reactive solute by soil is instantaneous and linearly related with solution concentration, the diffusion of sorbed solutes into the sphere can be expressed as,

$$\frac{\partial C}{\partial t} = \frac{D_s}{1 + R} \left(\frac{\partial^2 C}{\partial r^2} + \frac{2}{r} \frac{\partial C}{\partial r}\right) \qquad (B.2)$$

where R = a retardation factor which is equivalent to $\frac{\rho_b k}{\theta}$
ρ_b = soil bulk density ($M\ L^{-3}$), θ is volumetric water content ($L^3\ L^{-3}$), and k is the solution distribution coefficient obtained from the linear adsorption isotherm ($L^3\ M^{-1}$) (Eq. 1.7).

For unsteady state diffusion, when the surface concentration is maintained constant and the initial concentration in the sphere of radius a is uniform, then the solution for the total amount of diffusing substance entering or leaving the sphere (M_t) can be expressed as a fraction of the corresponding quantity after infinite time (M_∞) by the relation,

$$\frac{M_t}{M_\infty} = 1 - \frac{6}{\pi^2} \sum_{n=1}^{\infty} \frac{1}{n^2} \exp\left(-Dn^2\pi^2 t/a^2\right) \qquad (B.3)$$

where D is D_s for non-adsorbed solutes and is $D_s/(1 + R)$ for adsorbed solutes. Figure B.1 shows the relationship between M_t/M_∞ and $(Dt/a^2)^{\frac{1}{2}}$ given by Crank (1956).

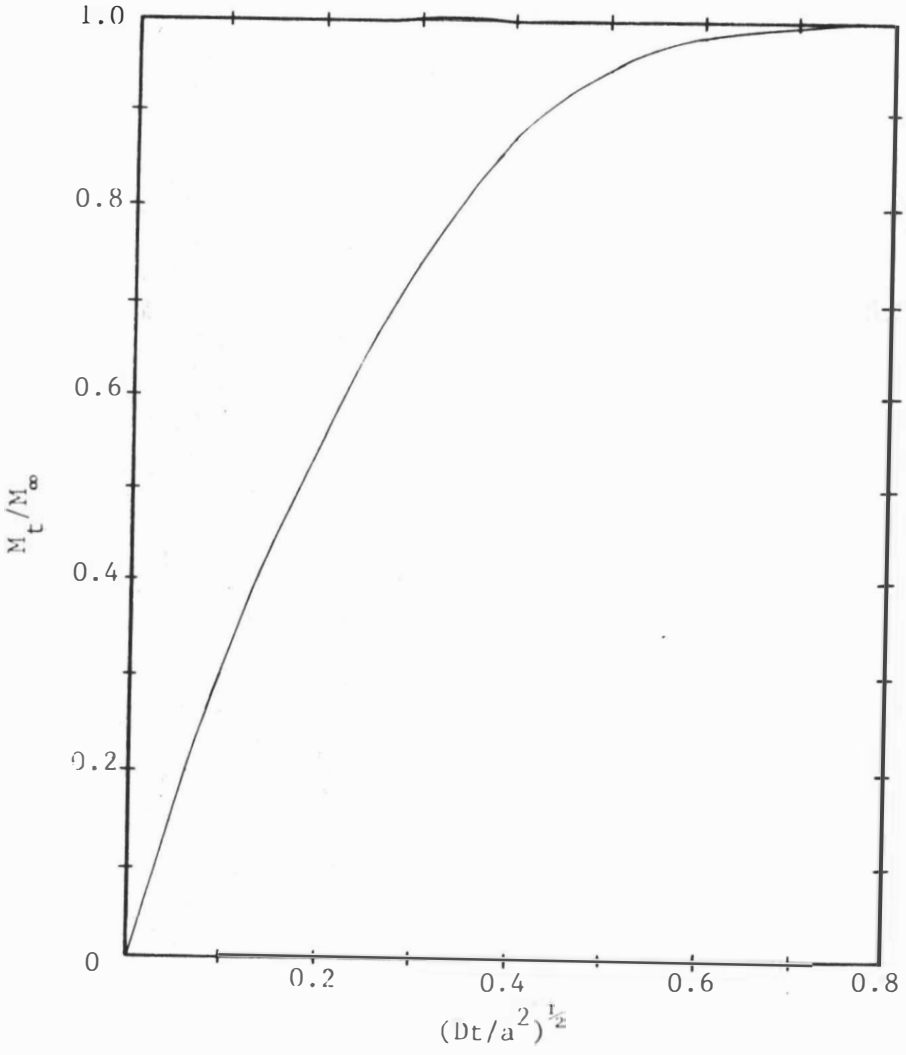

Fig. B.1 Relationship between M_t/M_∞ and $(Dt/a^2)^{\frac{1}{2}}$, as shown by Crank (1956).

APPENDIX C

THEORY OF PREFERENTIAL SOLUTE MOVEMENT THROUGH LARGER SOIL VOIDS AND TYPICAL COMPUTOR PROGRAMMES

C.1 "Preferential solute movement through larger soil voids. I Some computations using simple theory". by D.R. Scotter reprinted from Australian Journal Soil Research. 16:257-67

Aust. J. Soil Res., 1978, **16**, 257-67

Preferential Solute Movement through Larger Soil Voids. I Some Computations Using Simple Theory

D. R. Scotter

Department of Soil Science, Massey University,
Palmerston North, New Zealand.

Abstract

Viscous solution flow down vertical cylindrical channels and planar cracks, with simultaneous molecular diffusion of the solute into the surrounding soil, was modelled. Chloride and phosphate were chosen as representative of non-sorbed and adsorbed ions respectively. In channels at least 0·2 mm in diameter, and cracks at least 0·1 mm wide, almost instantaneous preferential movement of both chloride and phosphate was predicted. Little or no preferential movement was predicted in smaller channels or cracks. For example phosphate was predicted to move to a depth of 200 mm within 10 min in saturated soil containing 0·2 mm diameter continuous channels. However, it would take phosphate over 2 months to reach the same depth in similar soil with the same hydraulic conductivity, but containing only 0·05 mm diameter channels.

Channels and cracks permitting preferential solute movement would be solution-filled only at pressure potentials above −0·2 m, so such movement can only occur in near saturated soil. Although highly idealized soil-void geometries were assumed, the results have a number of practical implications related to the movement of nutrients and pollutants in field soils.

Introduction

Growing concern for groundwater and stream pollution, and continued interest in salt and fertilizer leaching, are the main reasons for the present strong interest in the movement of solutes in soil. Theory describing miscible fluid displacement in uniform soils exists (Nielsen and Biggar 1962; Kirkham and Powers 1972), and experimental results for packed columns of sand or soil aggregates are in general accord with the theory (Biggar and Nielsen 1967). Hydrodynamic dispersion occurs at the interface between the displacing and displaced solution, but in general non-adsorbed solute applied at one end of a saturated column breaks through after the application of approximately one pore volume of solution. Adsorbed solutes appear in the effluent even later, after a number of pore volumes have been displaced.

Field experiments have often shown quite different behaviour, however, with some of the applied solute moving through the soil much faster than expected. Kolenbrander (1970) found surface applied nitrate became more dispersed in cracking-clay soils than in more uniform soils, while Kissel *et al.* (1973), using a solution of chloride and fluorescein dye, showed preferential movement down the cracks in a swelling-clay soil. Even in a weakly structured loamy sand, field experiments by Wild and Babiker (1976) showed asymmetric leaching patterns for both chloride and nitrate. They attributed this to preferential solute movement down larger channels, such as earthworm channels typically 5 mm in diameter, and possible smaller channels.

Comparisons between chloride breakthrough curves for 'undisturbed' cores and repacked columns for a silt loam (Ellrick and French 1966), and a swelling-clay (Kissel *et al.* 1973), show the chloride appearing earlier from the cores in both cases. The authors attributed this to the presence of continuous channels and cracks in the undisturbed cores and their absence in the repacked columns. Bouma *et al.* (1976) found very pronounced preferential chloride movement in saturated cores of Dutch 'knik' clay soils, with the solute appearing in the effluent after the application of only a thousandth of a pore volume of solution. They attributed this to the bulk of the flow being through a relatively few large, continuous soil pores. Other data, showing preferential chloride movement in saturated cores of silty clay loam soil with sub-angular blocky structure, are given by Anderson and Bouma (1977). The same authors (Anderson and Bouma 1973) earlier applied a water–Rhodamine D dye mixture to soil cores which were then dried, impregnated with plastic, sectioned, and polished. They present diagrams showing dye movement down continuous channels and planar voids, but not through the bulk of the soil.

While preferential solute movement through relatively large continuous voids is well documented, no attempts to describe the phenomenon theoretically appear to have been made. The existing miscible displacement theory already referred to treats the soil as a continuum on a 'macroscopic' level (Raats and Klute 1968), and does not describe fluid and solute behaviour at a 'microscopic' level in and adjacent to individual voids. An exception is the theory of Passioura (1971) for hydrodynamic dispersion in aggregated media, which is developed from a microscopic viewpoint for viscous flow in the intra-aggregate pore space, coupled with molecular diffusion within the aggregates. It is predicted that slight preferential movement may occur in aggregated media under certain conditions (see Fig. 2 of Passioura 1971). However, the size of the intra-aggregate voids is not considered explicitly, and neither is the effect of solute adsorption.

The work described here is also microscopic in viewpoint, but involves a different approach. The effect of isolated relatively large channels or cracks of known size on solute movement, with and without solute adsorption, is investigated. Particular attention is addressed to three questions. Firstly, how large does a continuous channel or crack have to be for solutes to move through it preferentially? Secondly, at what water potential do such pores drain, and so cease to conduct solutes? Thirdly, as adsorbed and non-adsorbed ions are known to move differentially in packed soil columns, to what degree to strongly adsorbed solutes move preferentially through larger continuous voids?

Theory

Brewer (1964) suggests the larger interconnected soil voids fall into two broad classes, channels and planes. Two idealized pore geometries will be considered here, vertical cylindrical channels, and vertical planar voids.

Cylindrical Channels

The Hagen–Poiseuille equation for viscous flow through a hollow cylinder, applied to gravity induced flow in a vertical channel, gives (Childs 1969)

$$q = (\pi \rho_l g a^4)/(8\eta), \qquad (1)$$

where q is the flow rate ($m^3 s^{-1}$), ρ_l is the fluid density ($kg m^{-3}$), g is the acceleration due to gravity ($m s^{-2}$), a is the radius of the tube (m), and η the viscosity (Pa s). The solute flux into such a tube is qC_i (mol s^{-1}) where C_i is the concentration of the applied solution (mol m^{-3}).

The simple model, used for flow through a saturated soil containing channels, considers viscous flow down a number of uniformly spaced cylindrical channels of a certain diameter, with negligible viscous flow in the rest of the soil. The fourth power relationship between pore radius and flow means that, while the presence of a few larger channels may make only a very minor contribution to the total soil porosity, nearly all the flow is through these channels (Bouma and Anderson 1973).

In the soil surrounding the cylindrical channels, assuming radial symmetry, molecular diffusion of the solute may be described by (Gardner 1965)

$$j = -D_s f dC/dr, \tag{2}$$

where j is the solute flux crossing unit cross-sectional area per unit time (mol $m^{-2} s^{-1}$), D_s is the effective solute diffusivity in the soil ($m^2 s^{-1}$), f is the soil porosity ($m^3 m^{-3}$), C is the concentration of the soil solution (mol m^{-3}), and r is radial distance (m). It is assumed that the channels contribute negligibly to f. For transient diffusion of a solute following a linear adsorption isotherm

$$\frac{\partial C}{\partial t} = \frac{1}{r}\frac{\partial}{\partial r}\left(\frac{rD_s}{1+R}\frac{\partial C}{\partial r}\right) \tag{3}$$

where t is time (s), and R is the dimensionless ratio of the amount of adsorbed solute to solution solute per unit soil volume. With R defined this way, fR corresponds to the capacity factor of Olsen *et al.* (1965). For non-sorbed ions R is zero, unless negative adsorption occurs. Non-linear adsorption is readily treated numerically, but would constitute an unwarranted complication in the present study.

At any instant the change in average solute flow in the cylindrical channels due to diffusion into the surrounding soil is given by

$$q\frac{\partial C}{\partial z} = 2\pi a D_s f \left.\frac{\partial C}{\partial r}\right|_{r=a}, \tag{4}$$

where z is the vertical coordinate. There will be some variation in solute concentration across the channel, and hydrodynamic dispersion will occur in the channel itself (Taylor 1953). However, the molecular diffusivity of solute in the channel is greater than in the surrounding soil. It is assumed that C at $r = a$ is the average concentration in the channel at that depth. Radial concentration gradients within the channel would result in less diffusion into the surrounding soil, and so more preferential solute movement down the channel than predicted.

If values for the saturated hydraulic conductivity K ($m s^{-1}$) and the channel radius are assumed, then $n = K/q$, where n is the number of vertical channels per unit cross-section of soil (m^{-2}). The effective maximum radius of the diffusion shell around each channel is $(\pi n)^{-\frac{1}{2}}$. For short times and/or large channels, however, the diffusion is effectively into a semi-infinite soil volume.

A computer programme is CSMP73 was written to solve equations (3) and (4) simultaneously. For the larger channels considered, the solute flow down the channel is much greater than the radial diffusion, so the concentration in the tube varies

only slightly with time and depth. In such cases the analytical solution for the radial diffusive flux at $r = a$ when C is constant there, and the diffusion volume effectively semi-infinite, may be used to estimate the small changes that occur in C in the channel, and to provide a check for the computer solution of equation (3). The results of the analytical solution are presented graphically by Carslaw and Jaeger (1959); when applying analagous solutions for heat flow in solids to solute diffusion into soil, the thermal conductivity is put equal to D_s, the thermal diffusivity equal to $D_s/(1 + R)$, temperature equal to concentration, and the flux at $r = a$ is multiplied by the porosity.

The pressure potential at which a cylindrical channel will drain, assuming zero contact angle, is given by

$$\psi = -2s/(\rho_f g a), \tag{5}$$

where s is the surface tension between the solution and air (N m^{-1}).

Planar Voids

The gravity-induced flow down a vertical planar slit is (Childs 1969)

$$p = (\rho_f g d^3)/(12\eta), \tag{6}$$

where p is the flow rate per unit length of slit (m^3 m^{-1} s^{-1}) and d is the width of the slit (m). If viscous flow is assumed to occur only in the slits, then $m = K/p$, where m is the length of slit per unit horizontal cross-section of soil (m^{-1}).

A commonly observed pattern for interpedal vertical cracks is approximately hexagonal in the horizontal plane (Brewer 1964; Bouma and Anderson 1973). A regular hexagon with side length c has a perimeter of $6c$ and an area of $3c^2 \sin \frac{1}{3}\pi$. Each slit serves as a side for two hexagons, so assuming the area in the slits makes a negligible contribution to the total cross-sectional area,

$$c = 1/(m \sin \tfrac{1}{3}\pi). \tag{7}$$

However, to make the description of diffusion away from the slits more tractable, the hexagonal geometry was approximated by annuli constructed to have the same area and outer perimeter. The required annulus is

$$\begin{aligned} Y &= 3c/\pi \\ y &= c[(9/\pi^2)(3/\pi)\sin \tfrac{1}{3}\pi]^{\frac{1}{2}}, \end{aligned} \tag{8}$$

where Y and y are the outer and inner radii of the annulus respectively. Fig. 1 shows a hexagon with the annulus used to approximate it superposed. Equation (3) now applies, and the solution concentration in the slits is described by an equation very similar to equation (4)

$$\frac{p}{2}\frac{\partial C}{\partial z} = -2\pi Y D_s f \left.\frac{\partial C}{\partial r}\right|_{r=Y}. \tag{9}$$

To take account of diffusion into the soil on both sides of the slit $p/2$ rather than p appears. Equations (3) and (9) were solved simultaneously using a very similar computer programme to the one previously referred to.

For wider cracks an analytical solution for diffusion into the soil can be used for comparison, in this case for diffusion into a semi-infinite medium from a planar

source. Adaptation of the Carslaw and Jaeger (1959) solution in the manner described previously gives

$$J = D_s C_i f\left[\frac{\pi D_s t}{1+R}\right]^{-\frac{1}{2}}, \tag{10}$$

where J is the solute flux due to diffusion out of the slit (mol m^{-2} s^{-1}).

The pressure potential at which a planar void will drain is

$$\psi = -2s/(\rho_l g d). \tag{11}$$

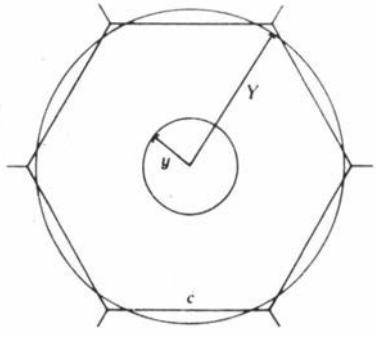

Fig. 1. A regular hexagon with an annulus having the same area and outer perimeter superposed. The symbols are defined in the text.

Diffusion Across the Soil Surface

It is possible that when a solution is ponded on the soil surface, diffusion across the surface may significantly lower the concentration of the solution entering the larger voids in which preferential movement occurs. The maximum rate of diffusion across the surface may be found by assuming $C = C_i$ at the soil surface, and that the soil initially contains no solute and is effectively semi-infinite, reasonable assumptions for soil with preferential movement down widely spaced larger voids and relatively little movement through the bulk of the soil. The solute flux across the surface (J) is then also given by equation (10). If $J/K \ll C_i$ for all except very short times, the concentration of the solution entering the larger voids (C_s) maybe approximated as

$$C_s = C_i - J/K. \tag{12}$$

Computations

Chloride and phosphate movement through 200 mm depth of hypothetical soil with a porosity of 0·5 and a saturated hydraulic conductivity of 10 mm/h was modelled. Thus the time for one pore volume of solution to pass through this soil depth was 10 h. The diffusivity of chloride in the soil was taken as 6×10^{-10} m^2 s^{-1}. When compared with the diffusivity of sodium chloride in dilute solution of $1{\cdot}6 \times 10^{-9}$ m^2 s^{-1} (Robinson and Stokes 1959) this gives a tortuosity–transmission factor of 0·4, a value in general agreement with the values found near saturation by Porter *et al.* (1960). In simulating phosphate movement, the diffusivity of phosphate in solution of 5×10^{-10} m^2 s^{-1} (Olsen *et al.* 1965) was multiplied by the same tortuosity factor to give a soil diffusivity of 2×10^{-10} m^2 s^{-1}. The factor $(1 + R)$ was taken as unity for chloride and 200 for phosphate, a value within the range found

by Olsen *et al.* (1965) and Olsen and Watanabe (1970). The viscosity of the solution was taken as 10^{-3} Pa s, its density as 10^{3} kg m^{-3}, and the surface tension between the solution and air as $7{\cdot}3 \times 10^{-2}$ N m^{-1}.

In the CSMP73 programmes, the soil volume around each channel or inside each slit was divided into four layers along the z-axis of 0·02, 0·04, 0·06 and 0·08 m thickness. Each layer was divided into usually eight, or sometimes four, geometrically spaced annuli. Each annulus was 1·2–1·8 times as thick as the one preceding it, with the thinnest annulus adjacent to the channel or slit. The method used to solve equation (3) was very similar to that described by de Wit and van Keulen (1972). The rectangular integration method was used, with finite difference methods to compute the flux in and out of each annulus. The thickness of the first annulus was chosen to minimize computer time, while avoiding serious computational errors at short times. This could be checked by comparing the computed flux into the first annulus in the top layer with the analytical solution. The integration time increment was chosen so that C/C_i in the first annulus in the top layer was less than 0·2 after the first iteration, ensuring numerical stability. To account for adsorption the real

Table 1. Channel sizes assumed and related data

Diameter of channels (mm)	Maximum diffusion radius (mm)	Pressure potential to drain (m)	Fraction of soil volume occupied by channels
0·05	0·4	−0·60	0·0036
0·1	1·6	−0·30	0·0009
0·2	6·6	−0·15	0·0002
0·4	26	−0·07	0·00006

volume of each annulus was multiplied by $(1 + R)$ to give an effective volume. If, as sometimes happened for narrow channels or slits at short times, the computed flux into the first annulus was greater than the solute flow through the channel or slit at that depth, then the flux was put equal to $C_L q/L$ for channels or $C_L p/2L$ for slits, where L is the thickness of the layer and C_L the concentration of solution entering the layer. For solution of this kind of transport problem in soil, CSMP was found convenient and inexpensive to use.

Four channel sizes were considered, with different spacings between channels so as to give the same hydraulic conductivity. The diameters assumed, and related data, are given in Table 1. The channels constitute a negligible fraction of the total pore volume, in all cases less than 0·8%. The Reynolds number for the largest channel considered is 160, so equation (1) would apply in all cases (Bird *et al.* 1960).

Computed breakthrough curves for chloride and phosphate are shown in Fig. 2. C_e is the solution concentration at 200 mm depth. For soil with 0·4 mm diameter channels both ions broke through effectively instantaneously, with C_e/C_i reaching 0·8 or higher before 0·01 pore volumes or 6 min had passed. The spacing between the channels was such that even after 20 h there was no interference between the diffusion shells around each channel. Further computations, assuming a 2 m soil depth also containing 0·4 mm vertical channels and the same K, showed C_e/C_i still reaching 0·8 after 0·01 pore volumes or 1 h.

The breakthrough curves for 200 mm soil depth containing 0·2 mm diameter channels also show marked preferential movement of both ions down the channels. After 20 h or two pore volumes there was some interference between adjacent diffusion shells for chloride, but not for phosphate.

For soil containing 0·1 mm diameter channels the breakthrough curve for chloride shows little preferential movement and almost 'classical' behaviour, resem-

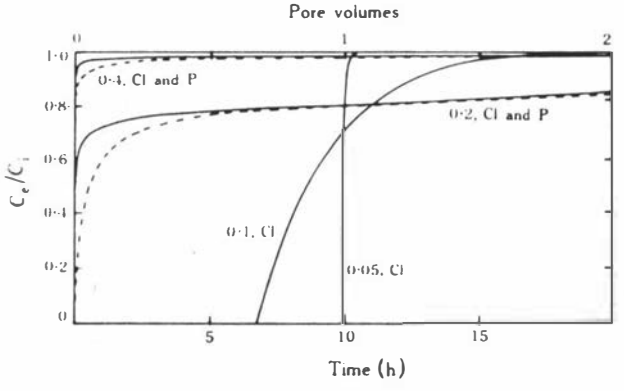

Fig. 2. Breakthrough curves for chloride (———) and phosphate (– – – –) moving through 200 mm of soil depth containing cylindrical channels. The numbers on the curves are channel diameters (mm). C_e/C_i is the ratio of effluent to influent concentration.

bling the S-shaped breakthrough curves symmetrical about one pore volume found for sand or disturbed soil (Biggar and Nielsen 1967). The breakthrough curve for phosphate in this case is shown in Fig. 3. Note that the horizontal scale has been expanded by a factor of 200, and phosphate is not predicted in the effluent until four pore volumes or 2 days have passed, and then the effluent concentration rises only very slowly. For soil containing 0·05 mm diameter channels very steep breakthrough

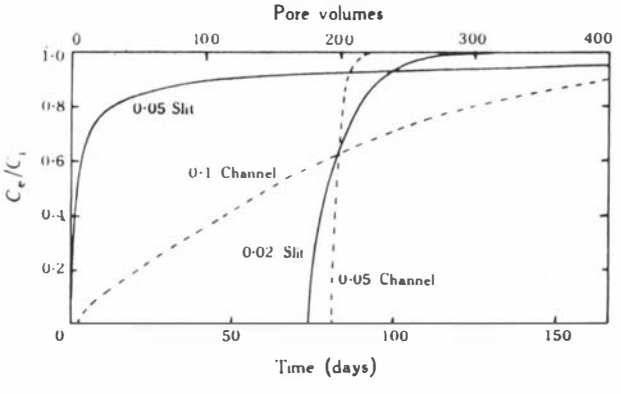

Fig. 3. Breakthrough curves for phosphate in soil containing channels (– – – –) or slits (———). The numbers on the curves are either the channel diameter or slit width (mm).

curves, suggestive of 'piston flow' (Nielsen and Biggar 1962) are predicted for both ions (Figs 2 and 3). Similar steep breakthrough curves have been found for chloride in uniformly sized glass beads (Biggar and Nielsen 1967). Phosphate is not predicted in the effluent until 194 pore volumes or 80 days have passed.

Four planar void widths were considered, again spaced so as to give the same hydraulic conductivity of 10 mm/h. The slit widths assumed and related data are

given in Table 2. The slits occupy only a small part of the total porosity, less than 2% in all cases. The computed breakthrough curves are shown in Figs 3 and 4.

Fig. 4 shows that with 0·2 mm slit width both chloride and phosphate appear almost instantaneously in the effluent. With 0·1 mm slit width, preferential movement still occurs with both ions, but is less pronounced for phosphate. With 0·05 mm slit width, chloride still appears within a few minutes, but phosphate (shown in both Figs 3 and 4) is not predicted in the effluent until 7 h have passed.

Table 2. Planar void widths assumed and related data

Width of slit (mm)	Outer radius of soil annulus enclosed by slit (mm)	Pressure potential to drain (m)	Fraction of soil volume occupied by slits
0·02	2·6	−0·74	0·0085
0·05	41	−0·30	0·0014
0·1	320	−0·15	0·0003
0·2	2600	−0·07	0·0001

With 0·02 mm width slits, the data in Fig. 4 show a steep breakthrough curve for chloride which appears after one pore volume, indicating negligible preferential movement. In Fig. 3 the curve for phosphate movement in the same soil shows a similar shape, but with no phosphate appearing in the effluent until 176 pore volumes or 73 days have passed.

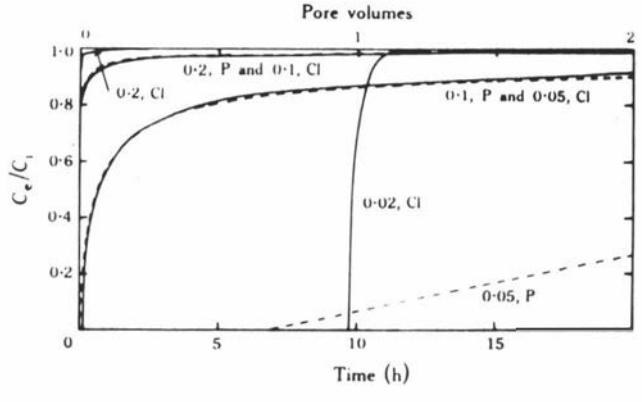

Fig. 4. Breakthrough curves for chloride (———) or phosphate (– – – –) moving through 200 mm depth of soil containing vertical planar slits. The numbers on the curves are slit widths (mm).

The computations described do not take account of diffusion across the soil surface from a ponded solution before it enters the larger voids. Fig. 5 shows the solutions to equations (10) and (12) for the values of K, f, D_s and R used in the computations, and gives an indication of the importance of such diffusion. The curves for both chloride and phosphate indicate that when pronounced preferential movement does occur, the effect of surface diffusion may be the same order of magnitude as the radial diffusion out from the larger voids in the soil. However, in these cases both diffusion processes effect only relatively slight changes in the concentration of the percolating solution.

Discussion

The two soil–void geometries considered are highly idealized, so care must be taken in interpreting the significance of these results to solute movement in field soils. While only continuous vertical channels and slits of uniform width have been considered, in real soil a short constriction in an otherwise uniform channel or slit may very significantly affect its solution conducting capacity.

Some of the results of the analysis were unexpected, in particular the strongly contrasting behaviour predicted for solute movement through 0·2 mm and 0·05 mm diameter channels. Phosphate could move through 200 mm long 0·2 mm diameter channels in soil within a few minutes, but would not emerge from 0·05 mm channels until over 2 months after it was applied. The minimum channel diameter for preferential flow of both non-sorbed and strongly adsorbed solutes is approximately 0·2 mm. The minimum crack width for preferential flow is approximately 0·1 mm.

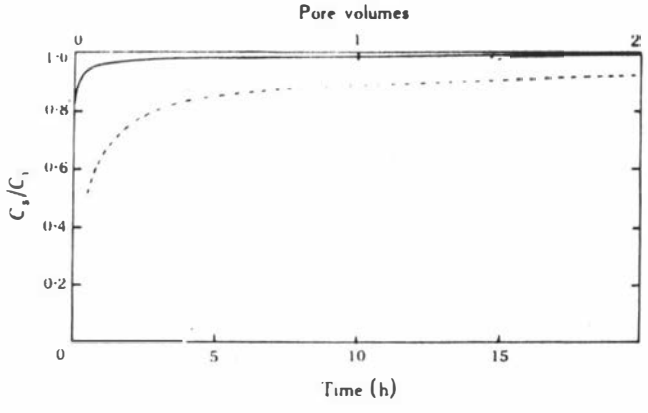

Fig. 5. Estimated concentration change due to diffusion through soil surface from ponded solution before it enters larger voids, for chloride (———) and phosphate (– – – –).

The less pronounced influence of sorption on preferential movement in channels as compared to planar voids is a result of the different diffusion geometries in the soil adjacent to the voids. For radial diffusion from a channel, the soil close to the channel provides a larger part of the 'diffusion resistance' than for planar voids, but contains a relatively small soil volume per unit radial distance. Thus the diffusive flux there quickly approaches a steady state, and so is less dependent on sorption.

In the root-zone horizons of many soils it is probable there are some channels greater than 0·2 mm diameter resulting from the activity of roots and soil fauna, and so some preferential solute movement is likely. Seminal and first lateral roots of wheat have been measured as 0·3–0·45 mm in diameter (Russell 1973), and presumably when decayed may leave channels approaching the same dimensions. Structural cracks are also common, particularly in swelling soils. Although cracks often close partly or completely when the soil is at or near saturation, the associated swelling takes some time, and meanwhile preferential water and solute movement can take place.

The data presented here for soil containing continuous larger voids show that preferential solute movement in such soil may be much more pronounced than indicated by Passioura's theory for aggregated media. His maximum dispersion occurred in the limiting case of zero Brenner number and gave C_e/C_i equal to only 0·2 after 0·2 of a pore volume.

Practical Implications

The results have several practical implications. Channels larger than 0·2 mm in diameter and planar voids wider than 0·1 mm will be air-filled if the pressure potential in the soil is less than −0·15 m, so preferential solute movement can occur only in soil considerably wetter than the usual 'field capacity'. If it does occur, both non-sorbed and strongly adsorbed ions will move preferentially. When potential groundwater pollutants are applied by sprinkler irrigation, and a long solute residence time in the topsoil is desired to allow biodegradation or plant uptake, the application rate or frequency should be such that the soil stays slightly unsaturated, and the pressure potential is maintained below −0·15 m. Preferential movement would not then occur.

Another implication is that movement of solutes, particularly strongly adsorbed solutes, through columns of disturbed and repacked soil, is likely to be very different from movement through undisturbed soil in the field. The soil chemical properties may be relatively unchanged, but in many situations the pore geometry may be more important than the sorption capacity in determining the movement of nutrients and pollutants. Coarser-textured soils with high saturated hydraulic conductivity are often considered unsuitable for effluent disposal, but finer-textured soils with a lower conductivity, but containing cracks or channels, may in fact allow more groundwater pollution.

While the movement of solutes into the soil has been considered here, the results are of course just as relevant to the leaching of solutes out of soils. When water movement occurs preferentially, the concentration of the percolating water will be very much lower than the concentration in the bulk of the soil, and little leaching will take place.

References

Anderson, J. L., and **Bouma, J.** (1973). Relationships between saturated hydraulic conductivity and morphometric data of an argillic horizon. *Soil Sci. Soc. Am. Proc.* **37**, 408–13.

Anderson, J. L., and **Bouma, J.** (1977). Water movement through pedal soils: I. Saturated flow. *J. Soil Sci. Soc. Am.* **41**, 413–18.

Bird, R. B., Stewart, W. E., and **Lightfoot, E. N.** (1960). 'Transport Phenomena.' (John Wiley: New York.)

Biggar, J. W., and **Nielsen, D. R.** (1967). Miscible displacement and leaching phenomenon. *In* 'Irrigation of Agricultural Lands'. *Agronomy* **11**, 254–74. (Eds. R. M. Hagan, H. R. Haise and T. W. Edminster.) (Am. Soc. Agron.: Madison, Wisc.)

Bouma, J., and **Anderson, J. L.** (1973). Relationships between soil structure characteristics and hydraulic conductivity. *In* 'Field Soil Water Regime'. (Eds. R. R. Bruce *et al.*) (Soil Sci. Soc. Am.: Madison, Wisc.)

Bouma, J., Dekker, L. W., and **Verlinden, H. L.** (1976). Drainage and vertical hydraulic conductivity of some Dutch 'knik' clay soils. *Agric. Water Manage.* **1**, 67–78.

Brewer, R. (1964). 'Fabric and Mineral Analysis of Soils.' (John Wiley: New York.)

Carlslaw, H. S., and **Jaeger, J. C.** (1959). 'Conduction of Heat in Solids.' 2nd Edn. (Oxford Univ. Press: London.)

Childs, E. C. (1969). 'An Introduction to the Physical Basis of Soil Water Phenomena.' (John Wiley: London.)

Gardner, W. R. (1965). Movement of nitrogen in soil. *In* 'Soil Nitrogen'. *Agronomy* **10**, pp. 550–72. (Eds. W. V. Bartholomew and F. E. Clark.) (Am. Soc. Agron.: Madison, Wisc.)

Kirkham, D., and **Powers, W. L.** (1972). 'Advanced Soil Physics.' (John Wiley: New York.)

Kissel, D. E., Ritchie, J. T., and **Burnett, E.** (1973). Chloride movement in undisturbed swelling clay soil. *Soil Sci. Soc. Am. Proc.* **37**, 21–4.

Kolenbrander, G. J. (1970). Calculation of parameters for the evaluation of the leaching of salts under field conditions, illustrated by nitrate. *Plant Soil* **32**, 439–53.

Nielsen, D. R., and **Biggar, J. W.** (1962). Miscible displacement: III. Theoretical considerations. *Soil Sci. Soc. Am. Proc.* **26**, 216–21.

Olsen, S. R., Kemper, W. D., and **van Schaik, J. C.** (1965). Self-diffusion coefficients of phosphorus in soil measured by transient and steady-state methods. *Soil Sci. Soc. Am. Proc.* **29**, 154–8.

Olsen, S. R., and **Watanabe, F. S.** (1970). Diffusive supply of phosphorus in relation to soil textural variations. *Soil Sci.* **110**, 318–27.

Passioura, J. B. (1971). Hydrodynamic dispersion in aggregated media: 1. Theory. *Soil Sci.* **111**, 339–44.

Porter, L. K., Kemper, W. D., Jackson, R. D., and **Stewart, B. A.** (1960). Chloride diffusion in soils as influenced by moisture content. *Soil. Sci. Soc. Am. Proc.* **24**, 460–3.

Raats, P. A. C., and **Klute, A.** (1968). Transport in soils: The balance of mass. *Soil. Sci. Soc. Am. Proc.* **32**, 161–6.

Robinson, R. A., and **Stokes, R. H.** (1959). 'Electrolyte Solutions.' 2nd Edn. (Butterworths: London.)

Russell, E. W. (1973). 'Soil Conditions and Plant Growth.' 10th Edn. (Longman: London.)

Taylor, G. I. (1953). Dispersion of soluble matter in solvent flowing slowing through a tube. *Proc. R. Soc.* (*London*) **219A**, 186–203.

Wild, A., and **Babiker, I. A.** (1976). The asymmetric leaching pattern of nitrate and chloride in a loamy sand under field conditions. *J. Soil. Sci.* **27**, 460–6.

de Wit, G. T., and **van Keulen, H.** (1972). 'Simulation of Transport Processes in Soils.' (Pudoc: Wageningen.)

Manuscript received 5 December 1977

C.2 List of Symbols in CSMP Programmes.

A, B, C, D, E, and F	=	Suffix indicating layer from the soil surface downwards, with A nearest the surface
BB	=	(1 + R), where R is the retardation factor described in text
C	=	relative concentration of solutes in soil solution
CSA, CSB,...	=	relative concentration of solute in macropores
CSO	=	concentration imposed at the soil surface
D	=	molecular diffusion coefficient of solutes in soil (L^2 T^{-1}) (for programme in Section C. 2.2 only)
DELT	=	computation time interval (T)
DIFC	=	molecular diffusion coefficient of solute in soil (L^2 T^{-1}) (for programme in Section C. 2.3. only)
DIFD	=	distance between the centers of two succeeding annuli (L) (see Fig. C.1 and C.2)
DIST	=	distance from the centre of the channel to the middle of any annulus (L) (see Fig. C.1 and C.2)
F	=	flux of solute between two adjacent annuli (M L^{-2} T^{-1})

FINTIM	=	final time for computation (T)
FLOW	=	viscous flow rate of solution in the cylindrical channel ($L^3\ T^{-1}$)
LA, LB, ...	=	thickness of column layer (L)
N	=	number of annuli around the channel
OUTDEL	=	time interval when output is given (T)
PI2	=	2π
POR	=	water filled porosity
RAD	=	radius of cylindrical channel (L)
RITCOM	=	a factor giving a geometric increase in the thickness of adjacent annuli
S	=	net flux of solute into or out of an annulus ($M\ L^{-1}\ T^{-1}$)
SFLUX	=	flux of solute across the soil surface ($M\ L^{-2}\ T^{-1}$)
TCOM	=	thickness of annulus (L) (see Fig. C.1 and C.2)
THCKNS	=	maximum diffusion radius from the channel (L)
TOPA	=	cross-sectional area of the soil surface (L^2)
VA, VB, ...	=	relative amount of solute in each soil layer ($M\ L^{-1}$)

C. 3 Programme for miscible displacement of solutes in a soil with uniform vertical cylindrical channels.

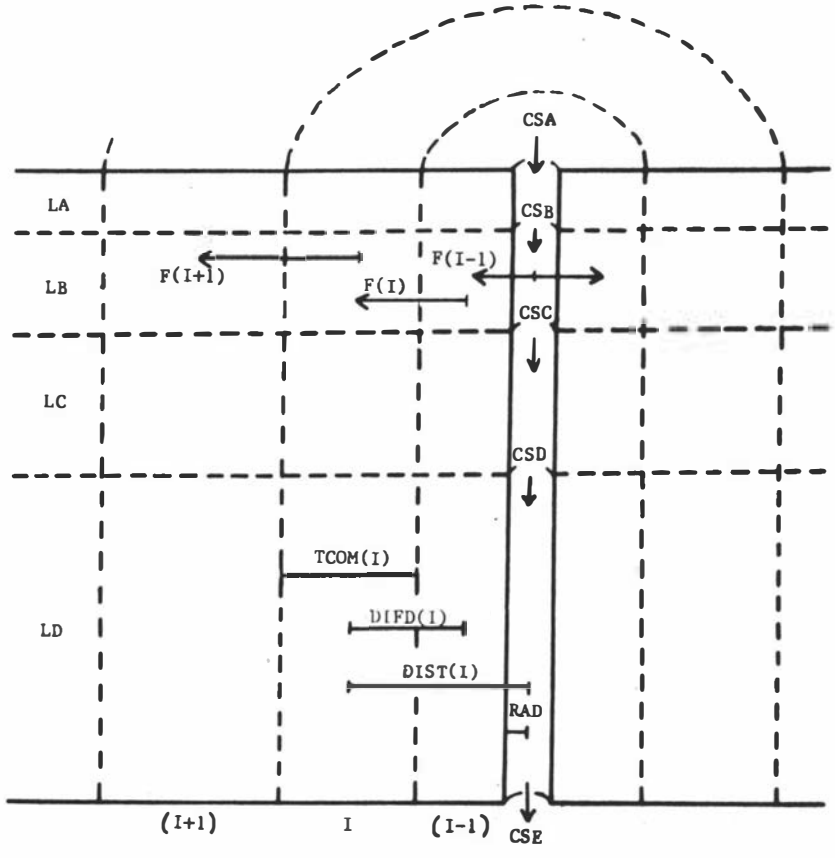

Fig. C.1 Geometry of the system and symbols used in the programme for miscible displacement of solutes in a soil column with uniformly spaced vertical cylindrical channels. Arrows indicate direction of flow.

```
* CSMP73 INPUT LIST *  25.003.000
0001        METHOD RECT
0002        TITLE RADIAL DIFFUSION
0003        TIMER FINTIM=25,DELT=0.1,OUTDEL=0.2
0004        PARAM D=1.2E-04,BB=70
0005        PARAM RAD=0.023,THICKNS=0.3
0006        PARAM TOPA=17.35,POR=0.365
0007        PARAM RITCUM=1.6,PI2=6.2832
0008        PARAM LA=1,LB=1,LC=1,LD=1.5
0009        STORAGE AREA(9),VOL(8),C(8),F(9),S(8),TCUM(8),DIFD(8),DIST(8),X(8)
0010        STORAGE VA(8),VB(8),VC(8),VD(8)
0011        FIXED I,N
0012        INITIAL
0013        * V IS AMOUNT SALT, S IS NET FLOW, TIME IN MINS, DIST IN CM,
0014        NOSORT
0015              N=8
0016              CSO=1.
0017              DIFC=POR*D
0018              FLOW=2.31E06*RAD**4.
0019              F(N+1)=0.
0020              TCUM(1)=(THICKNS-RAD)*(RITCUM-1.)/(RITCUM**N-1.)
0021              AREA(1)=(0.25*TCUM(1)*RAD)*PI2
0022              DIFD(1)=0.5*TCUM(1)
0023              DIST(1)=DIFD(1)*RAD
0024              X(1)=AREA(1)*DIFC/DIFD(1)
0025              DO 1 I=2,N
0026              TCUM(I)=RITCUM*TCUM(I-1)
0027              DIFD(I)=0.5*(TCUM(I-1)+TCUM(I))
0028              DIST(I)=DIST(I-1)+DIFD(I)
0029            1 CONTINUE
0030              DO 5 I=1,N
0031              VA(I)=0.
0032              VB(I)=0.
0033              VC(I)=0.
0034              VD(I)=0.
0035              VOL(I)=DIST(I)*PI2*TCUM(I)*POR*BB
0036              AREA(I+1)=(DIST(I)+0.5*TCUM(I))*PI2
0037            5 CONTINUE
0038              DO 70 I=2,N
0039              X(I)=AREA(I)*DIFC/DIFD(I)
0040           70 CONTINUE
0041              WRITE(6,100)DIST
0042              WRITE(6,101)
0043          100 FORMAT(1H ,4HDIST//(8F12.5))
0044          101 FORMAT(1H1)
0045        DYNAMIC
0046        NOSORT
0047              SFLUX=POR*D*CSO/SQRT(0.5*PI2*D*(TIME+DELT/2)/BB)
0048              CSA=CSO-(SFLUX*TOPA)/FLOW
0049              IF(CSA)91,92,92
0050           91 CSA=0
0051              SFLUX=FLOW*CSO/TOPA
0052           92 CONTINUE
0053              DO 2 I=1,N
0054            2 C(I)=VA(I)/VOL(I)
0055              F(1)=(CSA-C(1))*X(1)
0056              CSB=CSA-F(1)*LA/FLOW
0057              IF(CSB)51,51,52
0058           51 F(1)=CSA*FLOW/LA
0059              CSB=0.
0060           52 CONTINUE
0061              FA=F(1)
0062              DO 3 I=2,N
0063            3 F(I)=(C(I-1)-C(I))*X(I)
0064              DO 4 I=1,N
0065            4 S(I)=F(I)-F(I+1)+(SFLUX*VOL(I))/(LA*BB)
0066              SA1=S(1)
0067              SA2=S(2)
0068              SA3=S(3)
0069              SA4=S(4)
0070              SA5=S(5)
0071              SA6=S(6)
0072              SA7=S(7)
0073              SA8=S(8)
0074              CA1=C(1)
0075              CA4=C(4)
0076              CA8=C(8)
0077              DO 6 I=1,N
0078            6 C(I)=VB(I)/VOL(I)
0079              F(1)=(CSB-C(1))*X(1)
0080              CSC=CSB-F(1)*LB/FLOW
0081              IF(CSC)53,53,54
0082           53 F(1)=CSB*FLOW/LB
0083              CSC=0.
0084           54 CONTINUE
0085              DO 7 I=2,N
0086            7 F(I)=(C(I-1)-C(I))*X(I)
0087              DO 8 I=1,N
0088            8 S(I)=F(I)-F(I+1)
0089              SB1=S(1)
0090              SB2=S(2)
0091              SB3=S(3)
0092              SB4=S(4)
0093              SB5=S(5)
0094              SB6=S(6)
0095              SB7=S(7)
0096              SB8=S(8)
0097              DO 9 I=1,N
0098            9 C(I)=VC(I)/VOL(I)
0099              F(1)=(CSC-C(1))*X(1)
```

```
0100            CSD=CSC*F(1)*LC/FLOW
0101            IF(CSD) 55,55,56
0102         55 F(1)=CSC*FLOW/LC
0103            CSD=0.
0104         56 CONTINUE
0105            DO 10 I=2,N
0106         10 F(I)=(C(I-1)-C(I))*A(I)
0107            DO 11 I=1,N
0108         11 S(I)=F(I)*F(I+1)
0109            SC1=S(1)
0110            SC2=S(2)
0111            SC3=S(3)
0112            SC4=S(4)
0113            SC5=S(5)
0114            SC6=S(6)
0115            SC7=S(7)
0116            SC8=S(8)
0117            DO 12 I=1,N
0118         12 C(I)=VOL(I)/VOL(1)
0119            F(1)=(CSD-C(1))*A(1)
0120            CSE=CSD*F(1)*LC/FLOW
0121            IF(CSE) 57,57,58
0122         57 F(1)=CSD*FLOW/LC
0123            CSE=0.
0124         58 CONTINUE
0125            DO 13 I=2,N
0126         13 F(I)=(C(I-1)-C(I))*A(I)
0127            DO 14 I=1,N
0128         14 S(I)=F(I)*F(I+1)
0129            SD1=S(1)
0130            SD2=S(2)
0131            SD3=S(3)
0132            SD4=S(4)
0133            SD5=S(5)
0134            SD6=S(6)
0135            SD7=S(7)
0136            SD8=S(8)
0137            CD4=C(4)
0138            CD6=C(8)
0139         SORT
0140         VA1=INTGRL(0.,SA1)
0141         VA2=INTGRL(0.,SA2)
0142         VA3=INTGRL(0.,SA3)
0143         VA4=INTGRL(0.,SA4)
0144         VA5=INTGRL(0.,SA5)
0145         VA6=INTGRL(0.,SA6)
0146         VA7=INTGRL(0.,SA7)
0147         VA8=INTGRL(0.,SA8)
0148         VB1=INTGRL(0.,SB1)
0149         VB2=INTGRL(0.,SB2)
0150         VB3=INTGRL(0.,SB3)
0151         VB4=INTGRL(0.,SB4)
0152         VB5=INTGRL(0.,SB5)
0153         VB6=INTGRL(0.,SB6)
0154         VB7=INTGRL(0.,SB7)
0155         VB8=INTGRL(0.,SB8)
0156         VC1=INTGRL(0.,SC1)
0157         VC2=INTGRL(0.,SC2)
0158         VC3=INTGRL(0.,SC3)
0159         VC4=INTGRL(0.,SC4)
0160         VC5=INTGRL(0.,SC5)
0161         VC6=INTGRL(0.,SC6)
0162         VC7=INTGRL(0.,SC7)
0163         VC8=INTGRL(0.,SC8)
0164         VD1=INTGRL(0.,SD1)
0165         VD2=INTGRL(0.,SD2)
0166         VD3=INTGRL(0.,SD3)
0167         VD4=INTGRL(0.,SD4)
0168         VD5=INTGRL(0.,SD5)
0169         VD6=INTGRL(0.,SD6)
0170         VD7=INTGRL(0.,SD7)
0171         VD8=INTGRL(0.,SD8)
0172         NOSORT
0173            VA(1)=VA1
0174            VA(2)=VA2
0175            VA(3)=VA3
0176            VA(4)=VA4
0177            VA(5)=VA5
0178            VA(6)=VA6
0179            VA(7)=VA7
0180            VA(8)=VA8
0181            VB(1)=VB1
```

```
0182              VB(2)=VB2
0183              VB(3)=VB3
0184              VB(4)=VB4
0185              VB(5)=VB5
0186              VB(6)=VB6
0187              VB(7)=VB7
0188              VB(8)=VB8
0189              VC(1)=VC1
0190              VC(2)=VC2
0191              VC(3)=VC3
0192              VC(4)=VC4
0193              VC(5)=VC5
0194              VC(6)=VC6
0195              VC(7)=VC7
0196              VC(8)=VC8
0197              VD(1)=VD1
0198              VD(2)=VD2
0199              VD(3)=VD3
0200              VD(4)=VD4
0201              VD(5)=VD5
0202              VD(6)=VD6
0203              VD(7)=VD7
0204              VD(8)=VD8
0205        PRINT FA,CA1,CAB,SFLUX,CSA,CSB,CSC,CSE
0206        END
0207        ENDJOB
```

DIST

0.02441 0.02725 0.03236 0.04155 0.05809 0.08707 0.14140 0.23791

RADIAL DIFFUSION — RECT INTEGRATION

TIME	FA	CA1	CAB	SFLUX	CSA	CSB	CSC	CSE
0.00	0.00	0.00	0.00	3.99196E-02	0.00	0.00	0.00	0.00
2.00000E-01	1.72686E-05	5.70276E-05	5.70276E-05	3.98196E-02	2.5779E-03	2.55306E-03	2.52776E-03	2.49506E-03
4.00000E-01	1.75476E-03	3.77056E-04	1.70936E-04	2.96776E-02	2.5057E-01	2.54036E-01	2.51526E-01	2.48356E-01
6.00000E-01	2.37806E-03	3.42386E-02	2.61406E-04	2.40936E-02	3.8143E-01	3.77996E-01	3.74576E-01	3.66196E-01
8.00000E-01	2.54696E-03	8.69366E-02	3.35026E-04	2.15936E-02	4.5907E-01	4.55336E-01	4.51746E-01	4.42716E-01
1.00000E 00	2.52826E-03	1.42736E-01	3.90716E-04	1.94206E-02	5.1331E-01	5.09646E-01	5.06006E-01	4.96706E-01
1.20000E 00	2.45316E-03	1.95796E-01	4.55646E-04	1.78006E-02	5.5394E-01	5.50406E-01	5.46876E-01	5.36136E-01
1.40000E 00	2.34136E-03	2.44016E-01	5.07606E-04	1.65336E-02	5.8584E-01	5.82466E-01	5.78906E-01	5.67076E-01
1.60000E 00	2.22506E-03	2.88696E-01	5.55706E-04	1.54906E-02	6.1175E-01	6.08346E-01	6.04776E-01	5.93136E-01
1.80000E 00	2.11416E-03	3.32466E-01	6.00686E-04	1.46376E-02	6.3334E-01	6.30296E-01	6.26726E-01	6.15066E-01
2.00000E 00	2.01296E-03	3.57816E-01	6.43096E-04	1.39046E-02	6.5169E-01	6.48706E-01	6.45086E-01	6.33656E-01
2.20000E 00	1.92256E-03	3.86846E-01	6.83326E-04	1.32726E-02	6.6753E-01	6.64756E-01	6.61906E-01	6.50076E-01
2.40000E 00	1.84276E-03	4.12356E-01	7.21676E-04	1.27196E-02	6.8139E-01	6.78726E-01	6.76076E-01	6.63446E-01
2.60000E 00	1.77206E-03	4.38486E-01	7.58406E-04	1.22296E-02	6.9364E-01	6.91066E-01	6.88536E-01	6.76216E-01
2.80000E 00	1.71106E-03	4.62476E-01	7.93686E-04	1.17926E-02	7.0459E-01	7.02126E-01	6.99656E-01	6.87496E-01
3.00000E 00	1.65686E-03	4.87556E-01	8.27676E-04	1.13996E-02	7.1444E-01	7.12056E-01	7.09636E-01	7.03696E-01
3.20000E 00	1.60876E-03	4.88496E-01	8.60516E-04	1.10436E-02	7.2336E-01	7.21046E-01	7.18726E-01	7.12976E-01
3.40000E 00	1.56606E-03	5.02876E-01	8.92316E-04	1.07106E-02	7.3150E-01	7.29246E-01	7.26906E-01	7.21546E-01
3.60000E 00	1.52706E-03	5.17946E-01	9.23166E-04	1.04206E-02	7.3896E-01	7.36766E-01	7.34556E-01	7.29056E-01
3.80000E 00	1.49296E-03	5.27876E-01	9.53146E-04	1.01466E-02	7.4583E-01	7.43666E-01	7.41526E-01	7.36146E-01
4.00000E 00	1.46146E-03	5.30836E-01	9.82326E-04	9.89236E-03	7.5219E-01	7.50086E-01	7.47976E-01	7.42706E-01
4.20000E 00	1.43246E-03	5.48096E-01	1.01086E-03	9.62676E-03	7.5809E-01	7.56026E-01	7.53956E-01	7.48076E-01
4.40000E 00	1.40576E-03	5.58366E-01	1.03856E-03	9.43726E-03	7.6359E-01	7.61566E-01	7.59536E-01	7.53466E-01
4.60000E 00	1.38096E-03	5.67126E-01	1.06566E-03	9.23216E-03	7.6873E-01	7.66736E-01	7.64746E-01	7.59706E-01
4.80000E 00	1.35706E-03	5.75336E-01	1.09226E-03	9.03976E-03	7.7355E-01	7.71596E-01	7.69636E-01	7.64736E-01
5.00000E 00	1.33586E-03	5.83056E-01	1.11816E-03	8.85896E-03	7.7808E-01	7.76156E-01	7.74226E-01	7.69406E-01
5.20000E 00	1.31526E-03	5.90336E-01	1.14366E-03	8.68856E-03	7.8233E-01	7.80456E-01	7.78526E-01	7.73806E-01
5.40000E 00	1.29566E-03	5.97216E-01	1.16856E-03	8.52706E-03	7.8638E-01	7.84506E-01	7.82636E-01	7.77906E-01
5.60000E 00	1.27706E-03	6.03756E-01	1.19306E-03	8.37536E-03	7.9019E-01	7.88356E-01	7.86506E-01	7.81906E-01
5.80000E 00	1.25936E-03	6.09966E-01	1.21706E-03	8.23096E-03	7.9381E-01	7.92006E-01	7.90176E-01	7.85636E-01
6.00000E 00	1.24236E-03	6.15876E-01	1.24066E-03	8.09376E-03	7.9725E-01	7.95456E-01	7.93666E-01	7.89176E-01
6.20000E 00	1.22606E-03	6.21526E-01	1.26396E-03	7.96326E-03	8.0052E-01	7.98756E-01	7.96976E-01	7.92556E-01
6.40000E 00	1.21036E-03	6.26936E-01	1.28676E-03	7.83876E-03	8.0363E-01	8.01896E-01	8.00146E-01	7.95776E-01
6.60000E 00	1.19536E-03	6.32106E-01	1.30926E-03	7.71996E-03	8.0661E-01	8.04886E-01	8.03156E-01	7.98846E-01
6.80000E 00	1.18076E-03	6.37076E-01	1.33136E-03	7.60646E-03	8.0945E-01	8.07756E-01	8.06046E-01	8.01706E-01
7.00000E 00	1.16676E-03	6.41846E-01	1.35316E-03	7.49776E-03	8.1217E-01	8.10496E-01	8.08806E-01	8.04596E-01
7.20000E 00	1.15326E-03	6.46426E-01	1.37466E-03	7.39306E-03	8.1476E-01	8.13126E-01	8.11456E-01	8.07296E-01
7.40000E 00	1.14016E-03	6.50846E-01	1.39586E-03	7.29376E-03	8.1729E-01	8.15646E-01	8.13996E-01	8.09906E-01
7.60000E 00	1.12746E-03	6.55096E-01	1.41686E-03	7.19776E-03	8.1969E-01	8.18066E-01	8.16436E-01	8.12306E-01
7.80000E 00	1.11526E-03	6.59196E-01	1.43746E-03	7.10546E-03	8.2200E-01	8.20396E-01	8.18786E-01	8.14756E-01

RADIAL DIFFUSION — RECT INTEGRATION

TIME	FA	CA1	CAB	SFLUX	CSA	CSB	CSC	CSE
8.00000E 00	1.1033E-03	6.6315E-01	1.4577E-03	7.0166E-03	8.2423E-01	8.2263E-01	8.2104E-01	8.1700E-01
8.20000E 00	1.0910E-03	6.6098E-01	1.4779E-03	6.9310E-03	8.2637E-01	8.2477E-01	8.2322E-01	8.1927E-01
8.40000E 00	1.0808E-03	6.7067E-01	1.4977E-03	6.8463E-03	8.2844E-01	8.2688E-01	8.2537E-01	8.2141E-01
8.60000E 00	1.0698E-03	6.7425E-01	1.5173E-03	6.7689E-03	8.3043E-01	8.2887E-01	8.2734E-01	8.2340E-01
8.80000E 00	1.0592E-03	6.7771E-01	1.5367E-03	6.6920E-03	8.3236E-01	8.3081E-01	8.2930E-01	8.2534E-01
9.00000E 00	1.0489E-03	6.8107E-01	1.5559E-03	6.6176E-03	8.3422E-01	8.3271E-01	8.3119E-01	8.2724E-01
9.20000E 00	1.0391E-03	6.8434E-01	1.5749E-03	6.5457E-03	8.3602E-01	8.3452E-01	8.3302E-01	8.2927E-01
9.40000E 00	1.0295E-03	6.8747E-01	1.5936E-03	6.4760E-03	8.3777E-01	8.3626E-01	8.3479E-01	8.3106E-01
9.60000E 00	1.0201E-03	6.9052E-01	1.6122E-03	6.4086E-03	8.3946E-01	8.3794E-01	8.3651E-01	8.3283E-01
9.80000E 00	1.0110E-03	6.9349E-01	1.6305E-03	6.3432E-03	8.4110E-01	8.3964E-01	8.3818E-01	8.3452E-01
1.00000E 01	1.0022E-03	6.9637E-01	1.6487E-03	6.2797E-03	8.4269E-01	8.4124E-01	8.3979E-01	8.3617E-01
1.02000E 01	9.9355E-04	6.9917E-01	1.6667E-03	6.2182E-03	8.4423E-01	8.4279E-01	8.4136E-01	8.3777E-01
1.04000E 01	9.8517E-04	7.0189E-01	1.6845E-03	6.1584E-03	8.4573E-01	8.4430E-01	8.4288E-01	8.3932E-01
1.06000E 01	9.7702E-04	7.0454E-01	1.7021E-03	6.1003E-03	8.4718E-01	8.4577E-01	8.4436E-01	8.4083E-01
1.08000E 01	9.6910E-04	7.0711E-01	1.7196E-03	6.0438E-03	8.4860E-01	8.4720E-01	8.4580E-01	8.4229E-01
1.10000E 01	9.6139E-04	7.0962E-01	1.7369E-03	5.9889E-03	8.4997E-01	8.4859E-01	8.4719E-01	8.4372E-01
1.12000E 01	9.5382E-04	7.1206E-01	1.7541E-03	5.9354E-03	8.5131E-01	8.4994E-01	8.4856E-01	8.4511E-01
1.14000E 01	9.4649E-04	7.1443E-01	1.7711E-03	5.8833E-03	8.5262E-01	8.5125E-01	8.4989E-01	8.4646E-01
1.16000E 01	9.3934E-04	7.1674E-01	1.7879E-03	5.8326E-03	8.5389E-01	8.5253E-01	8.5117E-01	8.4776E-01
1.18000E 01	9.3237E-04	7.1900E-01	1.8046E-03	5.7832E-03	8.5513E-01	8.5378E-01	8.5243E-01	8.4902E-01
1.20000E 01	9.2556E-04	7.2120E-01	1.8212E-03	5.7350E-03	8.5633E-01	8.5500E-01	8.5366E-01	8.5031E-01
1.22000E 01	9.1892E-04	7.2334E-01	1.8376E-03	5.6880E-03	8.5751E-01	8.5618E-01	8.5485E-01	8.5155E-01
1.24000E 01	9.1244E-04	7.2544E-01	1.8539E-03	5.6421E-03	8.5866E-01	8.5734E-01	8.5602E-01	8.5277E-01
1.26000E 01	9.0610E-04	7.2748E-01	1.8700E-03	5.5973E-03	8.5978E-01	8.5847E-01	8.5716E-01	8.5396E-01
1.28000E 01	9.0002E-04	7.2948E-01	1.8861E-03	5.5536E-03	8.6088E-01	8.5958E-01	8.5828E-01	8.5512E-01
1.30000E 01	8.9401E-04	7.3142E-01	1.9020E-03	5.5109E-03	8.6195E-01	8.6066E-01	8.5936E-01	8.5624E-01
1.32000E 01	8.8814E-04	7.3333E-01	1.9177E-03	5.4691E-03	8.6299E-01	8.6171E-01	8.6043E-01	8.5732E-01
1.34000E 01	8.8240E-04	7.3519E-01	1.9334E-03	5.4283E-03	8.6402E-01	8.6274E-01	8.6148E-01	8.5837E-01
1.36000E 01	8.7679E-04	7.3700E-01	1.9489E-03	5.3884E-03	8.6502E-01	8.6375E-01	8.6249E-01	8.5939E-01
1.38000E 01	8.7132E-04	7.3878E-01	1.9644E-03	5.3493E-03	8.6599E-01	8.6474E-01	8.6347E-01	8.6039E-01
1.40000E 01	8.6598E-04	7.4052E-01	1.9797E-03	5.3111E-03	8.6695E-01	8.6570E-01	8.6443E-01	8.6136E-01
1.42000E 01	8.6077E-04	7.4222E-01	1.9949E-03	5.2737E-03	8.6789E-01	8.6665E-01	8.6540E-01	8.6229E-01
1.44000E 01	8.5569E-04	7.4389E-01	2.0100E-03	5.2371E-03	8.6881E-01	8.6757E-01	8.6633E-01	8.6324E-01
1.46000E 01	8.5073E-04	7.4552E-01	2.0249E-03	5.2012E-03	8.6970E-01	8.6848E-01	8.6724E-01	8.6417E-01
1.48000E 01	8.4588E-04	7.4712E-01	2.0398E-03	5.1661E-03	8.7058E-01	8.6936E-01	8.6814E-01	8.6508E-01
1.50000E 01	8.4087E-04	7.4868E-01	2.0546E-03	5.1316E-03	8.7145E-01	8.7023E-01	8.6902E-01	8.6598E-01
1.52000E 01	8.3617E-04	7.5021E-01	2.0693E-03	5.0979E-03	8.7229E-01	8.7109E-01	8.6988E-01	8.6686E-01
1.54000E 01	8.3156E-04	7.5171E-01	2.0839E-03	5.0648E-03	8.7312E-01	8.7192E-01	8.7072E-01	8.6771E-01
1.56000E 01	8.2705E-04	7.5319E-01	2.0984E-03	5.0323E-03	8.7394E-01	8.7274E-01	8.7154E-01	8.6855E-01
1.58000E 01	8.2263E-04	7.5463E-01	2.1128E-03	5.0005E-03	8.7473E-01	8.7355E-01	8.7235E-01	8.6936E-01

RADIAL DIFFUSION — RECT INTEGRATION

TIME		FA	CA1	CA8	SFLUX	CSA	CSB	CSC	CSE
1.60000E	01	8.1029E-04	7.5605E-01	2.1271E-03	4.9692E-03	8.7552E-01	8.7434E-01	8.7315E-01	8.7017E-01
1.62000E	01	8.1404E-04	7.5788E-01	2.1413E-03	4.9385E-03	8.7629E-01	8.7511E-01	8.7393E-01	8.7094E-01
1.64000E	01	8.0787E-04	7.5080E-01	2.1555E-03	4.9084E-03	8.7704E-01	8.7587E-01	8.7470E-01	8.7171E-01
1.66000E	01	8.0570E-04	7.4814E-01	2.1695E-03	4.8789E-03	8.7776E-01	8.7662E-01	8.7545E-01	8.7245E-01
1.68000E	01	8.0177E-04	7.4614E-01	2.1835E-03	4.8490E-03	8.7851E-01	8.7735E-01	8.7619E-01	8.7329E-01
1.70000E	01	7.9785E-04	7.4274E-01	2.1973E-03	4.8213E-03	8.7922E-01	8.7807E-01	8.7692E-01	8.7403E-01
1.72000E	01	7.9397E-04	7.4401E-01	2.2111E-03	4.7933E-03	8.7992E-01	8.7878E-01	8.7763E-01	8.7476E-01
1.74000E	01	7.9017E-04	7.4525E-01	2.2248E-03	4.7657E-03	8.8061E-01	8.7947E-01	8.7833E-01	8.7547E-01
1.76000E	01	7.8645E-04	7.4647E-01	2.2385E-03	4.7386E-03	8.8129E-01	8.8016E-01	8.7902E-01	8.7617E-01
1.78000E	01	7.8278E-04	7.4767E-01	2.2520E-03	4.7120E-03	8.8196E-01	8.8083E-01	8.7970E-01	8.7686E-01
1.80000E	01	7.7919E-04	7.4886E-01	2.2655E-03	4.6858E-03	8.8262E-01	8.8149E-01	8.8036E-01	8.7754E-01
1.82000E	01	7.7565E-04	7.5002E-01	2.2789E-03	4.6601E-03	8.8326E-01	8.8214E-01	8.8102E-01	8.7821E-01
1.84000E	01	7.7217E-04	7.5116E-01	2.2923E-03	4.6348E-03	8.8390E-01	8.8278E-01	8.8166E-01	8.7887E-01
1.86000E	01	7.6875E-04	7.5228E-01	2.3055E-03	4.6099E-03	8.8452E-01	8.8341E-01	8.8229E-01	8.7951E-01
1.88000E	01	7.6539E-04	7.5339E-01	2.3187E-03	4.5853E-03	8.8513E-01	8.8403E-01	8.8292E-01	8.8015E-01
1.90000E	01	7.6209E-04	7.5447E-01	2.3318E-03	4.5612E-03	8.8574E-01	8.8464E-01	8.8353E-01	8.8078E-01
1.92000E	01	7.5883E-04	7.5554E-01	2.3449E-03	4.5374E-03	8.8633E-01	8.8524E-01	8.8414E-01	8.8139E-01
1.94000E	01	7.5563E-04	7.5660E-01	2.3579E-03	4.5140E-03	8.8692E-01	8.8583E-01	8.8473E-01	8.8200E-01
1.96000E	01	7.5248E-04	7.5763E-01	2.3708E-03	4.4910E-03	8.8750E-01	8.8641E-01	8.8532E-01	8.8260E-01
1.98000E	01	7.4938E-04	7.5866E-01	2.3836E-03	4.4683E-03	8.8806E-01	8.8698E-01	8.8590E-01	8.8319E-01
2.00000E	01	7.4632E-04	7.5966E-01	2.3964E-03	4.4460E-03	8.8862E-01	8.8755E-01	8.8647E-01	8.8378E-01
2.02000E	01	7.4331E-04	7.6065E-01	2.4091E-03	4.4240E-03	8.8918E-01	8.8810E-01	8.8703E-01	8.8436E-01
2.04000E	01	7.4035E-04	7.6163E-01	2.4216E-03	4.4023E-03	8.8972E-01	8.8865E-01	8.8758E-01	8.8493E-01
2.06000E	01	7.3743E-04	7.6259E-01	2.4344E-03	4.3809E-03	8.9025E-01	8.8919E-01	8.8812E-01	8.8549E-01
2.08000E	01	7.3455E-04	7.6354E-01	2.4469E-03	4.3599E-03	8.9078E-01	8.8972E-01	8.8866E-01	8.8604E-01
2.10000E	01	7.3171E-04	7.6447E-01	2.4594E-03	4.3391E-03	8.9130E-01	8.9025E-01	8.8919E-01	8.8658E-01
2.12000E	01	7.2892E-04	7.6539E-01	2.4718E-03	4.3186E-03	8.9181E-01	8.9076E-01	8.8971E-01	8.8710E-01
2.14000E	01	7.2616E-04	7.6630E-01	2.4841E-03	4.2984E-03	8.9232E-01	8.9127E-01	8.9022E-01	8.8759E-01
2.16000E	01	7.2344E-04	7.6720E-01	2.4964E-03	4.2785E-03	8.9282E-01	8.9177E-01	8.9073E-01	8.8811E-01
2.18000E	01	7.2076E-04	7.6808E-01	2.5087E-03	4.2589E-03	8.9331E-01	8.9227E-01	8.9123E-01	8.8862E-01
2.20000E	01	7.1811E-04	7.6895E-01	2.5209E-03	4.2396E-03	8.9380E-01	8.9276E-01	8.9172E-01	8.8912E-01
2.22000E	01	7.1550E-04	7.6981E-01	2.5330E-03	4.2205E-03	8.9427E-01	8.9324E-01	8.9220E-01	8.8961E-01
2.24000E	01	7.1293E-04	7.7066E-01	2.5451E-03	4.2016E-03	8.9475E-01	8.9372E-01	8.9268E-01	8.9010E-01
2.26000E	01	7.1039E-04	7.7150E-01	2.5571E-03	4.1830E-03	8.9521E-01	8.9419E-01	8.9316E-01	8.9059E-01
2.28000E	01	7.0788E-04	7.7232E-01	2.5690E-03	4.1647E-03	8.9567E-01	8.9465E-01	8.9362E-01	8.9106E-01
2.30000E	01	7.0540E-04	7.7314E-01	2.5809E-03	4.1466E-03	8.9612E-01	8.9511E-01	8.9408E-01	8.9153E-01
2.32000E	01	7.0295E-04	7.7394E-01	2.5926E-03	4.1287E-03	8.9657E-01	8.9556E-01	8.9454E-01	8.9199E-01
2.34000E	01	7.0054E-04	7.7474E-01	2.6046E-03	4.1111E-03	8.9701E-01	8.9600E-01	8.9499E-01	8.9245E-01
2.36000E	01	6.9815E-04	7.7552E-01	2.6164E-03	4.0936E-03	8.9745E-01	8.9644E-01	8.9543E-01	8.9290E-01
2.38000E	01	6.9580E-04	7.7630E-01	2.6281E-03	4.0764E-03	8.9788E-01	8.9688E-01	8.9587E-01	8.9335E-01
2.40000E	01	6.9347E-04	7.7706E-01	2.6397E-03	4.0595E-03	8.9831E-01	8.9731E-01	8.9630E-01	8.9379E-01
2.42000E	01	6.9117E-04	7.7782E-01	2.6514E-03	4.0427E-03	8.9873E-01	8.9773E-01	8.9673E-01	8.9423E-01
2.44000E	01	6.8890E-04	7.7856E-01	2.6629E-03	4.0261E-03	8.9914E-01	8.9815E-01	8.9715E-01	8.9466E-01
2.46000E	01	6.8665E-04	7.7930E-01	2.6744E-03	4.0097E-03	8.9955E-01	8.9856E-01	8.9757E-01	8.9509E-01
2.48000E	01	6.8443E-04	8.0003E-01	2.6859E-03	3.9930E-03	8.9996E-01	8.9897E-01	8.9798E-01	8.9552E-01
2.50000E	01	6.8224E-04	8.0075E-01	2.6973E-03	3.9770E-03	9.0036E-01	8.9937E-01	8.9838E-01	8.9594E-01

C. 4 Programme for leaching of surface applied solutes under ponded water in a soil column containing uniformly distributed vertical cylindrical channels.

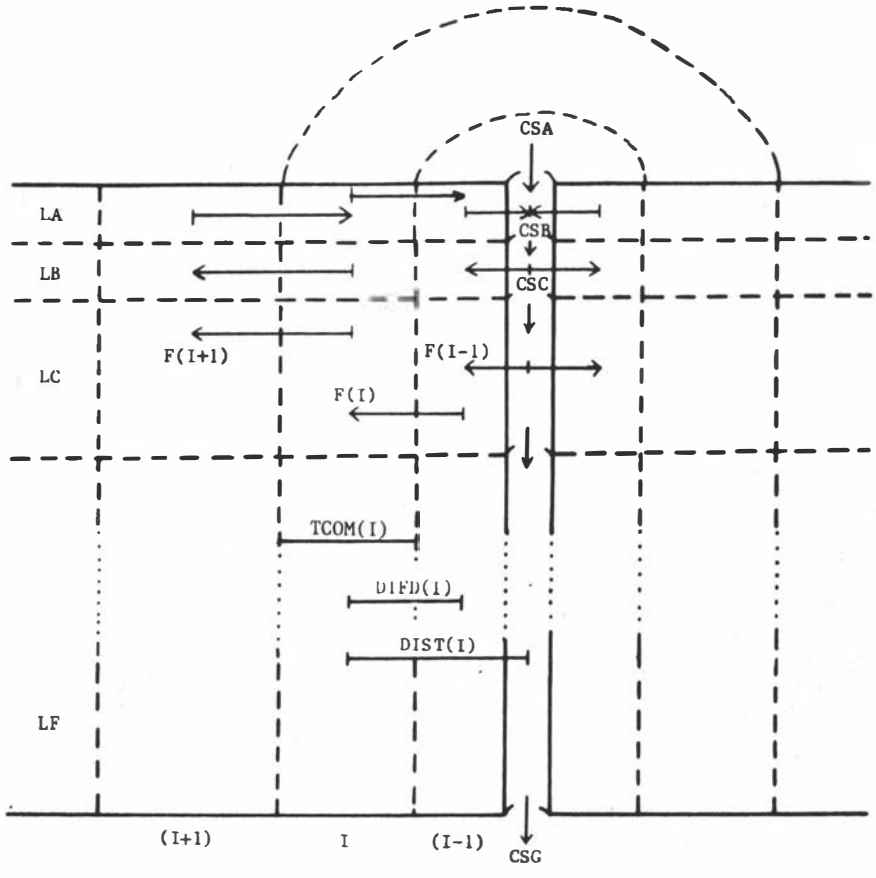

Fig. C.2 Geometry of the system and symbols used in the programme for leaching of the surface applied solutes under ponding water,in a soil column containing a uniform distribution of vertical cylindrical channels. Arrows indicate predominant direction of flow.

```
* CSMP/3 INPUT LIST * 25.003.000

0001        METHOD RECT
0002        TITLE BROMIDE DIFFUSION , PONDING WATER
0003        TIMER FINTIM=20,DELT=0.4,OUTDEL=20
0004        PARAM RITCOM=1.5
0005        PARAM CSA=0
0006        PARAM POR=0.52
0007        PARAM RAD=0.005,THCKNS=0.2807
0008        PARAM LA=1,LB=1,LC=2,LD=4,LE=8,LF=14
0009        PARAM PI2=6.2832
0010        PARAM DIFC=4.5E-04
0011        STORAG AREA(9),VOL(8),C(8),F(9),S(8),TCOM(8),DIFD(8),DIST(8),X(8)
0012        STORAG VA(8),VB(8),VC(8),VD(8),VE(8),VF(8)
0013        FIXED I,N
0014        INITIAL
0015        NOSORT
0016              FLOW=2.31E06*RAD**4.
0017              N=4
0018              F(N+1)=0.
0019              TCOM(1)=(THCKNS-RAD)*(RITCOM-1.)/(RITCOM**N-1.)
0020              AREA(1)=(0.25*TCOM(1)+RAD)*PI2
0021              DIFD(1)=0.5*TCOM(1)
0022              DIST(1)=DIFD(1)+RAD
0023              X(1)=AREA(1)*POR*DIFC/DIFD(1)
0024              DO 1 I=2,N
0025              TCOM(I)=RITCOM*TCOM(I-1)
0026              DIFD(I)=0.5*(TCOM(I-1)+TCOM(I))
0027              DIST(I)=DIST(I-1)+DIFD(I)
0028            1 CONTINUE
0029              DO 5 I=1,N
0030              VOL(I)=DIST(I)*PI2*TCOM(I)*POR
0031              AREA(I+1)=(DIST(I)+0.5*TCOM(I))*PI2
0032              VA(I)=VOL(I)
0033              VB(I)=0.
0034              VC(I)=0.
0035              VD(I)=0.
0036              VE(I)=0.
0037              VF(I)=0.
0038            5 CONTINUE
0039              VOL1=VOL(1)
0040              VOL2=VOL(2)
0041              VOL3=VOL(3)
0042              VOL4=VOL(4)
0043              DO 70 I=2,N
0044              X(I)=AREA(I)*POR*DIFC/DIFD(I)
0045           70 CONTINUE
0046              WRITE(6,100)DIST
0047              WRITE(6,101)
0048          100 FORMAT(1H ,4HDIST//(8F12.5))
0049          101 FORMAT(1H1)
0050        DYNAMIC
0051        NOSORT
0052              DO 2 I=1,N
0053            2 C(I)=VA(I)/VOL(I)
0054              F(1)=(CSA-C(1))*X(1)
0055              CSB=CSA-F(1)*LA/FLOW
0056              IF(CSB-C(1)) 51,51,52
0057           52 F(1)=C(1)*FLOW/LA
0058              CSB=C(1)
0059           51 CONTINUE
0060              DO 3 I=2,N
0061            3 F(I)=(C(I-1)-C(I))*X(1)
0062              DO 4 I=1,N
0063            4 S(I)=F(I)-F(I+1)
0064              SA1=S(1)
0065              SA2=S(2)
0066              SA3=S(3)
0067              SA4=S(4)
0068              CA1=C(1)
0069              CA2=C(2)
0070              CA3=C(3)
0071              CA4=C(4)
0072              DO 6 I=1,N
0073            6 C(I)=VB(I)/VOL(I)
0074              F(1)=(CSB-C(1))*X(1)
0075              CSC=CSB-F(1)*LB/FLOW
0076              IF(CSC)53,53,54
0077           53 F(1)=CSB*FLOW/LB
0078              CSC=0.
0079           54 CONTINUE
0080              DO 7 I=2,N
0081            7 F(I)=(C(I-1)-C(I))*X(1)
0082              DO 8 I=1,N
0083            8 S(I)=F(I)-F(I+1)
0084              SB1=S(1)
0085              SB2=S(2)
0086              SB3=S(3)
0087              SB4=S(4)
0088              CB1=C(1)
0089              CB2=C(2)
0090              CB3=C(3)
0091              CB4=C(4)
0092              DO 9 I=1,N
0093            9 C(I)=VC(I)/VOL(I)
0094              F(1)=(CSC-C(1))*X(1)
0095              CSD=CSC-F(1)*LC/FLOW
0096              IF(CSD) 55,55,56
0097           55 F(1)=CSC*FLOW/LC
0098              CSD=0.
0099           56 CONTINUE
```

```
0100            DO 10 I=2,N
0101         10 F(I)=(C(I-1)-C(I))*X(1)
0102            DO 11 I=1,N
0103         11 S(I)=F(I)-F(I+1)
0104            SC1=S(1)
0105            SC2=S(2)
0106            SC3=S(3)
0107            SC4=S(4)
0108            CC1=C(1)
0109            CC2=C(2)
0110            CC3=C(3)
0111            CC4=C(4)
0112            DO 12 I=1,N
0113         12 C(I)=VD(I)/VOL(I)
0114            F(1)=(CSD-C(1))*X(1)
0115            CSE=CSD-F(I)*LD/FLOW
0116            IF(CSE) 57,57,58
0117         57 F(1)=CSD*FLOW/LD
0118            CSE=0.
0119         58 CONTINUE
0120            DO 13 I=2,N
0121         13 F(I)=(C(I-1)-C(I))*X(1)
0122            DO 14 I=1,N
0123         14 S(I)=F(I)-F(I+1)
0124            SD1=S(1)
0125            SD2=S(2)
0126            SD3=S(3)
0127            SD4=S(4)
0128            CD1=C(1)
0129            CD2=C(2)
0130            CD3=C(3)
0131            CD4=C(4)
0132            DO 15 I=1,N
0133         15 C(I)=VE(I)/VOL(I)
0134            F(1)=(CSE-C(1))*X(1)
0135            CSF=CSE-F(I)*LE/FLOW
0136            IF(CSF) 59,59,60
0137         59 F(1)=CSE*FLOW/LE
0138            CSF=0.
0139         60 CONTINUE
0140            DO 16 I=2,N
0141         16 F(I)=(C(I-1)-C(I))*X(1)
0142            DO 17 I=1,N
0143         17 S(I)=F(I)-F(I+1)
0144            SE1=S(1)
0145            SE2=S(2)
0146            SE3=S(3)
0147            SE4=S(4)
0148            CE1=C(1)
0149            CE2=C(2)
0150            CE3=C(3)
0151            CE4=C(4)
0152            DO 18 I=1,N
0153         18 C(I)=VF(I)/VOL(I)
0154            F(1)=(CSF-C(1))*X(1)
0155            CSG=CSF-F(I)*LF/FLOW
0156            IF(CSG)61,61,62
0157         61 F(1)=CSF*FLOW/LF
0158            CSG=0.
0159         62 CONTINUE
0160            DO 19 I=2,N
0161         19 F(I)=(C(I-1)-C(I))*X(1)
0162            DO 20 I=1,N
0163         20 S(I)=F(I)-F(I+1)
0164            SF1=S(1)
0165            SF2=S(2)
0166            SF3=S(3)
0167            SF4=S(4)
0168            CF1=C(1)
0169            CF2=C(2)
0170            CF3=C(3)
0171            CF4=C(4)
0172         SORT
0173         VA1=INTGRL(VOL1,SA1)
0174         VA2=INTGRL(VOL2,SA2)
0175         VA3=INTGRL(VOL3,SA3)
0176         VA4=INTGRL(VOL4,SA4)
0177         VB1=INTGRL(0,SB1)
0178         VB2=INTGRL(0,SB2)
0179         VB3=INTGRL(0,SB3)
0180         VB4=INTGRL(0,SB4)
0181         VC1=INTGRL(0,SC1)
0182         VC2=INTGRL(0,SC2)
0183         VC3=INTGRL(0,SC3)
0184         VC4=INTGRL(0,SC4)
0185         VD1=INTGRL(0,SD1)
0186         VD2=INTGRL(0,SD2)
0187         VD3=INTGRL(0,SD3)
0188         VD4=INTGRL(0,SD4)
0189         VE1=INTGRL(0,SE1)
0190         VE2=INTGRL(0,SE2)
0191         VE3=INTGRL(0,SE3)
0192         VE4=INTGRL(0,SE4)
0193         VF1=INTGRL(0,SF1)
0194         VF2=INTGRL(0,SF2)
0195         VF3=INTGRL(0,SF3)
0196         VF4=INTGRL(0,SF4)
```

```
0197        NOSORT
0198              VA(1)=VA1
0199              VA(2)=VA2
0200              VA(3)=VA3
0201              VA(4)=VA4
0202              VB(1)=VB1
0203              VB(2)=VB2
0204              VB(3)=VB3
0205              VB(4)=VB4
0206              VC(1)=VC1
0207              VC(2)=VC2
0208              VC(3)=VC3
0209              VC(4)=VC4
0210              VD(1)=VD1
0211              VD(2)=VD2
0212              VD(3)=VD3
0213              VD(4)=VD4
0214              VE(1)=VE1
0215              VE(2)=VE2
0216              VE(3)=VE3
0217              VE(4)=VE4
0218              VF(1)=VF1
0219              VF(2)=VF2
0220              VF(3)=VF3
0221              VF(4)=VF4
0222        PRINT CA1,CA2,CA3,CA4,CSB
0223        PRINT CB1,CB2,CB3,CB4,CSC
0224        PRINT CC1,CC2,CC3,CC4,CSD
0225        PRINT CD1,CD2,CD3,CD4,CSE
0226        PRINT CE1,CE2,CE3,CE4,CSF
0227        PRINT CF1,CF2,CF3,CF4,CSG
0228        CONTIN
0229        TIMER FINTIM=60,DELT=0.4,OUTDEL=60
0230        CONTIN
0231        TIMER FINTIM=180,DELT=0.45,OUTDEL=180
0232        CONTIN
0233        TIMER FINTIM=720,DELT=0.45,OUTDEL=720
0234        CONTIN
0235        TIMER FINTIM=1200,DELT=0.48,OUTDEL=1200
0236        ENDJOB
```

DIST

0.02197 0.06438 0.12800 0.22344 0.00000 0.00000 0.00000 0.00000

BROMIDE DIFFUSION - PONDING WATER RECT INTEGRATION

TIME = 0.00	CA1 = 1.0000E 00	CA2 = 1.0000E 00	CA3 = 1.0000E 00	CA4 = 1.0000E 00
	CSB = 8.0930E-01	CB1 = 0.00	CB2 = 0.00	CB3 = 0.00
	CB4 = 0.00	CSC = 1.5433E-01	CC1 = 0.00	CC2 = 0.00
	CC3 = 0.00	CC4 = 0.00	CSD = 0.00	CD1 = 0.00
	CD2 = 0.00	CD3 = 0.00	CD4 = 0.00	CSE = 0.00
	CE1 = 0.00	CE2 = 0.00	CE3 = 0.00	CE4 = 0.00
	CSF = 0.00	CF1 = 0.00	CF2 = 0.00	CF3 = 0.00
	CF4 = 0.00	CSG = 0.00		
TIME = 2.0000E 01	CA1 = 3.7740E-01	CA2 = 6.9936E-01	CA3 = 8.8435E-01	CA4 = 9.7407E-01
	CSB = 3.0543E-01	CB1 = 1.9707E-01	CB2 = 1.0195E-01	CB3 = 4.3163E-02
	CB4 = 1.0936E-02	CSC = 2.1773E-01	CC1 = 1.2139E-01	CC2 = 6.8097E-02
	CC3 = 2.6776E-02	CC4 = 6.0022E-03	CSD = 8.8009E-02	CD1 = 3.7589E-02
	CD2 = 1.5624E-02	CD3 = 4.7322E-03	CD4 = 7.4626E-04	CSE = 0.00
	CE1 = 0.00	CE2 = 0.00	CE3 = 0.00	CE4 = 0.00
	CSF = 0.00	CF1 = 0.00	CF2 = 0.00	CF3 = 0.00
	CF4 = 0.00	CSG = 0.00		

BROMIDE DIFFUSION + PONDING WATER — RECT INTEGRATION

TIME = 6.0000E 01	CA1 =	3.1494E-01	CA2 =	5.8554E-01	CA3 =	7.5039E-01	CA4 =	8.5000E-01			
	CSB =	2.5486E-01	CB1 =	1.8031E-01	CB2 =	1.1519E-01	CB3 =	7.4105E-02			
	CB4 =	4.8064E-02	CSC =	1.9453E-01	CC1 =	1.3542E-01	CC2 =	8.4152E-02			
	CC3 =	5.2484E-02	CC4 =	3.2490E-02	CSD =	9.6847E-02	CD1 =	5.8479E-02			
	CD2 =	3.2742E-02	CD3 =	1.7735E-02	CD4 =	9.2384E-03	CSE =	0.00			
	CE1 =	0.00	CE2 =	0.00	CE3 =	0.00	CE4 =	0.00			
	CSF =	0.00	CF1 =	0.00	CF2 =	0.00	CF3 =	0.00			
	CF4 =	0.00	CSG =	0.00							
TIME = 1.8015E 02	CA1 =	2.0395E-01	CA2 =	3.7921E-01	CA3 =	4.8610E-01	CA4 =	5.5092E-01			
	CSB =	1.6506E-01	CB1 =	1.4475E-01	CB2 =	1.2665E-01	CB3 =	1.1475E-01			
	CB4 =	1.0085E-01	CSC =	1.4863E-01	CC1 =	1.2493E-01	CC2 =	1.0418E-01			
	CC3 =	9.1035E-02	CC4 =	8.2672E-02	CSD =	1.1026E-01	CD1 =	8.4902E-02			
	CD2 =	6.3237E-02	CD3 =	5.0017E-02	CD4 =	4.2032E-02	CSE =	2.8356E-02			
	CE1 =	7.6991E-03	CE2 =	1.1041E-03	CE3 =	2.1263E-03	CE4 =	1.0945E-03			
	CSF =	0.00	CF1 =	0.00	CF2 =	0.00	CF3 =	0.00			
	CF4 =	0.00	CSG =	0.00							

BROMIDE DIFFUSION + PONDING WATER — RECT INTEGRATION

TIME = 7.2015E 02	CA1 =	2.9004E-02	CA2 =	5.3927E-02	CA3 =	6.9128E-02	CA4 =	7.8346E-02			
	CSB =	2.3473E-02	CB1 =	3.8498E-02	CB2 =	5.1310E-02	CB3 =	5.9011E-02			
	CB4 =	6.3581E-02	CSC =	3.5633E-02	CC1 =	4.8340E-02	CC2 =	5.9152E-02			
	CC3 =	6.5013E-02	CC4 =	6.9409E-02	CSD =	5.6213E-02	CD1 =	6.3258E-02			
	CD2 =	6.9190E-02	CD3 =	7.2650E-02	CD4 =	7.4625E-02	CSE =	7.9018E-02			
	CE1 =	6.9256E-02	CE2 =	6.0813E-02	CE3 =	5.5597E-02	CE4 =	5.2335E-02			
	CSF =	1.5018E-02	CF1 =	2.0515E-03	CF2 =	9.4044E-04	CF3 =	3.7539E-04			
	CF4 =	1.1986E-04	CSG =	0.00							
TIME = 1.2001E 03	CA1 =	5.1219E-03	CA2 =	9.5231E-03	CA3 =	1.2207E-02	CA4 =	1.3835E-02			
	CSB =	4.1452E-03	CB1 =	9.6109E-03	CB2 =	1.4291E-02	CB3 =	1.7124E-02			
	CB4 =	1.8025E-02	CSC =	8.5686E-03	CC1 =	1.4980E-02	CC2 =	2.0401E-02			
	CC3 =	2.3766E-02	CC4 =	2.5741E-02	CSD =	1.8946E-02	CD1 =	2.0305E-02			
	CD2 =	3.2089E-02	CD3 =	3.6479E-02	CD4 =	3.8724E-02	CSE =	4.2903E-02			
	CE1 =	4.8230E-02	CE2 =	5.2675E-02	CE3 =	5.5202E-02	CE4 =	5.6702E-02			
	CSF =	7.7063E-02	CF1 =	3.3143E-02	CF2 =	2.7365E-02	CF3 =	2.3926E-02			
	CF4 =	2.1908E-02	CSG =	0.00							

APPENDIC D

DERIVATION OF EQUATION FOR FLOW THROUGH NON-UNIFORM CAPILLARY TUBES

The gravity induced, viscous flow through a vertical cylindrical, capillary tube of length L and radius r can be described by the Hagen-Poiseuille equation (Childs, 1969),

$$Q = \frac{\pi r^4 \rho_f g (\psi_1 - \psi_2)}{8\eta L} \qquad (D.1)$$

where Q = flow rate ($m^3 s^{-1}$)

ρ_f = fluid density ($kg\ m^{-3}$)

g = acceleration due to gravity ($m\ s^{-2}$)

η = viscosity of fluid (Pa s)

ψ_1 and ψ_2 = pressure potential at inflow and out flow respectively (m).

When viscous flow occurs through a tube made by joining together two different diameter capillary tubes A and B (as shown in the figure below), at steady state the rate of fluid flow in tube A is equal to the flow rate in tube B, thus

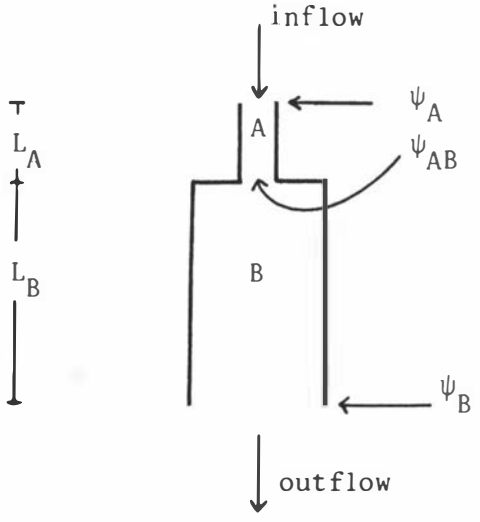

$$Q_A = Q_B$$

or
$$\frac{\pi r_A^4 \rho_f g(\psi_A - \psi_{AB})}{8 \eta L_A} = \frac{\pi r_B^4 \rho_f g(\psi_{AB} - \psi_B)}{8 \eta L_B} \qquad (D.2)$$

Rearrangement of equation (D.2) gives

$$\psi_{AB} = \left(\frac{\psi_A r_A^4}{L_A} + \frac{\psi_B r_B^4}{L_B}\right) / \left(\frac{r_A^4}{L_A} + \frac{r_B^4}{L_B}\right) \qquad (D.3)$$

Thus, once the potential at the join has been found using equation (D.3), equation (D.1) may be used to find Q.

APPENDIX E

BROMIDE CONCENTRATION MEASUREMENTS FOR INDIVIDUAL REPLICATES UNDER CONTINUOUS PONDING CONDITIONS

Table E.1 Bromide concentration measurements for individual replicates under continuous ponding condition in the pasture area. A log-normal distribution was assumed.

PLOT (a)

Preleaching

Depth (mm)	Bromide concentration (μg/ml)					$\bar{x}$	$\exp(\bar{x}_L)$	$\exp(s_L)$	C.V. %
	Core I	II	III	IV	V	(μg/ml)			
0-10	-	549	504	764	396	553	538	1.3	4.3
10-20		200	38	76	85	100	84	2.0	15.4
20-30	20	81	20	86	55	52	43	2.1	19.3
30-40	13	62	4	87	12	35	21	3.6	42.3
40-50	14	13	2	5	15	10	8	2.4	43.0
50-75	2	12	2	8	3	6	4	2.3	56.8
75-100	2	3	2	4	4	3	3	1.6	44.6

Post-Leaching

Depth (mm)	Bromide concentration (μg/ml)													$\bar{x}$	$\exp(\bar{x}_L)$	$\exp(s_L)$	C.V. %
	Core I	II	III	IV	V	VI	VII	VIII	IX	X	XI	XII	XIII	(μg/ml)			
0-20	119	196	189	149	130	124	161	117	223	155	160	108	166	154	150	1.3	4.5
20-40	90	96	148	71	46	38	48	40	102	97	120	47	90	79	73	1.6	10.6
40-60	59	68	122	47	45	36	56	27	114	41	89	35	33	59	50	1.6	12.0
60-80	56	90	67	18	102	45	73	30	168	31	107	57	18	66	56	2.0	17.2
80-100	29	97	24	3	184	26	46	33	70	30	63	67	13	53	38	2.8	28.4
100-120	23	55	8	2	161	10	19	25	21	24	15	62	5	33	19	3.1	38.5
120-140	13	13	4	5	146	22	33	23	12	11	4	40	3	25	14	3.0	42.1
140-160	12	8	2	9	143	31	42	26	9	12	5	28	3	25	13	3.2	44.8
160-180	12	11	7	8	110	32	64	15	8	9	15	13	3	24	14	2.6	36.0
180-200	7	7	10	8	85	36	117	7	8	8	13	17	3	25	12	2.9	42.6
200-225	7	7	12	5	25	34	96	7	5	8	15	24	4	19	12	2.5	37.3
225-250	19	7	6	4	13	27	50	9	5	5	12	18	4	14	10	2.2	34.2
250-300	6	27	6	3	14	17	35	5	6	7	12	12	3	12	2	1.3	35.3

PLOT (b)

Pre-leaching

Depth (mm)	Bromide concentration (μg/ml)					$\bar{x}$	$\exp(\bar{x}_L)$	$\exp(s_L)$	C.V. %
	Core I	11	III	IV	V	(μg/ml)			
0-10	602	882	452	741	884	712	691	1.3	4.4
10-20	31	61	1	167	102	72	33	6.8	54.3
20-30	44	-	1	108	7	40	14	7.2	74.3
30-40	12	3	1	3	6	5	5	2.7	85.1
40-50	2	0	0	0	0	0	x	x	x
50-75	0	0	0	0	0	0	x	x	x
75-100	0	0	0	0	0	0	x	x	x

Post-leaching

Depth (mm)	Bromide concentration (μg/ml)													$\bar{x}$	$\exp(\bar{x}_L)$	$\exp(s_L)$	C.V. %
	Core I	II	III	IV	V	VI	VII	VIII	IX	X	XI	XII	XIII	(μg/ml)			
0-20	136	164	95	89	133	119	113	110	103	159	149	151	192	132	129	1.3	4.8
20-40	97	84	48	56	-	73	94	99	69	71	125	127	117	88	85	1.4	7.0
40-60	92	57	25	41	87	69	79	88	61	56	104	96	69	71	67	1.5	9.4
60-80	64	69	28	50	85	58	72	82	64	86	75	92	53	68	70	1.4	7.6
80-100	41	70	33	41	83	48	67	102	62	113	80	143	35	71	64	1.6	11.2
100-120	18	80	27	51	85	42	80	70	59	104	74	117	18	63	61	1.9	15.6
120-140	8	51	10	53	71	36	58	71	55	29	51	88	7	43	35	2.4	24.6
140-160	4	45	5	42	74	13	68	52	46	28	67	91	7	42	29	3.0	32.5
160-180	1	47	6	35	72	6	56	27	37	18	63	93	9	36	22	3.7	42.4
180-200	2	40	12	29	61	3	42	20	29	13	81	108	5	34	20	3.5	41.7
200-225	2	40	13	17	49	3	45	9	30	15	63	84	4	29	18	3.4	42.7
225-250	4	38	12	16	31	6	27	10	20	13	67	55	5	23	15	2.4	32.0
250-300	5	24	4	13	21	4	18	9	12	16	61	42	6	18	19	2.7	33.9

CONTINUED ...

Table E.1 (continued)

PLOT (c)

Pre-leaching

Depth (mm)	Bromide concentration (µg/ml)					$\bar{x}$	$\exp(\bar{x}_L)$	$\exp(s_L)$	C.V. %
	Core I	II	III	IV	V	(µg/ml)			
0-10	442	565	481	741	465	539	529	1.2	3.3
10-20	248	96	65	36	9	91	54	3.4	30.7
20-30	54	52	42	23	3	35	24	3.2	36.5
30-40	26	1	1	1	3	6	2	4.5	191.8
40-50	21	2	0	1	1	5	1	6.8	520.9
50-75	0	1	0	0	0	0	+	+	+
75-100	0	0	0	0	0	0	+	+	+

Post-leaching

Depth (mm)	Bromide concentration (µg/ml)													$\bar{x}$	$\exp(x_L)$	$\exp(s_L)$	C.V. %
	Core I	II	III	IV	V	VI	VII	VIII	IX	X	XI	XII	XIII	(µg/ml)			
0-20	208	184	207	152	172	154	210	109	145	201	184	181	147	173	171	1.2	3.7
20-40	86	36	35	50	88	57	99	7	48	52	40	107	22	56	49	2.1	19.1
40-60	118	27	15	22	38	114	38	4	32	18	18	91	33	44	31	2.5	26.9
60-80	68	28	10	3	14	84	22	1	5	3	30	53	36	28	15	3.7	48.3
80-100	19	7	3	2	12	4	13	1	2	9	11	53	32	13	7	3.4	62.5
100-120	24	3	3	0	9	0	3	1	0	39	1	54	25	12	2	10.7	27.3
120-140	33	1	4	0	25	0	0	0	0	48	0	47	24	14	+	+	+
140-160	34	0	6	0	26	0	0	0	0	32	0	40	24	12	+	+	+
160-180	35	0	6	0	29	0	0	0	0	34	0	32	26	12	+	+	+
180-200	28	0	8	0	29	0	0	0	0	47	0	25	24	12	+	+	+
200-225	29	0	12	0	13	0	0	0	0	43	0	23	14	10	+	+	+
225-250	21	0	14	0	23	0	0	0	0	41	0	-	6	9	+	+	+
250-300	18	0	11	0	-	0	0	0	0	32	0	-	3	6	+	+	+

+ As ln 0 is not defined, these parameters cannot be computed.
Symbols used in the Table are defined in section 6.4.3.

Table E.2 Bromide concentration measurements for individual replicates under continuous ponding conditions in the cultivated area. A log-normal distribution was assumed.

PLOT (a)

Pre-leaching

Depth (mm)	Bromide concentration (µg/ml)					$\bar{x}$	$\exp(\bar{x}_L)$	$\exp(s_L)$	C.V. %
	Core I	II	III	IV	V	(µg/ml)			
0-10	600	744	600	682	789	683	679	1.1	1.9
10-20	6	13	21	13	58	18	15	2.0	26.2
20-30	3	20	13	2	14	10	7	2.9	54.6
30-40	4	3	1	1	5	2	4	2.5	64.4
40-50	2	3	0	1	5	2	2	2.8	250.9
50-75	2	2	2	2	2	2	2	1.1	17.2
75-100	3	3	2	1	2	2	2	1.6	86.7

Post-leaching

Depth (mm)	Bromide concentration (µg/ml)													$\bar{x}$	$\exp(\bar{x}_L)$	$\exp(s_L)$	C.V. %
	Core I	II	III	IV	V	VI	VII	VIII	IX	X	XI	XII	XIII	(µg/ml)			
0-20	297	302	287	308	217	205	226	244	300	234	268	221	286	261	259	1.2	2.6
20-40	210	262	189	292	189	145	294	276	408	217	288	161	258	245	155	1.3	5.2
40-60	41	66	40	69	127	43	156	137	126	104	119	24	86	88	75	1.8	13.6
60-80	4	5	4	7	28	6	23	29	74	39	12	1	11	19	10	3.2	49.6
80-100	3	2	1	2	3	1	2	5	53	4	3	1	3	6	3	2.8	99.3
100-120	3	3	1	4	3	1	2	2	19	3	21	2	3	5	3	2.5	80.0
120-140	2	4	1	9	4	1	1	1	10	6	54	2	7	8	4	3.3	95.0
140-160	3	3	1	24	4	2	1	1	25	17	94	1	20	15	5	4.7	95.8
160-180	4	12	6	31	11	1	6	1	37	18	52	1	38	17	8	4.2	68.1
180-200	11	26	16	41	13	1	17	2	49	24	48	3	31	22	2	3.5	199.7
200-225	22	31	24	44	10	3	23	2	46	34	11	6	19	21	15	2.7	36.9
225-250	11	14	18	40	9	3	13	12	42	30	26	8	14	18	15	2.1	26.8
250-300	13	9	12	27	6	3	14	3	22	19	24	4	15	13	23	21.3	102.9

PLOT (b)

Pre-leaching

Depth (mm)	Bromide concentration (µg/ml)					$\bar{x}$	$\exp(\bar{x}_L)$	$\exp(s_L)$	C.V. %
	Core I	II	III	IV	V	(µg/ml)			
0-10	386	684	795	709	684	652	389	1.3	4.4
10-20	9	16	647	104	20	159	45	5.7	45.6
20-30	2	11	349	8	1	74	8	11.4	114.8
30-40	1	9	60	6	1	15	4	7.1	140.1
40-50	0	9	12	8	0	6	2	12.0	598.5
50-75	0	1	2	1	0	1	+	+	+
75-100	0	1	1	0	0	0	+	+	+

Post-leaching

Depth (mm)		Bromide concentration (µg/ml)												$\bar{x}$	$\exp(\bar{x}_L)$	$\exp(s_L)$	C.V. %
	Core I	II	III	IV	V	VI	VII	VIII	IX	X	XI	XII	XIII	(µg/ml)			
0-20	169	193	342	231	335	269	194	257	232	167	190	220	139	226	212	1.3	4.9
20-40	67	64	200	115	232	144	105	190	161	90	92	251	50	135	117	1.68	10.9
40-60	32	29	40	65	53	33	38	45	39	31	9	115	26	43	10	1.8	16.4
60-80	24	7	31	34	29	1	18	6	4	7	1	29	33	17	10	3.6	54.7
80-100	8	11	17	21	83	1	1	1	1	24	1	7	47	17	6	5.2	89.7
100-120	8	5	5	1	198	1	1	0	0	6	1	0	31	20	3	5.3	136.8
120-140	27	2	5	1	238	2	1	0	4	1	0	0	8	22	2	10.4	486.8
140-160	45	0	22	1	169	11	0	1	1	0	1	1	43	23	2	12.5	333.1
160-180	22	0	70	0	124	20	0	22	1	2	33	0	33	25	3	17.4	235.9
180-200	18	10	69	0	110	55	0	59	0	25	79	0	21	34	6	19.28	160.3
200-225	71	52	66	17	80	74	18	85	6	52	61	10	60	50	41	2.6	25.8
225-250	64	4	70	77	54	63	51	88	36	49	33	51	4	50	38	2.76	28.0
250-300	21	2	39	79	50	72	66	63	59	19	37	59	0	42	27	4.1	42.9

+ As ln 0 is not defined, these parameters cannot be computed.
Symbols used in the Table are defined in section 6.4.3.

APPENDIX F

FRACTILE DIAGRAM CONSTRUCTION

Details concerning the construction of a fractile diagram have been given by Hald (1952) and Biggar and Nielsen (1976). The diagram is based on the cumulative distribution function P(x) for a normal distribution:

$$P(x) = \frac{1}{(2\pi)^{\frac{1}{2}}} \int_{-\infty}^{(x-\bar{x})/s} \exp\left(-\frac{u^2}{2}\right) du \qquad (F.1)$$

where in this case random variable x is the concentration of bromide in the soil (C, or ln C), $\bar{x}$ the mean value of C or ln C, and s the standard deviation. The values of P(x) are obtained by ranking the observed values of x in increasing order of magnitude. Pre-leaching data at 30-40 mm depth are given here as an example. P(x) is equal to i/n, where n = 48, the total number of the samples, and i = 1, 2, 3 ..., 47, 48. For the largest observed value of x, P(x) = 1 and for any value of x less than the smallest observed value, P(x) = 0. By using these values of P(x), the corresponding values of $(x-\bar{x})/s$ obtained from the tabular values of Eq. (F.1) (Mood and Graybill, 1963) were plotted versus C and ln C. The linearity of the resulting data was determined using linear regression analysis. In this example, the probability units were more linearly related to ln C (r = 0.993) than C (r = 0.808) as shown in Fig. 6.10C, thus bromide concentration variability in the soil after application to the soil surface was approximately log-normally distributed.

For a normal distribution, the mode (the most frequently observed value), the median (the value with an equal number of values above and below), and the mean are all identical. For a log-normal distribution, the mode, median and mean are obtained from:

$$\text{mode} = \exp(\bar{x}_L - s_L^2) = 5.4 \ \mu g/ml$$
$$\text{median} = \exp(\bar{x}_L) = 22.2 \ \mu g/ml$$
$$\text{mean} = \exp(\bar{x}_L + 0.5 s_L^2) = 45.0 \ \mu g/ml$$

where $\bar{x}_L$ and s_L for ln C were 3.1 and 1.2 μg/ml, respectively.

The results of the analysis for other leaching data under natural rainfall conditions are given in Table F.1 and F.2.

Table F.1 Results from fractile diagrams for experiment under natural rainfall.

Depth (mm)	n	r_1	r_2	$\bar{x}$	Mode	$\exp(\bar{x}_L)$	Median	$\exp(s_L)$	C.V. %
				(µg/ml)					
Pre-leaching									
0-10	48	0.975	0.987	413	346	389	380	1.41	5.8
10-20	48	0.917	0.979	141	93	123	117	1.70	11.0
20-30	48	0.817	0.980	65	24	47	41	2.25	21.0
30-40	48	0.808	0.993	45	5	22	24	3.28	38.3
40-50	48	0.745	0.980	41	3	16	14	3.91	49.0
Post-leaching (after 182 mm excess rainfall)									
0-50	40	0.923	0.986	30.5	22.3	27.4	24.6	1.58	13.8
50-100	40	0.878	0.978	13.1	11.3	12.5	12.0	1.37	12.4
100-150	40	0.919	0.968	11.4	10.4	11.0	10.4	1.30	11.0
150-200	40	0.889	0.978	12.4	10.7	11.8	11.1	1.36	12.5
200-250	40	0.969	0.992	11.9	10.9	11.5	11.4	1.28	10.0
250-300	40	0.964	0.998	12.6	11.0	12.0	11.6	1.36	12.2
300-400	40	0.955	0.979	14.3	11.6	13.3	12.3	1.46	14.6
400-500	40	0.934	0.985	14.3	11.9	13.4	12.8	1.42	13.6
500-600	40	0.957	0.984	11.1	8.9	10.3	9.8	1.46	16.4

r_1 and r_2 = correlation coefficients for $(x-\bar{x})/s$ vs concentration C and ln C, respectively, n = number of samples. Median = median obtained from experimental data. Other symbols used in the table are defined in section 6.4.3.

Table F.2 Data for bromide concentration distribution after infiltration of 46 mm excess rainfall over evapotranspiration. Four core samples obtained from 0.32 x 0.5 m subplots were bulked together in each replicate.

Depth (mm)	n*	Range	$\bar{x}$	$\exp(s_L)$	$\exp(x_L)$	C.V. %
		(µg/ml)				
0-20	10	37-105	71	1.38	68	7.6
20-40	10	27-49	38	1.16	38	4.0
40-60	10	26-60	37	1.26	36	6.5
60-80	10	22-59	38	1.36	37	8.6
80-100	10	21-73	44	1.45	41	10.0
100-120	10	22-70	48	1.45	44	9.8
120-140	10	22-63	47	1.41	50	8.8
140-160	10	25-67	48	1.36	47	8.0
160-180	10	28-67	49	1.35	49	7.7
180-200	10	28-61	45	1.33	43	7.6
200-250	10	24-70	40	1.44	38	10.0
150-300	10	14-60	32	1.64	29	14.7

* n = number of samples.

Other symbols are defined in section 6.4.3.

REFERENCES

Abdalla, N.A., and B. Lear. 1975. Determination of inorganic bromide in soil and plant tissues with a bromide selective-ion electrode. Commun. in Soil Science and Plant Analysis. 6: 489-494.

Allison, F.E. 1966. The fate of nitrogen applied to soils. Advan. Agron. 18:219-258.

Anderson, J.L., and J. Bouma. 1973. Relationships between saturated hydraulic conductivity and morphometric data of an Agrillic horizon. Soil Sci. Soc. Am. Proc. 37: 408-412.

Anderson, J.L., and J. Bouma. 1977a. Water movement through pedal soils. I. Saturated flow. Soil Sci. Soc. Am. J. 41: 413-418.

Anderson, J.L., and J. Bouma. 1977b. Water movement through pedal soils. II. Unsaturated flow. Soil Sci. Soc. Am. J. 41: 419-423.

Aylmore, L.A.G., and M. Karim. 1968. Leaching of fertilizer ions in soil columns. Int. Congr. Soil. Sci. Trans. 9th (Adelaide, Aust.), 1: 143-153.

Baker, F.G. 1978. Variability of hydraulic conductivity within and between nine Wisconsin soil series. Water Resour. Res. 14: 103-108.

Balasubramanian, V., Y. Kanehiro, P.S.C. Rao, and R.E. Green. 1973. Field study of solute movement in a highly aggregated oxisol with intermittent flooding. I. Nitrate. J. Environ. Qual. 2: 359-362.

Barrow, N.J., and T.C. Shaw. 1975. The slow reactions between soil and anions: 2. Effect of time and temperature on the decrease in phosphate concentration in the soil solution. Soil Sci. 119: 167-177.

Barrow, N.J. 1978. The description of phosphate adsorption curves. J. Soil Sci. 29: 447-462.

Biggar, J.W., and D.R. Nielsen. 1962. Miscible displacement; II. Behaviour of tracers. Soil Sci. Soc. Am. Proc. 26: 125-128.

Biggar, J.W., and D.R. Nielsen. 1963. Miscible displacement: V. Exchange processes. Soil Sci. Soc. Am. Proc. 27: 623-627.

Biggar J.W., and D.R. Nielsen. 1967. Miscible displacement and leaching phenomenon. p. 254-274. In R.M. Hagan et al. (eds.), Agronomy No. 11, Am. Soc. Agron., Madison, Wisconsin.

Biggar, J.W., and D.R. Nielsen. 1976. Spatial variability of the leaching characteristics of a field soil. Water Resour. Res. 12: 78-84.

Black, C.A. 1968. Soil-plant relationships. John Wiley, New York.

Blake, G., E. Schlichting, and U. Zimmerman. 1973. Water recharge in a soil with shrinkage cracks. Soil Sci. Soc. Am. Proc. 37: 669-672.

Bolton, E.F., J.W. Aylesworth, F.R. Hare. 1970. Nutrient losses through tile drains under three cropping systems and two fertility levels on Brookston clay loam. Can. J. Soil Sci. 50: 275-279.

Boswell, F.C., and O.E. Anderson. 1970. Nitrogen movement comparisons in cropped versus fallowed soils. Agron. J. 62: 499-503.

Bouma, J., and J.L. Anderson. 1973. Relationships between soil structure characteristics and hydraulic conductivity. Field soil water regime. Soil Sci. Soc. Am. Spec. Publ. No. 5. Am. Soc. of Agronomy. Madison, Wisconsin. p. 77-105.

Bouma, J., and J.L. Anderson. 1977. Water and chloride movement through soil columns simulating pedal soils. Soil Sci. Soc. Am. J. 41: 766-770.

Bouma, J., L.W. Dekker, and H.L. Verlinden. 1977a. Drainage and vertical hydraulic conductivity of some Dutch "knik" clay soils. Agricultural Water Management. Vol. 1: 67-78.

Bouma, J., A Jongerious, O. Boesma, A. Jager, and D. Schoonderbeek. 1977b. The function of different types of macropores during saturated flow through four swelling soil horizons. Soil Sci. Soc. Am. J. 41: 945-950.

Bouma, J., and L.W. Dekker. 1978. A case study on infiltration into dry clay soil. I. Morphological observation. Geoderma. 20: 27-40.

Bouma, J., L.W. Dekker, and J.H.M. Wösten. 1978. A case study on infiltration into dry clay soil. II. Physical measurement. Geoderma. 20: 41-51.

Bouma, J., and J.H.M. Wösten. 1979. Flow patterns during extended saturated flow in two, undisturbed swelling clay soils with different macrostructures. Soil Sci. Soc. Am. J. 43: 16-22.

Bowden, J.W., S. Nagarajah, N.J. Barrow, A.M. Posner, and J.P. Quirk. 1980. Describing the adsorption of phosphate, citrate, and selenite on a variable charge mineral surface. Aust. J. Soil Res. 18: 49-60.

Bower, C.A., and L.V. Wilcox. 1965. Soluble salts. In Methods of Soil Analysis. Agronomy. No. 9., p. 933-951, Am. Soc. Agron., Madison, Wisconsin.

Bowler, D.G. 1980. The drainage of wet soils. Hodder and Stoughton, Sydney. pp. 259.

Bresler, E., and R.J. Hanks. 1969. Numerical method for estimating simultaneous flow of water and salt in unsaturated soils. Soil Sci. Soc. Am. Proc. 33: 827-832.

Brewer, R. 1964. Fabric and mineral analysis of soils. John Wiley and Sons. Inc., New York. 470 pp.

Burns, I.G. 1974. A model for predicting the redistribution of salts applied to fallowed soils after excess rainfall or evapotranspiration. J. Soil Sci. 25: 165-178.

Burwell, R.E., D.R. Timmons, and R.F. Holt. 1975. Nutrient transport in surface run-off as influenced by soil cover and seasonal periods. Soil Sci. Soc. Am. Proc. 39: 523-528.

Cagauan, B.G., Jr., L.S. Lau, R.E. Green, and G. Uehara. 1962. Solute dispersion in two Hawiian soils under saturated flow. Trans. J. Meet. Comm. VI., Int. Soc. Soil Sci. p. 185-194.

Calvert, D.V. 1975. Nitrate, phosphate, and potassium movement into drainage lines under three soil management systems. J. Environ. Qual. 4: 183-186.

Cameron, D.R., and A. Klute. 1977. Convective-dispersive solute transport with a combined equilibrium and kinetic adsorption model. Water Resour. Res. 13: 183-188.

Cameron, D.R., C.G. Kowalenko, and K.C. Ivarson. 1978. Nitrogen and chloride distribution and balance in a clay loam soil. Can. J. Soil. Sci. 58: 77-88.

Cameron, D.R., C.G. Kowalenko, and C.A. Campbell. 1979. Factors affecting nitrate nitrogen and chloride leaching variability in a field plot. Soil Sci. Soc. Am. Proc. 43: 455-460.

Cassel, D.K. 1971. Water and solute movement in Svea loam for two water management regimes. Soil Sci. Soc. Am. Proc. 35: 859-866.

Cassel, D.K., T.H. Krueger, F.W. Schroer, and E.B. Norum. 1974. Solute movement through disturbed and undisturbed soil cores. Soil Sci. Soc. Am. Proc. 38: 36-40.

Cassel, D.K., M. Th. van Genuchten, and P.J. Wierenga. 1975. Predicting anion movement in disturbed and undisturbed soils. Soil Sci. Soc. Am. J. 39: 1015-1019.

Cho, C.M., J. Strong, and G.J. Racz. 1970. Convective transport of orthophosphate (P-31 and P-32) in several Manitoba soils. Can. J. Soil Sci. 50: 303-315.

Childs, E.C. 1969. The physical basis of soil water phenomena. John Wiley, New York. pp 493.

Coat, K.R., and B.D. Smith. 1964. Dead-end pore volume and dispersion in porous media. Soc. Pet. Eng. J. 4: 73-84.

Corker, R.B. 1977. Saturated hydraulic conductivity measurement on the Tokomaru silt loam. Dip. Agri. Sci. Thesis, Massey University, New Zealand.

Corey, J.C., D.R. Nielsen, and D. Kirkham. 1967. Miscible displacement of nitrate through soil columns. Ibid. 31: 497-501.

Couchat, Ph., F. Brissaud, and J.P. Gayraud. 1980. A study of strontium-90 movement in a sandy soil. Soil Sci. Soc. Am. J. 44: 7-13.

Crank, J. 1956. The mathematics of diffusion. Clarendon Press, Oxford, England.

Davidson, J.M., C.E. Reick, and P.W. Santleman. 1968. Influence of water flux and porous material on the movement of selected herbicides. Soil Sci. Soc. Am. Proc. 32: 629-633.

Davidson, J.M., and R.K. Chang. 1972. Transport of picloram in relation to soil physical conditions and pore-water velocity. Soil Sci. Soc. Am. Proc. 36: 257-261.

Davidson, J.M., and J.R. McDougal. 1973. Experimental and predicted movement of three herbicides in a water saturated soil. J. Environ. Qual. 2: 428-433.

Day, P.R. 1956. Dispersion of a moving salt-water boundary advancing through saturated sand. Trans. Am. Geophys. Union. 37: 595-601.

Dayananda, P.W.A., F.P.W. Winteringham, C.W. Rose, and J.Y. Parlange. 1980. Leaching of a sorbed solute: A model for peak concentration displacement. Irrigation Sci. 1: 169-175.

de Camargo, O.A., J.W. Biggar, and D.R. Nielsen. 1979. Transport of inorganic phosphorus in an Alfisol. Soil Sci. Soc. Am. J. 43: 884-890.

Duxbury, J.M., and J.H. Peverly. 1978. Nitrogen and phosphorus losses from organic soils. J. Environ. Qual. 7: 566-570.

Ehlers, W. 1973. Observation on earthworm channels and infiltration on tilled and untilled loess soil. Soil Sci. Soc. Am. Proc. 37: 242-249.

Elrick, D.E., and L.K. French. 1966. Miscible displacement patterns on disturbed and undisturbed soil cores. Soil Sci. Soc. Am. Proc. 30: 153-156.

Evans, G., and I. Levin. 1969. The distribution of salt by infiltration of water into dry soil and sand. Aust. J. Soil Res. 7: 21-27.

Evans, T.D., and J.K. Syers. 1971. An application of autoradiography to study the spherical distribution of ^{32}P-labelled orthophosphate added to soil crumb. Soil Sci. Soc. Am. Proc. 35: 906-909.

see below

Fox. R.L., E.J. Kamprath. 1970. Phosphate sorption isotherm for evaluating the phosphate requirement of soils. Soil Sci. Soc. Am. Proc. 32: 902-907.

Gandar, P.W., and P.E.H. Gregg. 1979. Designing a long-term nitrogen balance experiment. Proceeding of the Agronomy Society of New Zealand. 9: 29-34.

Gardner, W.R. 1965. Movement of nitrogen in soil. p. 550-572. In Bartholomew, W.V., and F.E. Clark. (eds.), Soil Nitrogen. Publ. Am. Soc. Agron., Inc., Madison, Wisconsin.

Gast, R.G., W.W. Nelson, and J.M. MacGregor. 1974. Nitrate and chloride accumulation and distribution in fertilized tile-drained soil. J. Environ. Qual. 4: 406-412.

Foth, D.H. 1978. Fundamentals of soil science. 6th Edition. John Wiley and Sons. New York. pp. 436.

Ghuman, B.S., S.M. Verma, and S.S. Prihar. 1975. Effect of application rate, initial soil wetness, and redistribution time on salt displacement by water. Soil Sci. Soc. Am. Proc. 39: 7-10.

Glover, J., and M.D. Gwynne. 1962. Light rainfall and plant survival in East Africa. I. Maize. J. Ecol. 50: 111-118.

Glover, P.E., J. Glover, and M.D. Gwynne. 1962. Light rainfall and plant survival and E. Africa. II. Dry grassland vegetation. J. Ecol. 50: 199-206.

Green, R.E., P.S.C. Rao, and J.C. Corey. 1972. Solute transport in aggregated soils: Tracer zone shape in relation to pore-velocity distribution and adsorption. Symposium on Fundamental of Transport Phenomenon in Porous Media. Proc. 2nd 2: 732-752.

Gunary, D. 1964. Phosphate diffusion in intact soil. 8th Intern. Congress of Soil Science, Bucharest, Romania. 573-578.

Hall, J.K., and N.L. Hartwig. 1978. Atrazine mobility in two soils under conventional tillage. J. Environ. Qual. 7: 63-68.

Hudson, A.W., H.G. Hopewell, and D.G. Bowler, and M.W. Cross. 1962. The drainage of farm lands. 2nd Ed. Massey College, Palmerston North.

Humphreys, F.R., and W.L. Prichett. 1971. Phosphorus adsorption and movement in some sandy forest soils. Soil Sci. Soc. Am. Proc. 35: 495-500.

John, M.K. 1972. Factors affecting the adsorption of tagged phosphorus by soils. Communication in Soil Sci. and Plant Analysis. 3: 197-205.

Johnston, W.R., F. Ittihadieh, R.M. Daum. and A.F. Pillsburry. 1965. Nitrogen and phosphorus in tile drainage effluent. Soil Sci. Soc. Am. Proc. 29: 287-289.

Jongerius, A. 1957. Morphometric investigations on soil structure. Versl. Landbouwkdi. Onder. 63: 12.

Kanchanasut, P., D.R. Scotter, and R.W. Tillman. 1978. Preferential solute movement through larger soil voids. II. Experiments with saturated soil. Aust. J. Soil Res. 16: 269-276.

Kay, B.D., and D.E. Elrick. 1967. Adsorption and movement of lindane in soils. Soil Sci. 104: 314-322.

Kirda, C., D.R. Nielsen, and J.W. Biggar. 1973. Simultaneous transport of chloride and water during infiltration. Soil Sci. Soc. Am. Proc. 37: 339-345.

Kirkham, D., and W.L. Powers. 1972. Advanced soil physics. Wiley-Interscience, New York. pp. 534.

Kissel, D.E., J.T. Ritchie, and E. Burnett. 1973. Chloride movement in undisturbed swelling clay soil. Soil Sci. Soc. Am. Proc. 37: 21-24.

Kissel, D.E., J.T. Ritchie, and Earl Burnett. 1974. Nitrate and chloride leaching in a swelling clay soil. J. Environ. Qual. 3: 401-404.

Krupp, H.K., and D.E. Elrick. 1969. Density effects in miscible displacement experiment. Soil Sci. 107: 372-380.

Krupp, H.K., J.W. Biggar, and D.R. Nielsen. 1972. Relative flow rates of salt and water in soil. Soil Sci. Soc. Am. Proc. 36: 412-417.

LaFleur, K.S., W.R. McCaskill, and D.S. Adams. 1974. Movement of Prometryne through Congaru soil into ground water. J. Environ. Qual. 4: 132-133.

LaFleur, K.S., G.A. Wojeck, and W.R. McCaskill. 1972. Movement of toxaphene and fluometron through Dunbar soil to underlying ground water. J. Environ. Qual. 2: 515-520.

Lapidus, L., and N.R. Amundson. 1952. Mathematics of adsorption in beds. VI. The effect of longitudinal diffusion in ion exchange chromatographic columns. J. Phys. Chem. 56: 984-988.

Lawes, J.B., J.H. Gilbert, and R. Warington. 1882. On the amount and composition of the rain and drainage waters collected at Rothamsted. William Clowes and Sons, LTD. London.

Levin, I. 1964. Movement of added nitrates through soil columns and undisturbed soil profiles. Trans. 8th Int. Congr. Soil Sci. (Bucharest), 4: 1011-1022.

Lindstrom, F.T., L. Boersma. 1971. The theory of mass transport of previously distributed chemicals in a water saturated sorbing porous medium. Soil Sci. 111: 192-199.

Loveday, J. 1974. Methods for soil analysis of irrigated soils. Tech. Commun. No. 54, Commonwealth Agricultural Bureaux, Farnham Royal.

MacGregor, A.N., J.K. Syers, M.A. Turner, and D.G. Bowler. 1975. Land disposal of untreated dairy shed effluent at Massey University. New Zealand Soil News. 23: 38-40.

MacLean, A.J. 1977. Movement of nitrate nitrogen with different cropping system in two soils. Can. J. Soil Sci. 57: 27-33.

Mansell, R.S., H.M. Selim, P. Kanchanasut, J.M. Davidson, and J.G.A. Fiskell. 1977. Experimental and simulated transport of phosphorus through sandy soils. Water Resour. Res. 13: 189-194.

Mason, D.D., J.F. Lutz, and R.G. Peterson. 1957. Hydraulic conductivity as realted to certain soil properties in a number of great soil groups, sampling errors involved. Soil Sci. Soc. Am. Proc. 21: 554-560.

McAuliffe, K.W. 1978. The effect of land disposal of dairy factory waste on soil properties. Master Thesis. Massey University, New Zealand.

McMahon, M.A., and G.W. Thomas. 1974. Chloride and tritiated water flow in disturbed and undisturbed soil cores. Soil Sci. Soc. Am. J. 38: 727-732.

Meek, B.D., L.B. Grass, A.J. McKenzie. 1969. Applied nitrogen losses in relation to oxygen status in soils. Soil Sci. Soc. Am. Proc. 33: 575-578.

Miller, R.J., J.W. Biggar, and D.R. Nielsen. 1965. Chloride displacement in Panoche clay loam in relation to water movement and distribution. Water Resour. Res. 1: 63-73.

Minshall, N., M.S. Nichols, and S.A. Witzel. 1969. Plant nutrients in base flow of streams in Southern Wisconsin. Water Resour. Res. 5: 706-713.

Mood, A.M., and F.A. Graybill. 1963. Introduction of theory of statistics. McGraw-Hill, New York. pp. 431.

Murphy, J., and J.P. Riley. 1962. A modified single solution method for the determination of phosphate in natural water. Anal. Chim. Acta. 27: 31-36.

New Zealand Soil Bureau Staff. 1968. Soil of New Zealand. Part I. Soil Bureau Bull. No. 26(1). (DSIR: Wellington).

Nielsen, D.R., and J.W. Biggar. 1961. Miscible displacement in soil: I Experiment information. Soil Sci. Soc. Am. Proc. 25: 1-5.

Nielsen, D.R., and J.W. Biggar. 1962. Miscible displacement: III Theoretical considerations. Soil Sci. Soc. Am. Proc. 26: 216-221.

Nielsen, D.R., J.W. Biggar, and K.T. Erh. 1973. Spatial variability of field measured soil-water properties. Hilgadia. 42: 215-259.

Olsen, R.J., R.F. Hensler, O.J. Attoe, S.A. Witzel, and L.A. Peterson. 1970. Fertilizer nitrogen and crop rotation in relation to movement of nitrate nitrogen through soil profiles. Soil Sci. Soc. Am. Proc. 34: 448-452.

Omoti, V., and A. Wild. 1979. Use of fluorescent dyes to marke the pathways of solute movement through soils under leaching conditions: 2. Field experiments. Soil Sci. 128: 98-104.

Oster, J.D., L.S. Willardson, and G.J. Hoffman. 1972. Sprinkling and ponding techniques for reclaiming saline soils. Trans. ASAE. 15: 1115-1117.

Passioura, J.B. 1971. Hydrodynamic dispersion in aggregated media. I. Theory. Soil Sci. 111: 339-344.

Pollok, J.A. 1975. A comparative study of certain New Zealand and German soils formed from loess. Ph.D. thesis, Friedrich-Wilhelms-Universität, Bonn.

Priestley, C.H.B., and R.J. Taylor. 1972. On the assessment surface heat flux and evaporation using large-scale parameters. Month. Weather Rev. 100: 81-92.

Quisenberry, V.L., and R.E. Phillips. 1976. Percolation of surface applied water in the field. Soil Sci. Soc. Am. J. 40: 484-489.

Quisenberry, V.L., and R.E. Phillips. 1978. Displacement of soil water by simulated rainfall. Soil Sci. Soc. Am. J. 42: 675-679.

Rao, P.S.C., R.E. Green, V. Balasubramanian, and Y. Kanehiro. 1974. Field study of solute movement in a highly aggregated oxisol with intermittent flooding. J. Environ. Qual. 3: 197-201.

Rao, P.S.C., J.M. Davidson, R.E. Jessup, and H.M. Selim. 1979. Evaluation of conceptual models for describing nonequilibrium adsorption-desorption of pesticides during steady flow in soils. Soil Sci. Soc. Am. J. 43: 22-28.

Rao, P.S.C., R.E. Jessup, D.E. Rolston, J.M. Davidson, and D.P. Kilcrease. 1980. Experimental and mathematical description of nonadsorbed solute transfer by diffusion in spherical aggregates. Soil Sci. Soc. Am. J. 44: 684-688.

Rennes, L., R.W. Tillman, J.K. Syers and D.G. Bowler. 1976. Effects of mole drainage on surface run-off from a soil under pasture. N.Z. J. Agric. Res. 20: 45-59.

Ritchie, J.T., D.E. Kissel, and E. Burnett. 1972. Water movement in undisturbed swelling clay soil. Soil Sci. Soc. Am. Proc. 36: 874-879.

Robinson, R.A., and R.H. Stokes. 1959. Electrolyte solution. 2nd Edn. Butterworths, London.

Rokowski, A.S. 1972. Watershed physics: Soil variability criteria. Water Resour. Res. 8: 1015-1023.

Rose, D.A., and J.B. Passioura. 1971a. The analysis of experiments on hydrodynamic dispersion. Soil Sci. 111: 252-257.

Rose, D.A., and J.B. Passioura. 1971b. Gravity seggregation during miscible displacement experiments. Soil Sci. 111: 258-265.

Ryden, J.C., J.K. Syers, and R.F. Harris. 1973. Phosphorus in run-off and streams. Advan. Agron. 25: 1-45.

Ryden, J.C., J.R. McLaughlin, and J.K. Syers. 1977. Mechanisms of phosphate sorption by soils and hydrous ferric oxide gel. J. Soil Sci. 28: 72-92.

Saffigna, P.G., C.B. Tanner, and D.R. Keeney. 1976. Non-uniform infiltration under potato canopies caused by interception, stemflow, and hilling. Agron. J. 68: 337-342.

Saffigna, P.G., D.R. Keeney, and C.B. Tanner. 1977. Lysimeter and field measurements of chloride and bromide leaching in an uncultivated loamy sand. Soil Sci. Soc. Am. J. 41: 478-482.

Scotter, D.R. 1978. Preferential solute movement through larger soil voids. I. Some computations using simple theory. Aust. J. Soil Res. 16: 257-267.

Scotter, D.R., B.E. Clothier, and R.B. Corker. 1979a. Soil water in a Fragiaqualf. Aust. J. Soil Res. 17: 443-453.

Scotter, D.R., B.E. Clothier, and M.A. Turner. 1979b. The soil water balance in a Fragiaqualf and its effect on pasture growth in central New Zealand. Aust. J. Soil Res. 17: 455-465.

Scott-Russel, R. 1977. Plant root systems: Their function and interaction with the soil. McGraw-Hill. London. pp.298.

Selim, H.M., P. Kanchanasut, R.S. Mansell, L.W. Zelazny, and J.M. Davidson. 1974. Phosphorus and chloride movement in a spodosol. Soil and Crop Sci. Soc. Fla. 34: 18-23.

Selim, H.M., J.M. Davidson, and R.S. Mansell. 1976. Evaluation of a two site adsorption-desorption model for describing solute transport in soil. Proc. of Summer Computer Simulation Conf., Washington, D.C.

Sharpley, A.N., and K.J. Syers. 1979a. Phosphorus input into a stream draining an agricultural watershed. II Amounts contributed and relative significance of run-off types. Water, Air, and Soil Polution. 11: 417-428.

Sharpley, A.N., and J.K. Syers. 1979b. Loss of nitrogen and phosphorus in tile drainage as influenced by area application and grazing animals. N.Z. Journal of Agricultural Research. 22: 127-131.

Shuford, W.J., D.D. Fritton, and D.E. Baker. 1978. Nitrate-nitrogen and chloride movement through undisturbed field soil. J. Environ. Qual. 6: 255-259.

Skopp. J., and A.W. Warrick. 1974. A two-phases model for the miscible displacement of reactive solutes in soils. Soil Sci. Soc. Am. 38: 545-550.

Soil Survey Staff. 1975. Soil taxonomy. Handb. No. 436. (U.S.D.A.: Washington).

Smith, S.J., and R.J. Davis. 1974. Relative movement of bromide and nitrate through soils. J. Environ. Qual. 3: 152-155.

Spencer, W.F. 1957. Distribution and availability of phosphate added to a Lakeland fine sand. Soil Sci. Soc. Am. Proc. 21: 141-144.

Starr, J.L., and J.Y. Parlange, 1976. Solute dispersion in saturated soil columns. Soil Sci. 121: 364-372.

Syers, J.K., M.G. Brownman, G.W. Smith, and R.B.Corey. 1973. Phosphate sorption by soils evaluated by the Langmuir adsorption equation. Soil Sci. Soc. Am. Proc. 37: 358-363.

Talsma, T. 1967. Leaching of tile-drained saline soils. Aust. J. Soil Res. 5: 37-46.

Taylor, N.H. 1956. Discussion on measurement of soil moisture. Proceedings of the conference on soil moisture. N.Z. Department of Scientific and Industrial Research. pp. 174.

Taylor, S.A. and G.L. Ascroft. 1972. Physical edaphology: The physics of irrigated and nonirrigated soils. W.H. Freeman and Company, San Francisco. pp. 533.

Thomas, G.W., and A.R. Swoboda. 1970. Anion exclusion effects on chloride movement in soils. Soil Sci. 110: 163-166.

Thomas, G.W., and R.E. Phillips. 1979. Consequences of water movement in macropores. J. Environ. Qual. 8: 149-152.

Turner, M.A., D.R. Scotter, D.G. Bowler, and R.W. Tillman. 1976. Water harvesting: The concept and use in a humid climate. Proceedings of Soil and Plant Water Symposium. Palmerston North. p. 168-174.

van De Pol, R.M., P.J. Wierenga, and D.R. Nielsen. 1977. Solute movement in a field soil. Soil Sci. Soc. Am. J. 41: 10-13.

van Genuchten, M. Th., J.M. Davidson, and P.J. Wierenga. 1974. An evaluation of kinetic equilibrium equations for the prediction of pesticide movement in porous media. Soil Sci. Soc. Am. J. 38: 29-35.

van Genuchten, M.Th., and P.J. Wierenga. 1976a. Mass transfer studies in sorbing porous media: I Analytical solutions. Soil Sci. Soc. Am. J. 40: 473-480.

van Genuchten, M. Th., and P.J. Wierenga. 1976b. Numerical solution for convective dispersion with intra-aggregate diffusion and non-linear adsorption. p. 275-292. In G. C. van Steenkiste (ed.) System Simulation in Water Resources North Holland Publ. Co., Amsterdam.

van Genuchten, M. Th., and P.J. Wierenga. 1977. Mass transfer studies in sorbing porous media: II. Experimental evaluation with tritium (^3H_2O). Soil Sci. Soc. Am. J. 41: 272-278.

van Genuchten, M. Th., P.J. Wierenga, and G.A. O'Connor. 1977. Mass transfer studies in sorbing porous media: III. Experimental evaluation with 2,4,5-T. Soil Sci. Soc. Am. J. 41: 278-285.

Warrick, A.W., J.W. Biggar, and D.R. Nielsen. 1971. Simultaneous solute and water transfer for an unsaturated soil. Water Resour. Res. 7: 1216-1225.

Wetselaar, R. 1962. Nitrate distribution in tropical soils. III. Downward movement and accumulation of nitrate in the subsoil. Plant and Sci. XVI: 19-31.

White, R.E., and A.W. Taylor. Effect of pH on phosphate adsorption and isotopic exchange in acid soils at low and high additions of soluble phosphate. J. Soil Sci. 28: 48-61.

Wild, A. 1972. Nitrate leaching under bare fallow at a site in northern Nigeria. J. Soil Sci. 23: 315-324.

Wild, A., and I.A. Babiker. 1976. The assymetric leaching pattern of nitrate and chloride in a loamy sand under field conditions. J. Soil Sci. 27: 460-466.

Williams, R.E., and D.W. Allman. 1969. Factors affecting infiltration and recharge in a loess covered basin. J. Hydrol. 8: 265-281.

Wilson, L.G., J.N. Luthin, and J.W. Biggar. 1961. Drainage salinity investigations of the Tulelake lease lands. Cal. Agr. Expt. Sta. Bull. 779.

Zimmerman, U., K.O. Munnich, and W. Roether. 1967. Downward movement of soil moisture traced by means of hydrogen isotopes. Geophysical Monograph. No. 11. Amer-Geophys. Union. p. 28-36.